

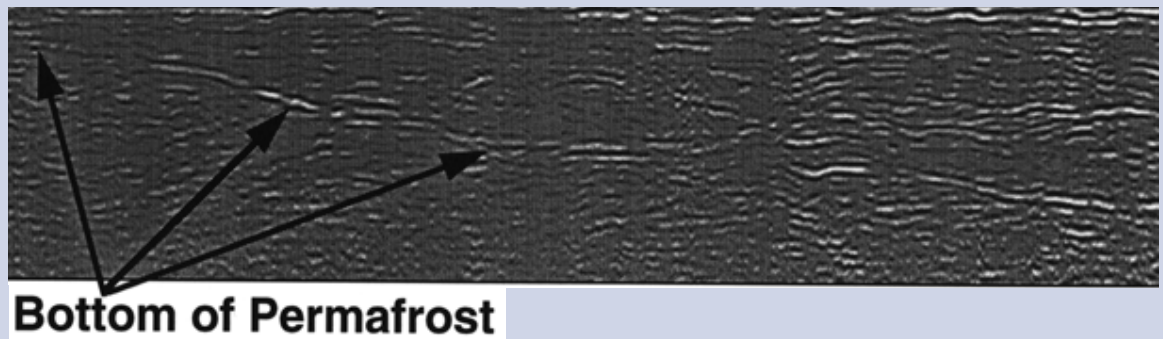
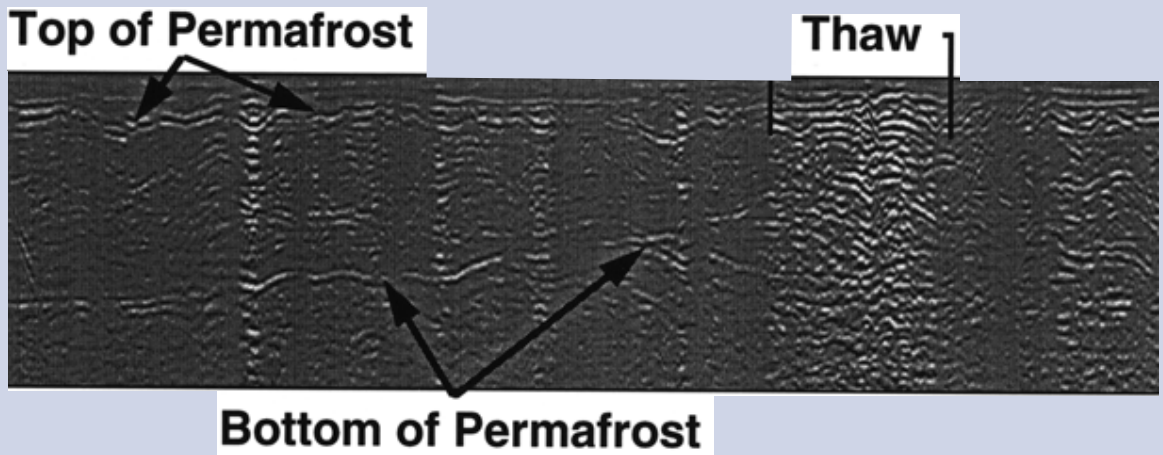


# Geological and Geophysical Investigations of the Hydrogeology of Fort Wainwright, Alaska

## Part II: North-Central Cantonment Area

Daniel E. Lawson, Steven A. Arcone, Allan J. Delaney, Jodie D. Strasser, Jeffrey C. Strasser, Christopher R. Williams, and Tommie J. Hall

August 1998



**Abstract:** Ongoing investigations of the permafrost and ground water conditions in the north-central area of the Fort Wainwright, Alaska, cantonment, north of the Chena River, show the hydrogeology of the site to be extremely complex. Permafrost, being impermeable and discontinuous, controls the distribution and dimensions of ground water aquifers to a great degree. Aquifers are above, below, and adjacent to permafrost, and in some locations are within unfrozen zones surrounded by it. This complexity makes it difficult to predict the direction and velocity of ground water flow, as

well as its seasonal and annual variability. Data have been obtained from ground-penetrating radar surveys, borehole logs, and ground water instruments. They have then been combined with interpretations of aerial photographs and ground observations to delineate the permafrost and aquifer distribution. They have also been used to develop conceptual hydrogeological models of the area. This information is necessary to remediate ground water contamination, while furthering the basic understanding of aquifer distribution and ground water flow in discontinuous permafrost terrain.

**Cover:** Two examples of ground-penetrating radar profiles of permafrost and ground water on Fort Wainwright, Alaska.

**How to get copies of CRREL technical publications:**

Department of Defense personnel and contractors may order reports through the Defense Technical Information Center:

DTIC-BR SUITE 0944  
8725 JOHN J KINGMAN RD  
FT BELVOIR VA 22060-6218  
Telephone 1 800 225 3842  
E-mail help@dtic.mil  
msorders@dtic.mil  
WWW <http://www.dtic.dla.mil/>

All others may order reports through the National Technical Information Service:

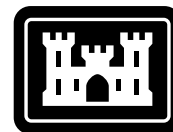
NTIS  
5285 PORT ROYAL RD  
SPRINGFIELD VA 22161  
Telephone 1 703 487 4650  
1 703 487 4639 (TDD for the hearing-impaired)  
E-mail orders@ntis.fedworld.gov  
WWW <http://www.fedworld.gov/ntis/ntishome.html>

A complete list of all CRREL technical publications is available from

USACRREL (CECRL-LP)  
72 LYME RD  
HANOVER NH 03755-1290  
Telephone 1 603 646 4338  
E-mail techpubs@crrel.usace.army.mil

**For information on all aspects of the Cold Regions Research and Engineering Laboratory, visit our World Wide Web site:**  
<http://www.crrel.usace.army.mil>

CRREL Report 98-6



**US Army Corps  
of Engineers®**

Cold Regions Research &  
Engineering Laboratory

# **Geological and Geophysical Investigations of the Hydrogeology of Fort Wainwright, Alaska**

## **Part II: North-Central Cantonment Area**

Daniel E. Lawson, Steven A. Arcone, Allan J. Delaney,  
Jodie D. Strasser, Jeffrey C. Strasser, Christopher R. Williams,  
and Tommie J. Hall

August 1998

Prepared for  
U.S. ARMY ENGINEER DISTRICT, ALASKA

Approved for public release; distribution is unlimited.

## PREFACE

This report was prepared by Dr. Daniel E. Lawson, Research Physical Scientist, Geological Sciences Division, Dr. Steven A. Arcone, Geophysicist, Snow and Ice Division, Allan J. Delaney, Physical Science Technician, Snow and Ice Division, Jodie D. Strasser, Physical Scientist, Geological Sciences Division, Dr. Jeffrey C. Strasser, former Physical Scientist, Geological Sciences Division, Christopher Williams, Electronics Engineer, and Tommie J. Hall, Electronics Technician, Engineering Resources Branch, of the U.S. Army Cold Regions Research and Engineering Laboratory.

The investigations described in this report were conducted as part of the OU4 remedial investigations through the U.S. Army Engineer District, Alaska, for the Environmental Resources Department, Public Works Directorate, U.S. Army Alaska, under two projects: *Geological and Geophysical Analyses of Permafrost and Ground Water Conditions, Fort Wainwright, Alaska*, and *Site-specific, In Situ Ground Water Flow Analyses at Fort Wainwright, Alaska*. The authors thank Cristal Fosbrook, Chief, Environmental Restoration Branch, and Douglas Johnson, Chief, Environmental Resources Department, USARAK, Fort Richardson, Alaska, for their continued support, encouragement, and assistance in many aspects of the work on Fort Wainwright.

The authors also thank the personnel in the Alaska District's Geotechnical Branch for obtaining and evaluating subsurface data by drilling the ground-truth boreholes essential for interpreting and applying the ground-penetrating radar transect data. In particular, they thank Jerome Raychel, Chief, Soils and Geology, Delwyn Thomas, Chief, Geotechnical Branch, and the many members of the District's field crews responsible for logging and sampling each borehole, including Daniel Ackerman, James Saucedo, Chuck Wilson, Joni Sue Minor, and Jeff Harmon. The Alaska District's drill crew, and the contracted drill crew for Ambler, Inc., including driller Daniel Finnegan, are to be commended for drilling and obtaining borehole information even under the most trying of field conditions and weather. Thanks to Lawrence Gatto and Dr. Lewis Hunter for critically reviewing this report, and Cora Farnsworth for preparing the manuscript.

The contents of this report are not to be used for advertising or promotional purposes. Citation of brand names does not constitute an official endorsement or approval of the use of such commercial products.

## CONTENTS

	Page
Preface .....	ii
Introduction .....	1
General background .....	2
Permafrost .....	2
Ground and surface water .....	2
Surface and bedrock geology .....	5
Methods of investigation .....	6
Ground-penetrating radar (GPR) .....	6
Drilling .....	7
Monitoring wells .....	7
Ground water flow system .....	8
Analysis and interpretation .....	9
Subsurface geology and permafrost distribution .....	9
Ground water aquifers .....	19
Site-specific seepage data .....	21
Hydrogeological concepts .....	23
Suprapermafrost aquifers and near-surface flow patterns .....	25
Subpermafrost and deep flow patterns .....	25
Discussion .....	25
Conclusion .....	27
Literature cited .....	28
Appendix A: Site-specific ground water data .....	31
Abstract .....	67

## ILLUSTRATIONS

Figure	
1. North-central cantonment area, showing the landfill site .....	1
2. Idealized sketch illustrating the configuration and nomenclature for discontinuous permafrost and ground water aquifers associated with it .....	2
3. Aerial photograph of the discontinuous permafrost region north of the Chena River on 20 May 1993 .....	3
4. Mosaic of aerial photographs of the region north of the Chena River on 9 September 1949 .....	4

Figure	Page
5. Assemblages of alluvial deposits as distinguished by the trends of point bars, meander scrolls, former channels, and levees north of the Chena River .....	5
6. GPR transects in the area north of the Chena River .....	6
7. Locations of boreholes used to interpret GPR data in the north-central cantonment area .....	7
8. Monitoring wells in which the CRREL ground water flow system is installed .....	8
9. Automated ground water flow system .....	9
10. Transect 94-78 with interpretation based on boreholes and other data .....	10
11. 50-MHz profile from three concatenated transects .....	11
12. 50-MHz profile of south to north transect 94-61, which lies west of the landfill .....	11
13. 50-MHz profile of transect 94-70, which trends west from near Canol Road and ends east of the landfill site .....	12
14. 50-MHz profile and interpretation of transect 93-11, which trends south-southwest to north-northeast approximately parallel to the base of Birch Hill .....	12
15. Elevation of permafrost .....	13
16. Characteristic depths of thaw and the locations of unfrozen zones in the north-central area of the cantonment .....	15
17. Locations of areas frozen into bedrock, areas where permafrost is underlain by unfrozen sediments that overlie unfrozen bedrock, and unfrozen zones that penetrate the permafrost completely .....	16
18. Depth to bedrock from boreholes drilled north of the Chena River .....	17
19. Buried bedrock surface topography based upon borehole data .....	17
20. Six interpretive cross sections illustrating subsurface distribution of discontinuous permafrost within the north-central cantonment area .....	18
21. Averaged flow vectors for subpermafrost and deep wells, shown with respect to permafrost distribution .....	22
22. Near-surface and suprapermafrost flow paths .....	24
23. Hydrogeological concepts of deep aquifer flow paths depicted for two scenarios: where Birch Hill dominates and where a sub-regional aquifer dominates .....	26
24. Idealized ground water flow patterns within and beneath the landfill .....	27

# Geological and Geophysical Investigations of the Hydrogeology of Fort Wainwright, Alaska

## Part II: North-Central Cantonment Area

DANIEL E. LAWSON, STEVEN A. ARCONE,  
ALLAN J. DELANEY, JODIE D. STRASSER, JEFFREY C. STRASSER,  
CHRISTOPHER R. WILLIAMS, AND TOMMIE J. HALL

### INTRODUCTION

The surface and ground water hydrology of Fort Wainwright, Alaska, is extremely complex because discontinuous permafrost (perennially frozen ground) is present. Ground water aquifers can occur in unfrozen sediments above, below, or adjacent to permafrost, and in thawed zones within it (e.g., Hopkins et al. 1955). The permafrost, acting as a low permeability boundary that constrains ground water movement and the locations of aquifer recharge or discharge (e.g., William 1970), may be present because of a number of factors, most notably human and natural disturbances to the terrain and vegetation. Identifying unfrozen aquifers in permafrost terrain is, therefore, extremely difficult. Standard techniques such as drilling or terrain analysis cannot readily locate frozen or unfrozen zones, except in the most obvious instances.

The fate of contaminants transported in ground water depends upon the distribution of discontinuous permafrost. These complex hydrogeological conditions have made it difficult for previous investigators to evaluate ground water contamination at Fort Wainwright. Contamination problems have included determining whether sites

were actually contaminated, defining the extent and nature of the contamination, identifying sources, defining transport paths, and evaluating the potential for off-site migration.

In this report, we summarize ongoing hydrogeological investigations of ground water and permafrost conditions in the north-central area of the cantonment of Fort Wainwright (Fig. 1). Our

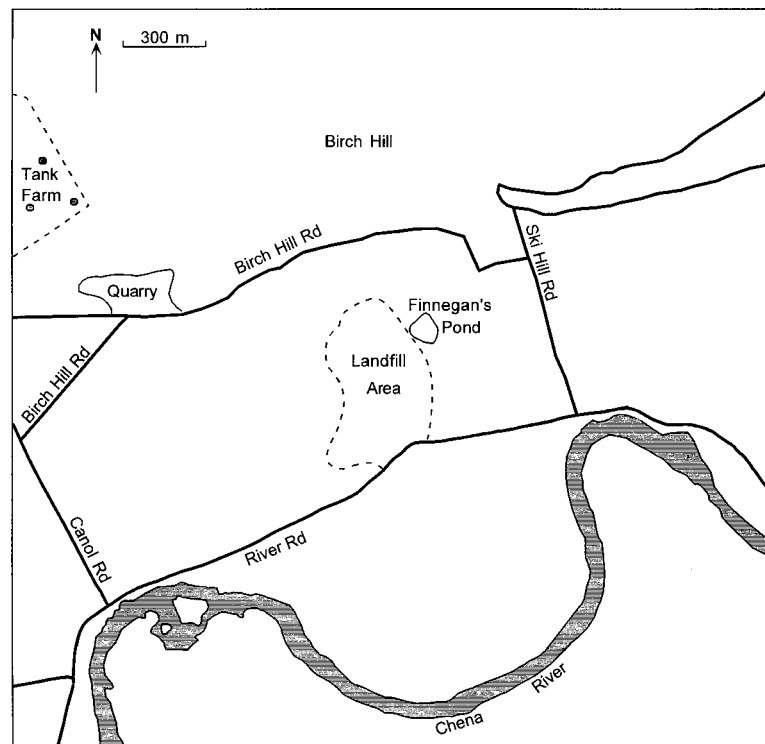


Figure 1. North-central cantonment area, showing the landfill site.

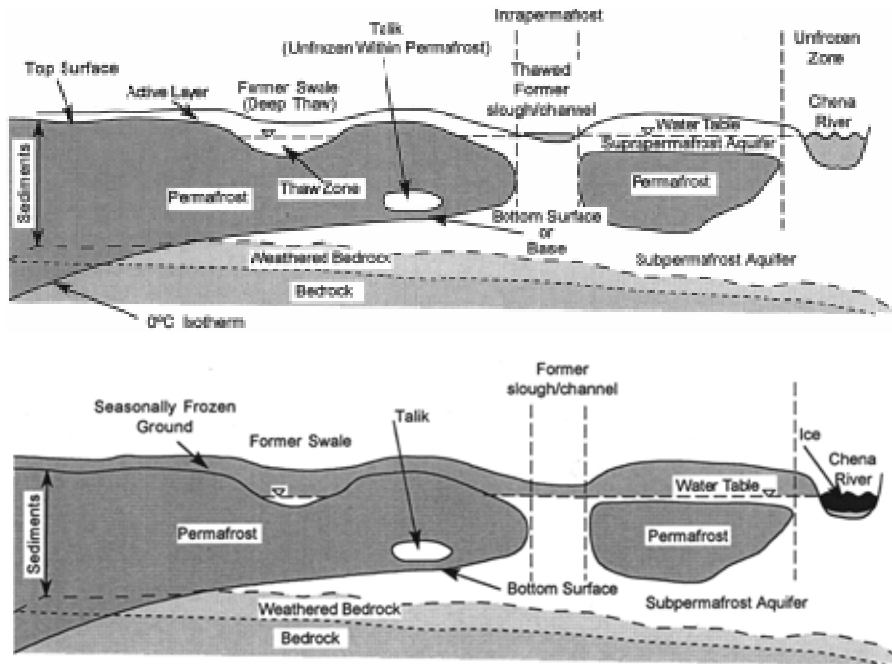


Figure 2. Idealized sketch illustrating the configuration and nomenclature for discontinuous permafrost and ground water aquifers associated with it; (top) summer conditions, and (bottom) winter conditions.

studies, part of the effort to remediate contaminant problems on the base, augments the results of Lawson et al. (1996). In addition, an active landfill (Ecology and Environment 1994) is one site in the north-central cantonment requiring hydrogeological data for remediation.

## GENERAL BACKGROUND

### Permafrost

The three-dimensional configuration and extent of discontinuous permafrost controls ground water flow to a large degree (Hopkins et al. 1955, Williams 1970). Changes from frozen to unfrozen conditions may be abrupt and without surface expression. The top and bottom surfaces, as well as lateral boundaries, of permanently frozen subsurface materials have highly irregular relief. Combined with the impermeability of permafrost, these characteristics can significantly affect ground water movement in the region (Fig. 2). The distribution of frozen ground is a function of not only the past and present environment, but also of terrain characteristics, historical use, surface disturbances, vegetative cover, and conductive heat transfer from the surface and ground water (e.g., Hopkins et al. 1955, Mackay 1970,

Ferrians and Hobson 1973, Williams and Van Everdingen 1973, Abele et al. 1984, Lawson 1986).

Permafrost exists at various depths throughout the Fairbanks region, ranging from less than 0.5 to over 20 m to its upper surface. The base of the permafrost commonly ranges from as little as 10 to over 50 m below the ground surface (e.g., Ferrians 1965, Williams 1970). Permafrost thins rapidly to a few meters adjacent to thawed areas. Thawed areas generally are deepest beneath geological features such as swales and former stream channels, or beneath man-made disturbances such as roads, buried pipelines, buildings, excavations, and areas cleared of vegetation (Lawson et al. 1994, 1996).

The landfill (Fig. 3) was built on discontinuous permafrost in about 1950 and it probably has disturbed the surface sufficiently for a thick thaw bulb to develop beneath it (Ecology and Environment 1994). Sediments and bedrock on southerly exposed slopes such as Birch Hill (Fig. 1) are generally unfrozen.

### Ground and surface water

Two ground water flow systems are present in the cantonment area. The first is discontinuous, near the surface, and perched above the perma-



Figure 3. Aerial photograph of the discontinuous permafrost region north of the Chena River on 20 May 1993. Arcuate landforms are usually former channels and sloughs, or point bar–swale complexes.

frost (suprapermafrost), while the second is deeper, below the permafrost (subpermafrost) (Fig. 2) (Williams 1970, Lawson et al. 1996). The suprapermafrost and subpermafrost aquifers communicate with one another where the frozen ground is perforated by thaw zones that are confined only laterally by permafrost, and through the unfrozen ground beneath the Chena River (Fig. 2). Isolated thaw zones may be areas of discharge or recharge to either aquifer, and may have upward or downward vertical gradients. Ground water may also be confined in taliks, which are unfrozen materials surrounded by

permafrost (Fig. 2). The water levels, flow rates, and flow directions in the suprapermafrost aquifer vary relatively rapidly each season and possibly each day. In part, these variations are caused by infiltrating surface water from rainfall, snow-melt, or flooding.

Surface water also enters the ground water system from Birch Hill via two pathways. First, water infiltrates through the unfrozen sediments and weathered bedrock of Birch Hill, flowing on the competent rock surface to the base of the slope where it enters the suprapermafrost aquifer. Second, water can enter the bedrock by migrating



Figure 4. Mosaic of aerial photographs of the region north of the Chena River on 9 September 1949. The approximate area of the active landfill site is outlined.

through fractures, but their locations and orientations are generally unknown and difficult to predict. Water within fractures that trend generally north-south will tend to flow in accord with the southerly slope of Birch Hill and enter unfrozen alluvial sediments from below (e.g., Williams 1970, Péwé et al. 1976). If such an aquifer is confined by permafrost, the resulting piezometric surface could become artesian, which will maintain isolated zones of unfrozen materials beneath and in the permafrost (e.g., Hopkins et al. 1955).

The migration pathways of contaminants will follow the aquifers and, thus, be affected by all the factors that determine ground water flow.

### Surface and bedrock geology

Unconsolidated materials with relief generally less than a meter make up most of the surface south of Birch Hill (Péwé et al. 1976). Alluvial deposits cover most of the area of the Chena River and its tributaries, and are represented at the surface by various landforms, including point bars, swales, channels, and sloughs (Fig. 4). Drilling has revealed that most of the unconsolidated sediments consist of gravels and sands, with spo-

radic layers and lenses of silt.\* The materials at depth were likely deposited by meandering or braided streams that were ancestral to the Chena and Tanana Rivers. In addition, a layer of wind-blown silt (loess), less than 1 m thick, commonly lies just below a thin (less than 0.5 m) surface layer of organic material.

Unconsolidated materials on Birch Hill have also moved downslope to form colluvial deposits composed of weathered bedrock, silt, and sand. These deposits extend up to several hundred meters south from the base of the hill and overlie the prevailing alluvial sediments (e.g., Péwé et al. 1976). In addition, runoff from gullies cut into Birch Hill has locally deposited sand and silt with thicknesses of up to 2-4 m. These deposits form fans that can extend several hundred meters south of Birch Hill.\*

The cross-cutting of alluvial landforms south of Birch Hill reflects the migration of the Chena River (Fig. 5). Meander scrolls with associated channels or swales generally trend east-west in

\* Unpublished borehole records, U.S. Army Engineer District, Alaska.

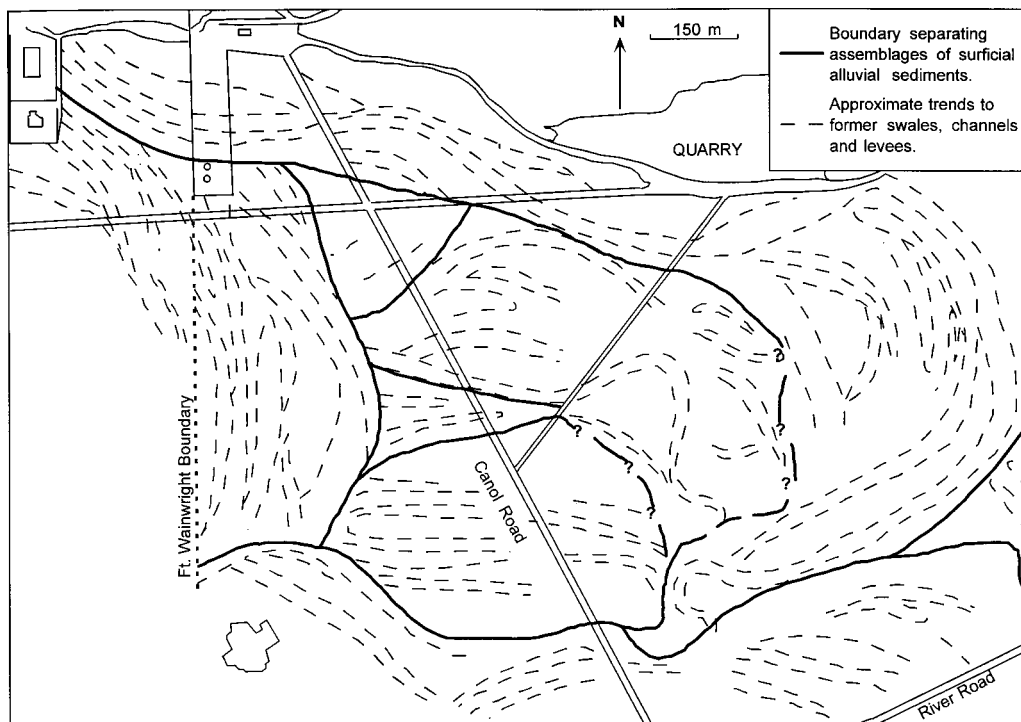


Figure 5. Assemblages of alluvial deposits as distinguished by the trends of point bars, meander scrolls, former channels, and levees north of the Chena River. Cross-cutting relationships of these features show that the surface deposits are of different ages. Compare with the aerial photograph in Figure 4.

the area immediately east of the landfill, while similar features trend north-south to the south and west (Fig. 4 and 5). Similarly, the north-south trending meander scrolls are crossed by east-west trending ridges and swales further to the south, meaning that the latter features were deposited more recently.

The relative age of the alluvial sediments can be an important factor hydrologically by dictating the three-dimensional relationship of layers that either do or don't conduct water (i.e., coarse gravel channel vs. fine-grained overbank deposits). The Chena River basin also received glacial runoff during the last major period of glaciation (Hamilton 1994), which implies that channel deposits of this age may be significantly coarser than material being transported by the Chena River today. Similarly, overbank deposits from this time may be thicker and contain more silt than recent deposits.

Former channels and swales tend to be slightly lower than the surrounding terrain, causing water to collect during wet times of the year. These topographic features generally retain their natural morphologies and are often the sites of slow moving streams, unless they are artificially excavated to improve drainage. There are unfrozen sediments beneath some of these alluvial features,

but others may be frozen to bedrock; the reasons for this difference are unknown.

The unconsolidated materials of the Chena River floodplain lie unconformably above dark pelitic schists of the Yukon-Tanana Complex, formerly identified as the Birch Creek Schist (King 1969, Péwé et al. 1976). This metamorphic unit is generally of lower greenschist facies, and is thought to be of Precambrian age (Péwé et al. 1976). Birch Hill, which rises approximately 200 m above the adjacent alluvial plain, is also composed of this highly fractured and foliated schist. In most areas of Birch Hill, the bedrock is overlain by eolian silt with thicknesses that may exceed 3 m or more.

## METHODS OF INVESTIGATION

Our investigations have been multifaceted. We used standard ground-penetrating radar (GPR) techniques, as well as new methods and equipment that we developed for this study, to define the extent and depth of permafrost and of saturated aquifer sediments (Arcone et al., in press). These data were combined with other data from drilling records, ground water flow sensors, aerial photographs, and surface observations to find out how aquifers were distributed. From these analyses, we have developed several hydrogeological concepts of the north-central cantonment area.

### Ground-penetrating radar

Ground-penetrating radar (GPR) analyses produced the data necessary to outline the three-dimensional permafrost and ground water stratigraphy of the area. Multiple GPR profiles were therefore acquired along numerous transects established on new and existing trails across the area (Fig. 6). Prior to profiling, the trails were cleared of vegetation by hydroax. Their locations were later surveyed by professional crews.

GPR data were obtained between 1993 and 1995, with most acquired in March-April 1994, August-September 1994, and March-April 1995. Our radars were Geophysical Survey Systems, Inc., SIR Models 4800 and 10a+ control units and antennas radiating wide bandwidth

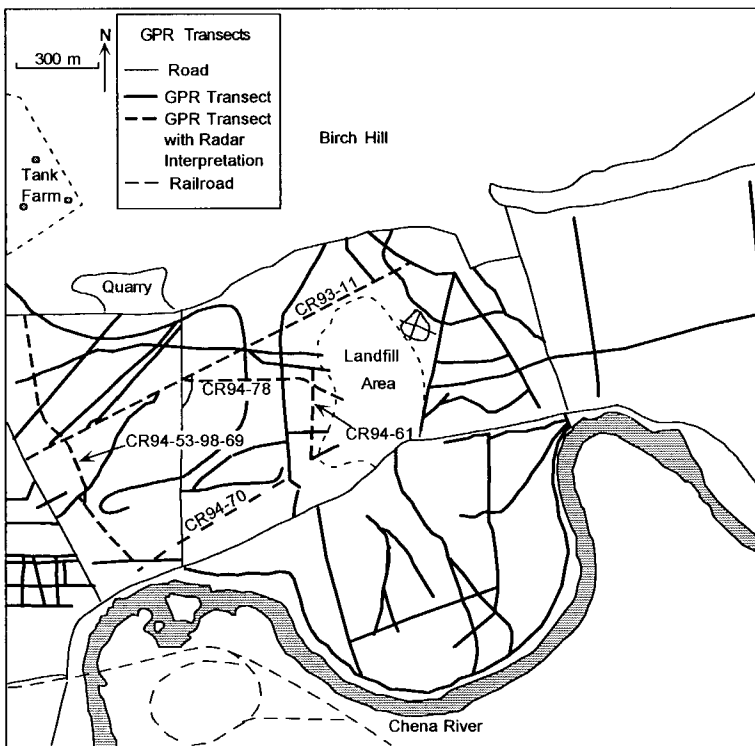


Figure 6. GPR transects in the area north of the Chena River.

signals centered near 50, 100, and 300 MHz. We profiled each transect by towing the antennas along the ground approximately 6–10 m behind a tracked vehicle moving at a constant velocity of about 1 m/s. Event markers were placed artificially on the records at 10-m intervals. Single trace time durations of 150, 600, and 1500 ns were commonly used for the 300-, 100-, and 50-MHz antennas respectively. For a more complete description of the GPR methods and theory, see Appendix A of Lawson et al. (1996).

GPR is reflected and diffracted at material interfaces, with a signal amplitude strength determined by the contrast in relative dielectric permittivity  $\epsilon$  across the interface. The thickness  $d$  of a layer was interpreted using the echo delay formula for normal incidence

$$d = ct^2 / \epsilon \quad (1)$$

where  $c$  is the free space speed of light ( $3 \times 10^8$  m/s),  $t$  is time, and the factor of two accounts for the round trip propagation path. Typically, the value of  $\epsilon$  for permafrost is about 5, and ranges between about 10 and 45 for unfrozen sediments of varying degrees of saturation and grain size. An outcrop of the local bedrock was measured at  $\epsilon = 11$  using a wide angle sounding technique. Arcone et al. (in press) provide details of the analysis and interpretation of permafrost and aquifers from GPR profiles.

### Drilling

We determined subsurface material types and permafrost horizons by drilling test boreholes in 1993 and 1994. Drill sites (Fig. 7) were chosen using preliminary interpretations of the site's geomorphic features and any available GPR data. We subsequently combined borehole and GPR records to make interpretive cross sections of permafrost and aquifer distribution. Data on the thickness of active layers (less than 1.5 m thick) were also obtained by probing with a hand-driven steel rod. We measured piezometric surfaces in wells installed in the suprapermfrost, subpermafrost, and unfrozen zone aquifers. Geological logging of each borehole followed standard procedures.

### Monitoring wells

Monitoring wells, generally in clusters of three at depths of about 10, 20, and 30 m, were drilled, logged, and developed for use with the CRREL ground water flow system (Fig. 8) (see following section). Monitoring well clusters are located in thawed zones above the permafrost or in unfrozen zones laterally confined by it. Additional wells were drilled through the permafrost into the subpermafrost aquifer; these wells were pressurized to keep ice growth from closing them. We used data from GPR surveys and borehole logs, and geomorphic features and other geological data, to select monitoring well locations that would provide representative ground water flow data.

Monitoring wells above and below the permafrost were built following standard procedures. Each monitoring well was drilled to a specified depth, where a 3-m-long well screen was installed. The well screens, of about 5 cm (2 in.) i.d., are made of continuous wire wrap stainless steel, with a 15-mm- (0.060-in.-) slot size and a filter sock of 120- to 150-mm mesh covering the outside. Laboratory testing at CRREL shows that this configuration minimally restricts water movement, while stopping finer sediments from infiltrating the well

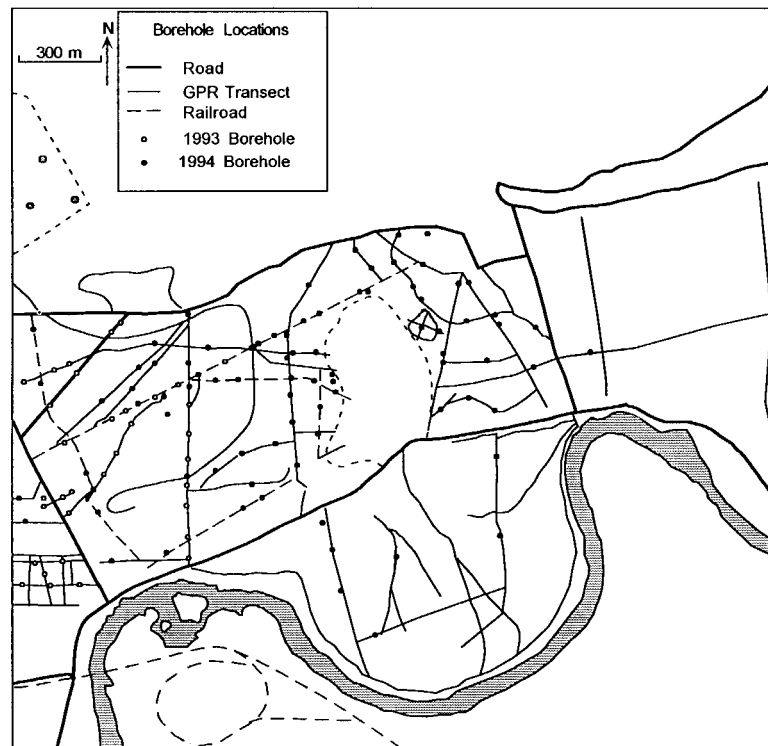


Figure 7. Locations of boreholes used to interpret GPR data in the north-central cantonment area.

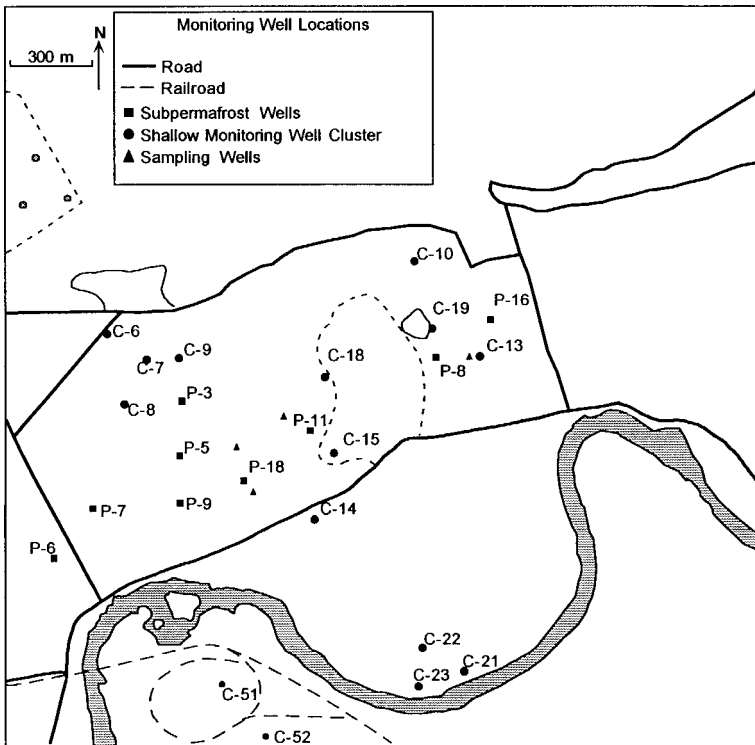


Figure 8. Monitoring wells in which the CRREL ground water flow system is installed.

and affecting measurements. During installation, each hole was allowed to collapse around the filter-covered screen as a way to minimize the well's effect on ground water movement. Monitoring wells set in the subpermafrost aquifer were screened at a depth beginning 3 m below the permafrost. Water levels were recorded in subpermafrost wells after they were completed.

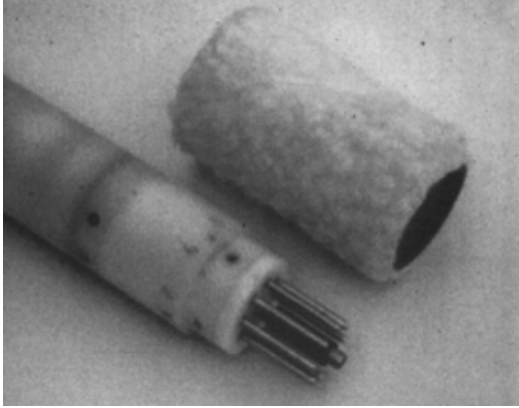
### Ground water flow system

CRREL's prototype ground water flow system uses the thermal tag and trace technique (e.g., Chapman and Robinson 1962, Hess 1982) to measure flow direction and seepage velocity. The system uses a sensor with four pairs of platinum resistive temperature devices (RTDs) in steel tynes arrayed in a circular pattern around a point source heater (Fig. 9a). Heat is transferred preferentially by ground water flow from the heater to the RTDs. Conductive heat transfer is enhanced by glass beads placed into the screen in which the RTD tynes are imbedded. Temperature fluctuations between paired RTDs, relative to background levels, are recorded. This temperature differential is then used to calculate the direction of flow and seepage velocity.

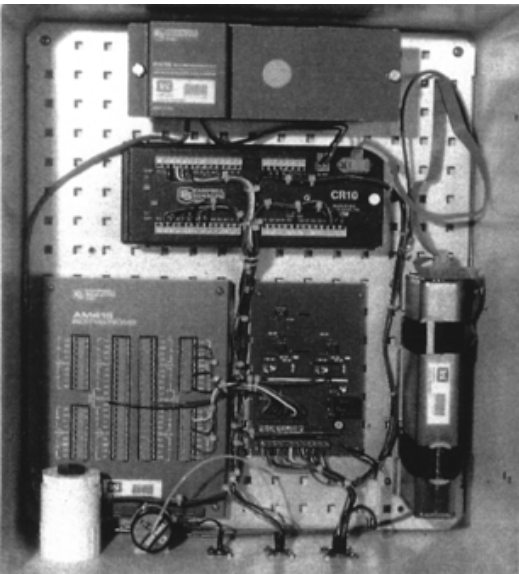
Each sensor was calibrated individually in a section of well screen set in a flume filled with materials generally representative of those in the

screened interval of the monitoring wells. This material consisted of a commercially available sand mixture (sieve no. 8–12), compacted to a porosity similar to most materials in the well screen intervals. A constant displacement pump was used to regulate seepage rates in the flume from 1 to 10 ft/day (0.3 to 3 m/day). An empirical linear relationship between sensor readings and seepage rates was determined for each system for a known direction of flow. The accuracy of the flow system is 0.1 ft/day (0.03 m/day) over the range of 0.5 to more than 10 ft/day (0.15 to more than 3 m/day). Direction, as defined by ten measurements in the flume, is accurate to within  $\pm 5^\circ$ . Details of the calibration procedure are given in Williams et al. (in prep).

Seepage direction and velocity are measured four times per day in summer and twice per day in winter, with system functions controlled by a Campbell CR10XT datalogger (Fig. 9b). Signals are transmitted by cable from the flow sensor, which is held by steel rods and a clamp at a specified depth. Power is provided by an external 12-V, deep cycle battery, charged by a solar panel mounted on a pole with the control unit (Fig. 9c). A pressure transducer (Druck PDCR-35D) installed in each well records water level (piezometric surface) fluctuations at the same time as flow measurements. Data are stored using a



a. Sensor.



b. Control unit with Campbell CR10a datalogger installed at field site.



c. Typical field installation with solar panels and 12-V battery for power at remote site.

Figure 9. Automated ground water flow system.

Campbell SM 716XT storage module and periodically downloaded to a portable computer for analysis and graphical display.

## ANALYSIS AND INTERPRETATION

### Subsurface geology and permafrost distribution

We defined the subsurface geology and permafrost distribution using GPR data from multiple transects for which we obtained ground truth using borehole logs from sites on each transect. These data were augmented by landform analyses using historical (1949) and recent (1993) aerial photography of the site. Our interpretations of the subsurface geology from borehole and GPR data were thus linked to the surface morphology, so that the spatial distribution of permafrost and aquifers could be defined.

### GPR data

GPR profiles of the landfill were generally unable to reveal the nature of the subsurface, despite our using low-frequency (50-MHz) antennas. The signals were extremely attenuated, penetrating to only 1 to 2 m depth. This probably resulted because fine-grained coal ash from the Fort Wainwright power plant is buried in the landfill.

Therefore, we investigated the area surrounding the landfill, so that stratigraphic and ground water data could be extrapolated to evaluate the state of the materials below it. The 1949 aerial photograph of the site (Fig. 4), taken before the landfill was built, shows a surface similar to the surrounding terrain beneath it. Assuming that the stratigraphy is similar to that of the surrounding area, we can infer the subsurface conditions beneath the landfill.

Radar reflections in the north-central cantonment area result mainly from changes in material type, such as from coarse to fine-grained deposits or from sedimentary units to bedrock, and from changes in water or ice content (Arcone et al., in press). Abrupt changes in the time delay of reflections in frozen sediments may indicate stratigraphic changes in grain size or the unfrozen water content. There is generally little attenuation where permafrost is very close to the surface. In this case, the signal can penetrate deep into the permafrost, to greater than 80 m below the ground surface. In contrast, signals are strongly attenuated in thawed or perennially unfrozen sediments.

The 50-MHz profiles described here were

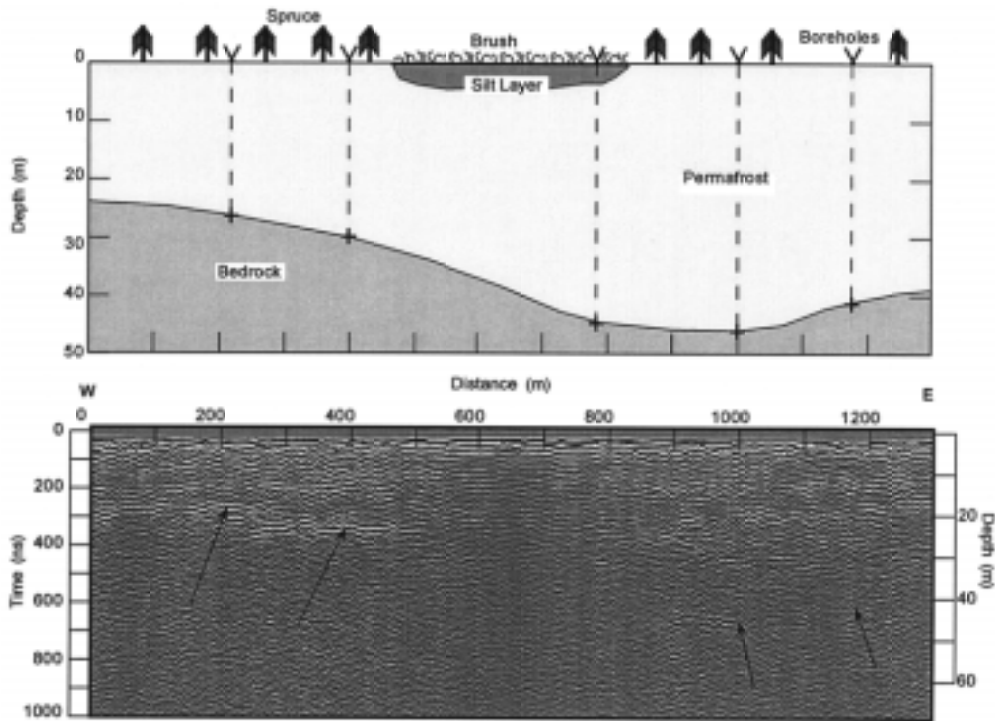


Figure 10. Transect 94-78 with interpretation based on boreholes and other data. The transect lies west of landfill and trends east to west (0–660 m). This profile was obtained in March 1995 using 50-MHz antennas. Arrows in radar traces indicate bedrock reflectors.

acquired in late March 1995, when the ground was frozen from 3 to 4 m deep. They are representative of GPR data and subsurface conditions across the area, and illustrate typical features of the radar records. Boreholes used to interpret the radar data are located on each profile figure.

Conditions in the area west of the landfill are interpreted from several transects, including profile CR94-78, which trends east–west and crosses several features with contrasting subsurface properties (Fig. 10). The ground is deeply thawed on its eastern end (600–650 m). Permafrost then thickens and extends to bedrock between the 600- and 90-m distance marks. Between 410 and 230 m, the transect traverses a marshy area with a prominent, abandoned slough between 290 and 250 m. Although much of the area was frozen to bedrock at the time of survey, the near-surface fine-grained sediments attenuated the signal and kept us from detecting the bedrock. A strong subhorizontal return only marks the surface of bedrock at shallow depths, such as those ranging from 25 to 35 m along the far western end of the profile. Bedrock is intermittently revealed on the eastern end at depths greater than 40 m.

The profiles of three transects (CR94-53, 98, and 69) are linked in Figure 11 to show several characteristics of the site. Bedrock is a prominent reflector at a depth of about 15 m at the 85-m distance mark. This reflector steadily deepens to the south, dropping sharply after about 500 m distance. Permafrost extends into bedrock in the northern end, but at about 400 m distance, a weak reflector suggests that unfrozen bedrock lies at a depth of 30–40 m. At about 950 m distance, permafrost extends to about 32 m depth, with unfrozen sediments between it and the top of the bedrock, which is undetected, but must be greater than 50 m deep.

Transect 94-61 (Fig. 12) is about 1 km long, trending south to north from River Road to the base of Birch Hill, and lies directly west of the landfill (see Fig. 6). Only one borehole, that at 100 m distance north of River Road, encountered the bottom of the permafrost. At this location, the bottom of permafrost lies at about 38 m depth. The permafrost bottom rises south of 100 m, and disappears at about 40 m distance, where there are unfrozen channel deposits under an artificially deepened drainage ditch. North of about 250 m,

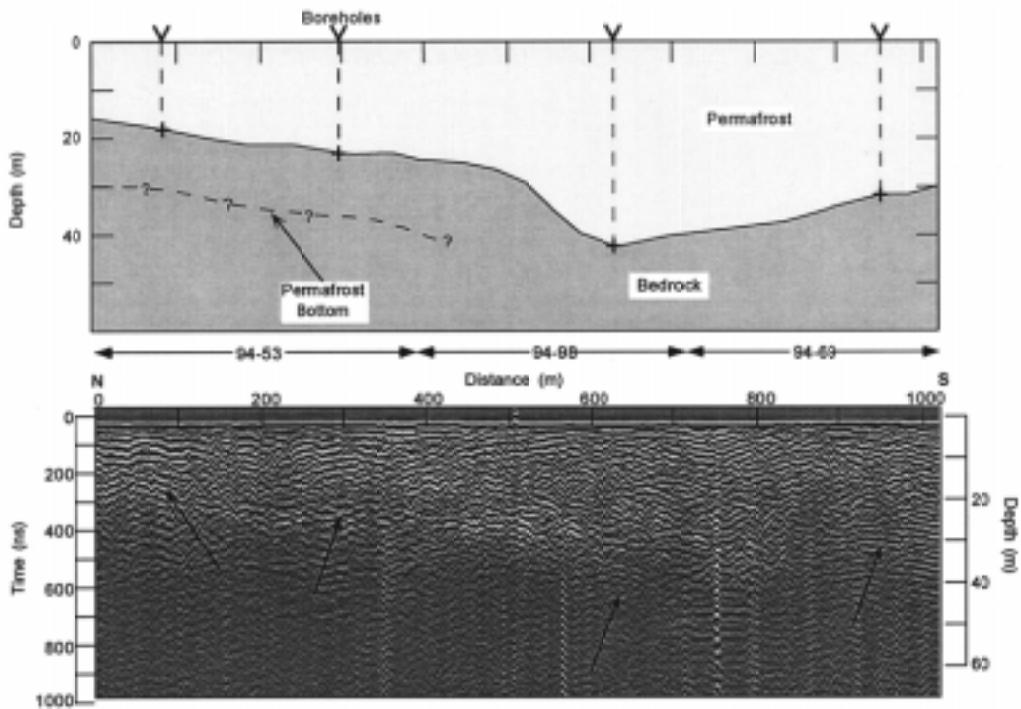


Figure 11. 50-MHz profile from three concatenated transects (CR94-53, 98, 69). Subpermafrost ground water was found only at the northern end. The interpreted permafrost horizon depicted with question marks is speculative. Arrows in radar traces indicate bedrock reflectors.

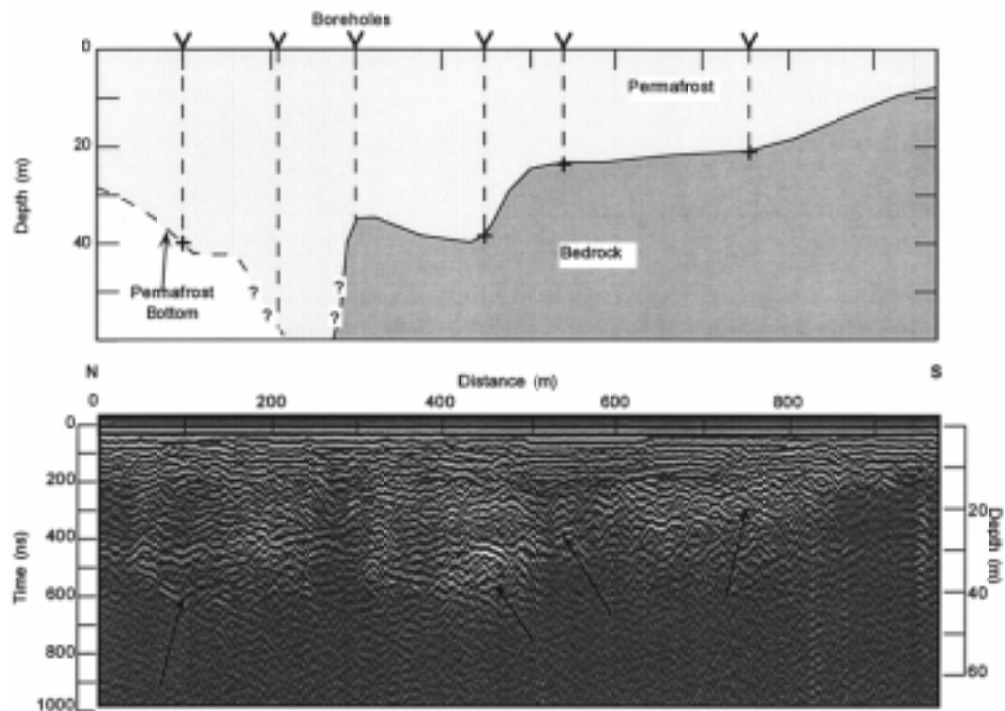


Figure 12. 50-MHz profile of south to north transect 94-61, which lies west of the landfill (see Fig. 6). Borehole locations are shown. The lower profile shows the interpretation of the borehole and GPR data. The bottom of permafrost was encountered only at the southern end. Permafrost appears to extend into bedrock along most of this line. Arrows in radar traces indicate bedrock reflectors.

permafrost extends into the bedrock. The bedrock shallows at the northern end of the transect near Birch Hill, ranging from about 10–12 m deep at 925 m distance and gradually deepening to about 21 m at 750 m distance. The bedrock depth then appears to hold steady to about 500 m distance, where it deepens sharply to about 44 m at about 450 m distance. Of note, bedrock returns are

not always the strongest events at depth (e.g., between 400 and 500 m), and south of 300 m, there are no returns from bedrock because of the unfrozen, saturated sediments that are between the base of permafrost and bedrock.

Transect 94-70 (Fig. 13) runs west to east, beginning near Canol Road. It has a well-defined sub-horizontal reflector from subpermafrost water

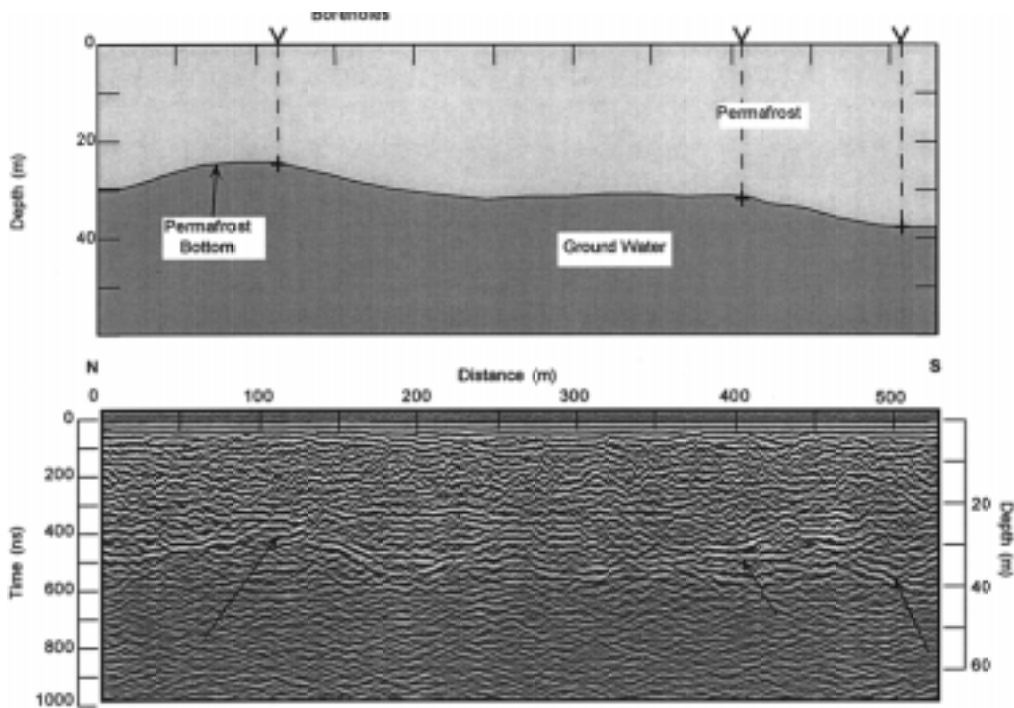


Figure 13. 50-MHz profile of transect 94-70, which trends west from near Canol Road and ends east of the landfill site (Fig. 6). Ground water is interpreted to occur beneath the entire transect.

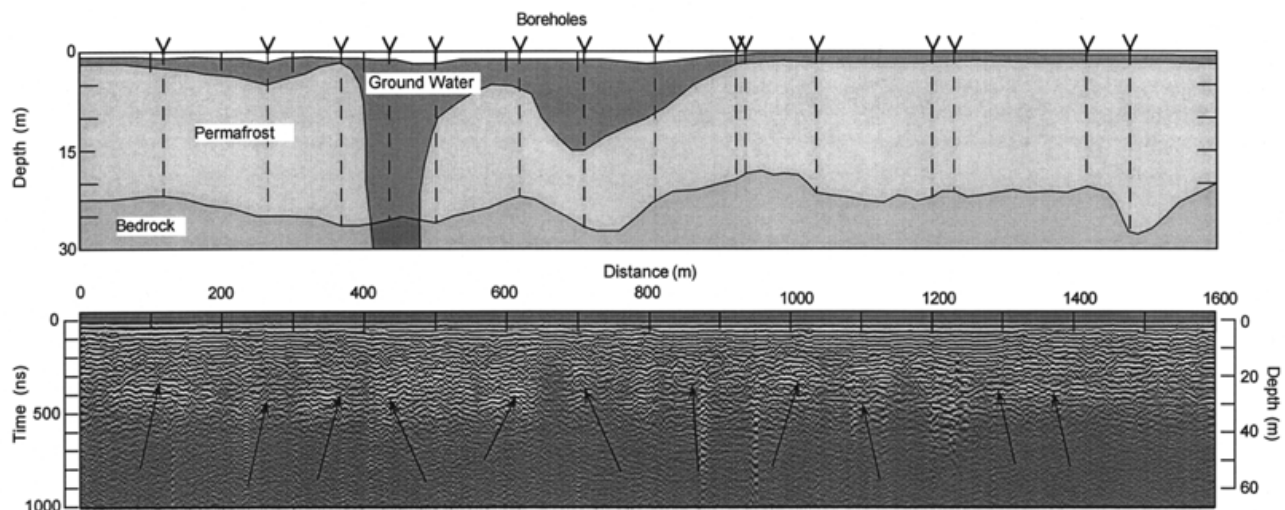


Figure 14. 50-MHz profile and interpretation of transect 93-11, which trends south-southwest to north-northeast approximately parallel to the base of Birch Hill (Fig. 6). Arrows in radar traces indicate bedrock reflectors.

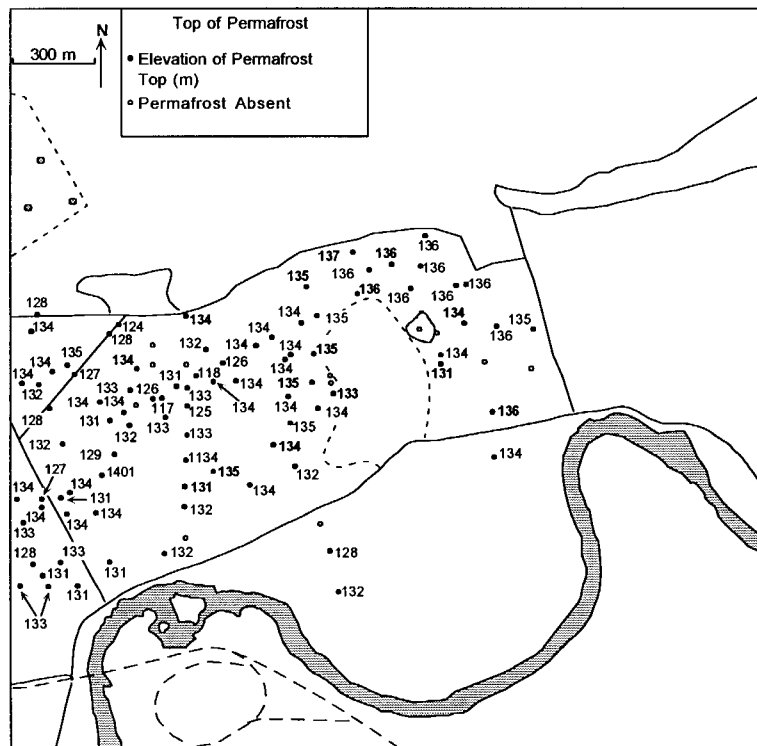
that is in contact with the base of the permafrost. Permafrost thickness is relatively constant, varying from about 28–35 m along the transect. There is no consistent reflection from bedrock beneath permafrost. Bedrock was also not encountered in any of the boreholes and apparently lies below 50 m depth. Reflectors in the permafrost are from features that may include strata of differing grain size, sedimentary structure, or higher ice volume.

Transect 93-11 is 1600 m long, trends west to east, and passes just north of the landfill (see Fig. 6). Bedrock is a prominent reflector at depths of 20 to 30 m along nearly its entire length (Fig. 14). Only where signals are attenuated by water, such as locations with standing water or where deeply thawed sediments are near the surface, is this reflector absent. A subpermafrost aquifer is

present at some locales in the center of the profile, but it is apparently absent elsewhere.

#### Permafrost distribution

Our data show that the extent and thickness of permafrost vary greatly across the north-central cantonment area (Fig. 15). Seasonal freezing depths often exceed 3.0 m, while active layers may have seasonal thaw depths as little as 0.3 m. The depth of thaw apparently varies with drainage, vegetative cover, organic content of the sediments, and other factors (e.g., Hopkins et al. 1955, Péwé 1958, Ferrians and Hobson 1973). Deeply thawed materials, ranging from several meters to over 20 m in depth, commonly exist beneath disturbed areas, such as roads, and in former swales and channels (Fig. 15a). Deep thaw may also be expected beneath the landfill; borehole and GPR



a. Elevations of the top of permafrost from borehole records. Active layer thickness (more than 2 m deep) was also measured in August and September 1994 using a hand-driven steel probe.

Figure 15. Elevation of permafrost (U.S. Army Engineer District, Alaska, unpublished borehole logs). Bold numbers show wells drilled between 1 March 1994 and 30 June 1995. All others were drilled between 1 July and 1 December 1995.



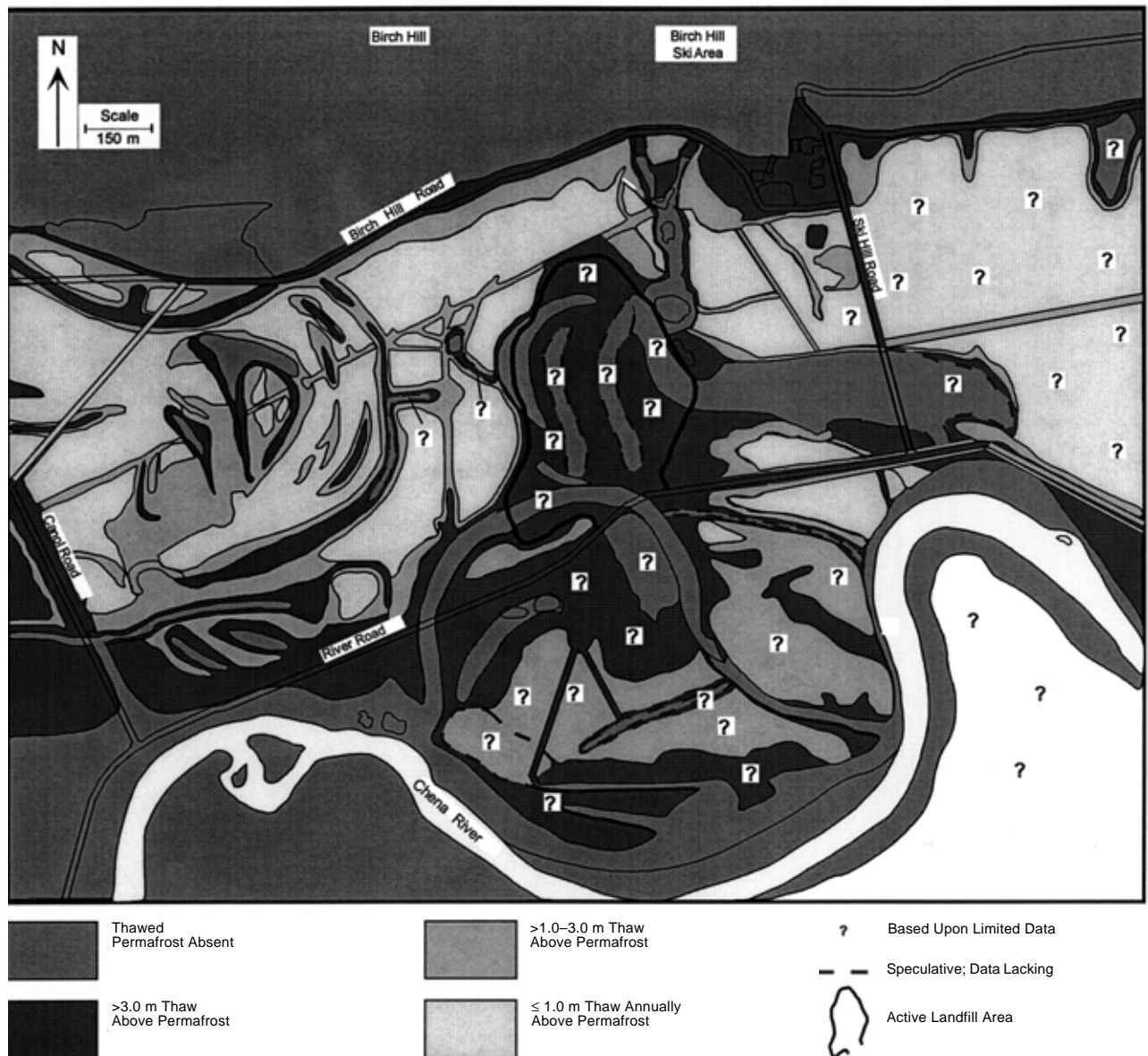
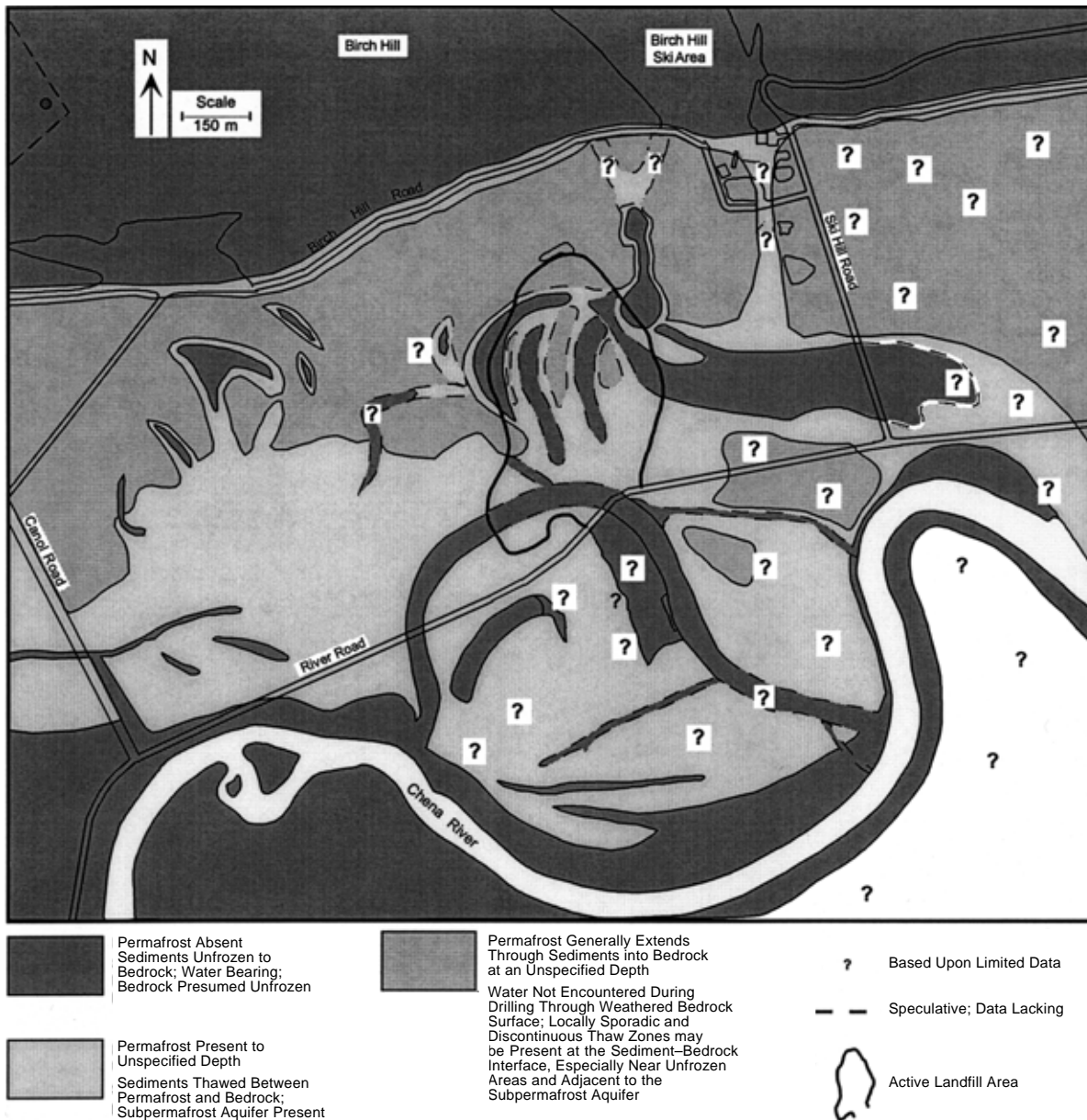


Figure 16. Characteristic depths of thaw and the locations of unfrozen zones in the north-central area of the cantonment. Deep thaw zones above permafrost are commonly associated with disturbed terrain, while thin active layers characterize undisturbed terrain covered by vegetation. Areas with shallow active layers (less than 1.0 m) severely reduce ground water movement and result in divergent flow patterns. Unfrozen materials are generally in former channels and sloughs, as is evident by their map patterns. Permafrost and aquifer distribution below the landfill are based upon interpretations from historical aerial photographs using data from the terrain surrounding the site. Very few subsurface data exist east of Ski Hill Road. Note that small, shallow drainages are not identified, thaw depths may exceed the cited depths by two to three times, and the unfrozen zones have peripheral shallow and deep thaw zones that may be omitted for clarity. This map was created on unrectified aerial photographs taken on 20 May 1993.

increase sharply at about several hundred meters distance south of Birch Hill. Comparing the depth to bedrock (Fig. 18) with the depth to the bottom of permafrost (Fig. 15b) shows that unfrozen sediments from a few meters to over 25 m thick underlie perennially frozen materials over much of the

area. The depth to bedrock presumably continues to increase south of River Road but there are only a limited number of borehole measurements in this area.

Contouring of the depth to bedrock data tells us that sediments bury gullies or valleys that were



*Figure 17. Locations of areas frozen into bedrock, areas where permafrost is underlain by unfrozen sediments that overlie unfrozen bedrock, and unfrozen zones that penetrate the permafrost completely. Unfrozen zones generally are within former sloughs or channels, and permit communication between supra- and subpermafrost aquifers. The large areas of materials that are frozen into bedrock constrain ground water interactions among aquifers in Birch Hill and the Tanana Valley alluvium; they also modify flow patterns by their impermeability. A bedrock aquifer in Birch Hill may communicate through fractures, such as the thaw zone associated with Finnegan's Pond (upper right of landfill). Subpermafrost aquifers communicate with the large unfrozen area of alluvium beneath and south of the Chena River. Data are practically nonexistent, however, on permafrost and bedrock depths east of Ski Hill Road, an area critical to understanding ground water conditions north of the Chena River. The mapping of unfrozen zones and aquifers beneath the landfill is based on our interpretations of subsurface conditions surrounding it, which were obtained from historical aerial photographs.*

formerly cut deep into the bedrock surface (Fig. 19). Above the valley surfaces, unconsolidated sediments that fill these bedrock valleys are thicker than in the surrounding area and are likely a focal zone for ground water flow where the sediment is unfrozen (e.g., Lawson et al. 1996).

Interpretive cross sections (Fig. 20) show the high variability of the subsurface distribution of permafrost, as well as the irregularity of unfrozen zones in and above the permafrost in relation to the bedrock surface. The abrupt and sometimes deep interfaces between unfrozen sediments and

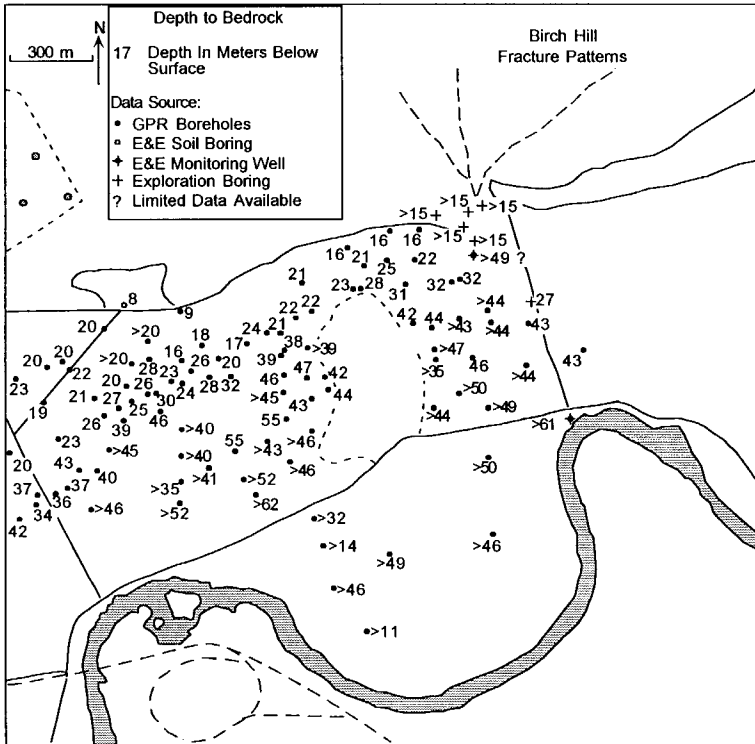


Figure 18. Depth to bedrock from boreholes drilled north of the Chena River. Maximum depth of drilling to bedrock was limited to 1 to 2 m or less. Values with "greater than" symbols are the depth penetrated by drilling without encountering bedrock.

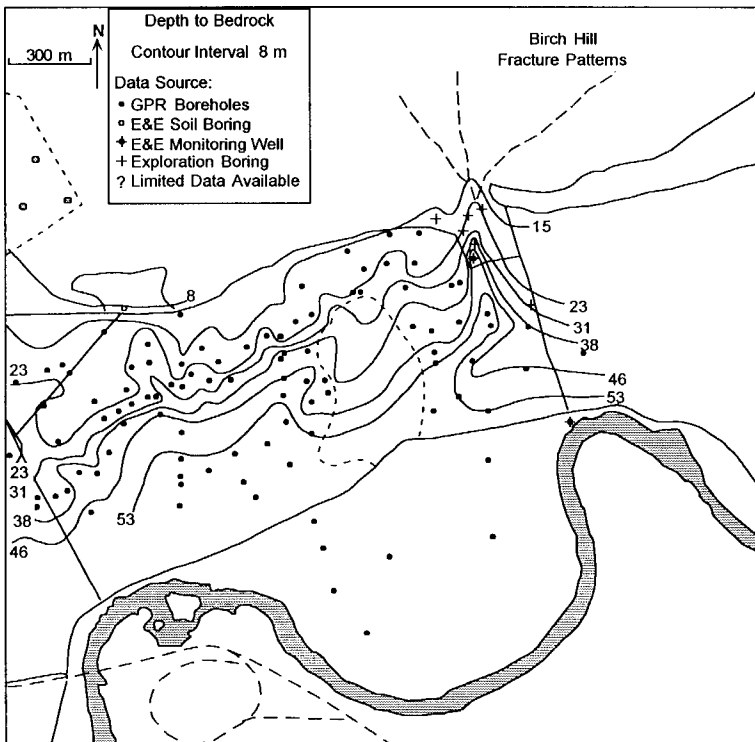
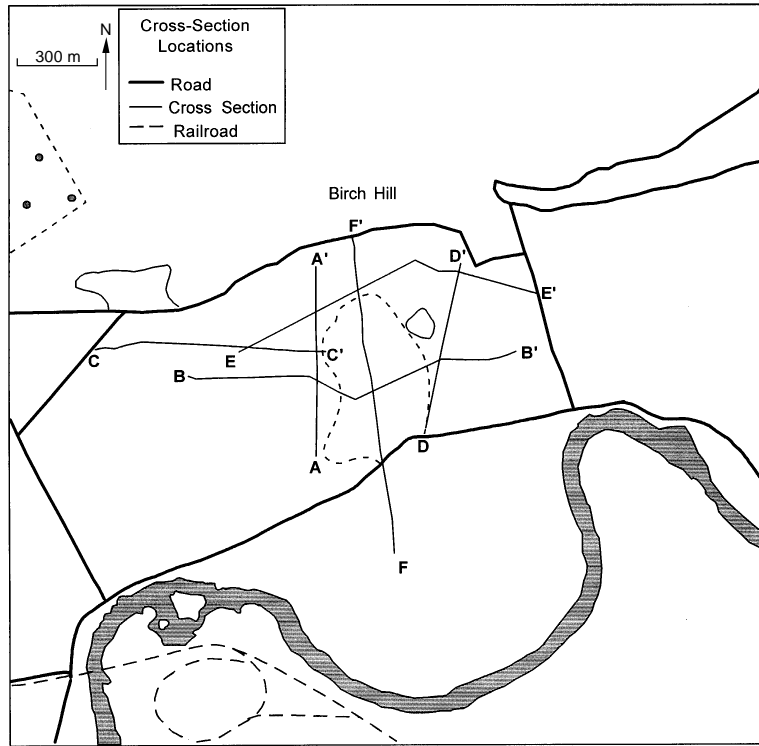
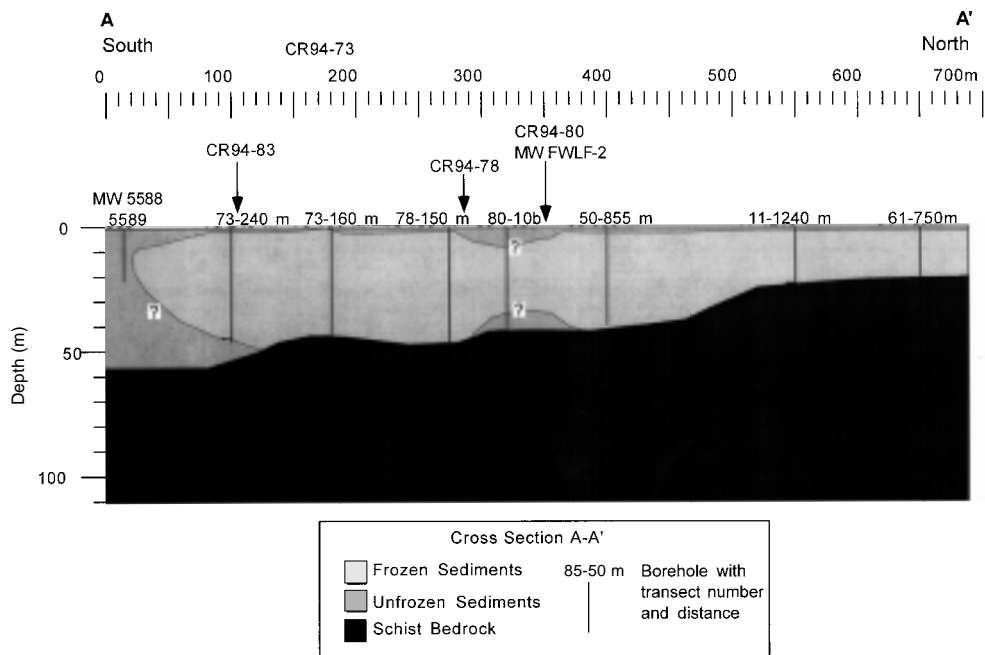


Figure 19. Buried bedrock surface topography based upon borehole data. The deep, trench-like valley just east and northeast of the landfill appears related to gullies in the ski slope on Birch Hill. These features may be associated with a fracture zone within the bedrock. Preferential flow of ground water below the permafrost within materials filling this buried valley may be an important factor locally controlling subpermafrost ground water movement. A smaller buried gully cut into the bedrock surface on the western edge may also be important in this regard.

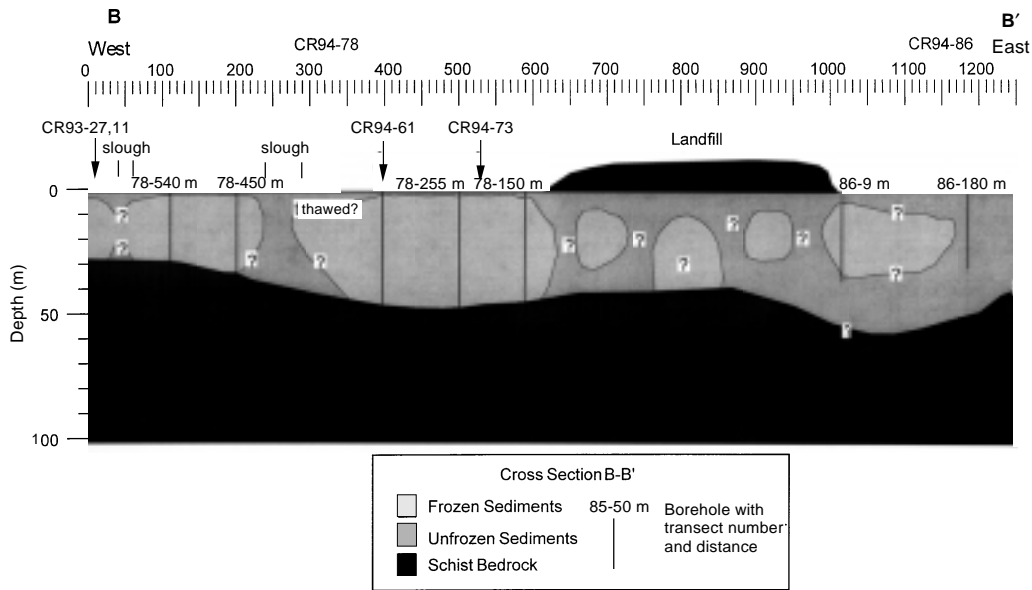


a. Locations

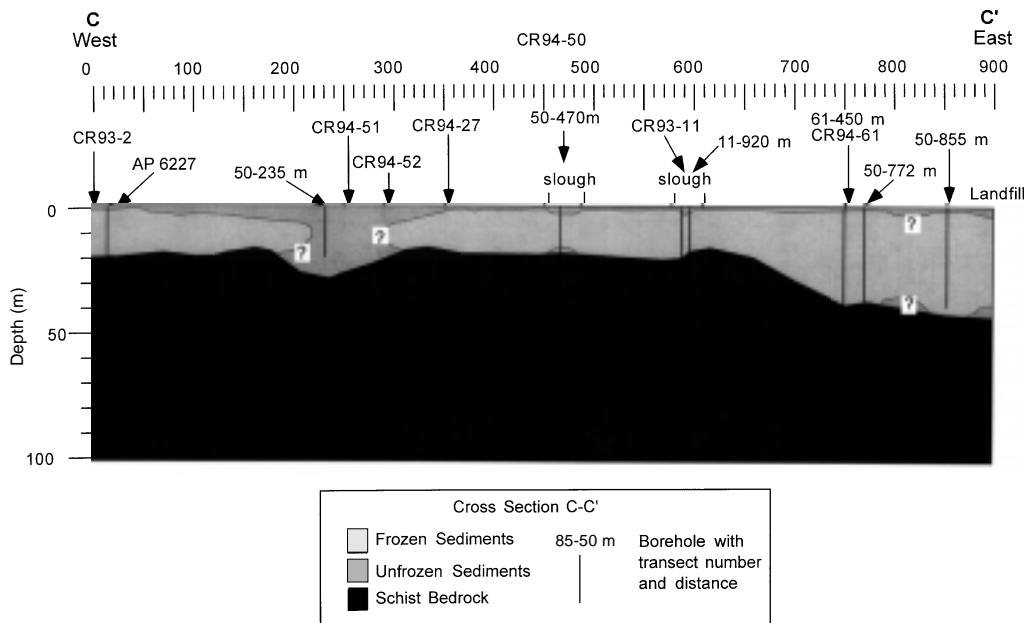


b. North-south cross section A-A'. Data from GPR transect 94-73 are included. The land-fill lies east of this cross section.

Figure 20. Six interpretive cross sections illustrating subsurface distribution of discontinuous permafrost within the north-central cantonment area. GPR transect data used in each cross section are indicated.



c. B-B'. Includes data from GPR transects 94-78 and 94-86.



d. C-C'. Located west of the landfill and includes transect CR94-50 data.

Figure 20 (cont'd).

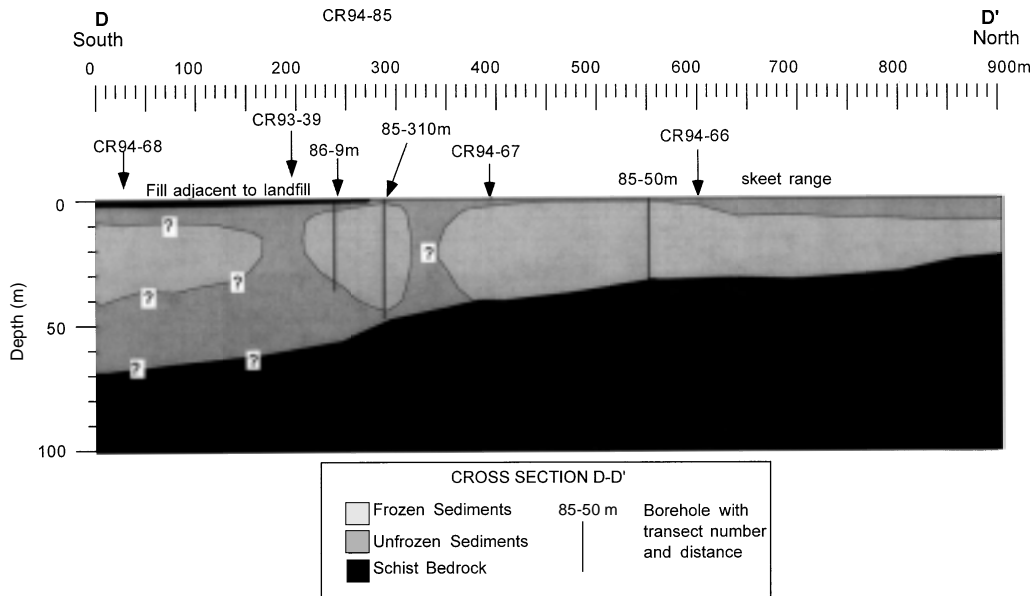
permafrost can control ground water movement, recharge, and discharge between different aquifers (e.g., Fig. 20d, e, f). Flow can even become channeled between frozen materials (e.g., Fig. 20c).

### Ground water aquifers

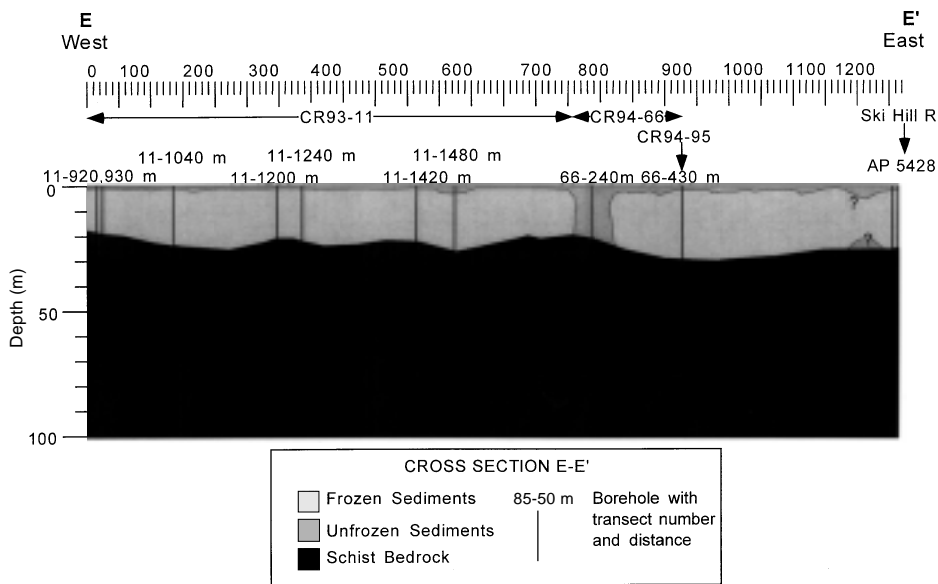
Unfrozen sediments around and inside the permafrost are potential locations of aquifers. In the north-central cantonment area, zones that are unfrozen at the surface and extend uninterrupted

into the bedrock are critical links between aquifers. Suprapermafrost aquifers generally exist in abandoned channels and, in some cases, beneath roads and other disturbed areas, such as the area around the landfill (Fig. 16). Deeply frozen areas restrict ground water movement and may isolate aquifers, while complicating flow patterns (Fig. 17).

Deeply frozen materials are extensive along the base of Birch Hill, where bedrock is relatively shal-



e. D-D'. Located east of the landfill and includes data from GPR transect 94-85.



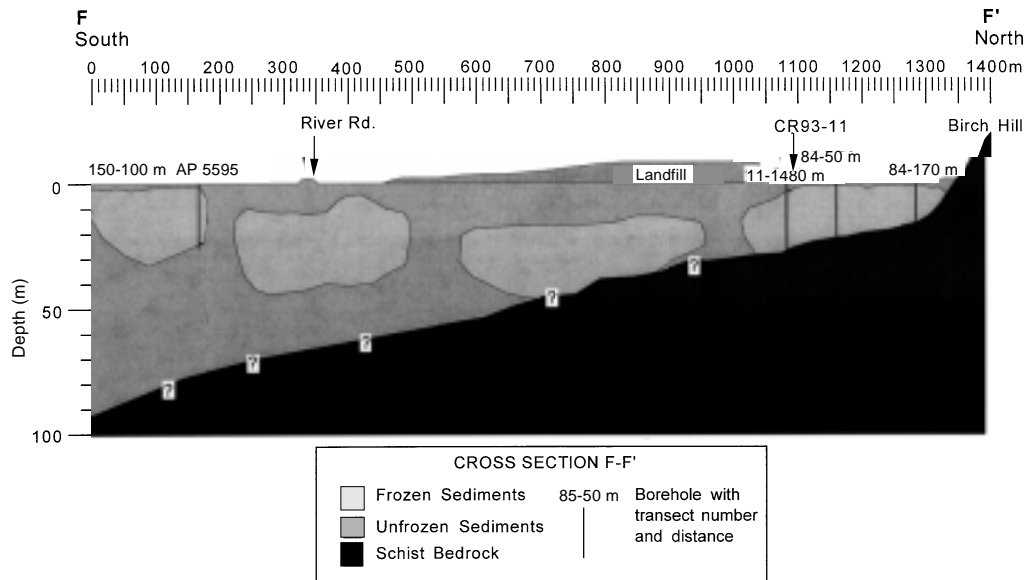
f. West-east cross section E-E'. Includes data from GPR transects 94-11 and 94-66 in the northern portion of the site.

Figure 20 (cont'd). Six interpretive cross sections illustrating subsurface distribution of discontinuous permafrost within the north-central cantonment area. GPR transect data used in each cross section are indicated.

low and both the sediments and bedrock below them are frozen. Because of its lateral extent, the permanently frozen area forms a nearly impenetrable barrier to ground water migration.

Only in narrow, north-south trending thaw zones does water move through this area; these thaw zones can strongly affect ground water

movement wherever they intercept the sub-permafrost aquifer on the south. One of these extends from Finnegan's Pond on the northeast corner of the landfill to the base of Birch Hill (Fig. 16). Two other smaller ponds lie within this thaw zone and appear to be where the ground water table comes to the surface. Hopkins et al. (1955)



*g. North-south cross section F-F' through the center of the landfill.*

*Figure 20 (cont'd).*

concluded that such unfrozen zones are developed and maintained by artesian flow. In this case, an unfrozen fracture zone in the bedrock of Birch Hill may be the artesian source. Cederstrom (1963) reported previously that individual fractures and fracture zones are the source of water in many, if not most, wells drilled into the schistose bedrock in the Fairbanks region.

Similarly, a buried bedrock valley that trends mainly north-northeast to south-southwest extends beneath the frozen sediments at the base of the ski slope on Birch Hill (Fig. 15 and 19). It appears to be a continuation of a prominent gully on the hillside and probably is a subsurface expression of a bedrock fracture zone. Data are insufficient to determine, however, if indeed water is flowing within this valley off of Birch Hill.

Near-surface aquifers in unfrozen zones that are laterally confined by permafrost commonly have flow parallel to the impermeable permafrost boundaries. Flow in the subpermafrost aquifers may cause deviations from this trend until, at depth, the near-surface flow parallels that of the lower aquifer. The subpermafrost aquifer can also recharge or discharge through these unfrozen materials. In general, the subpermafrost aquifer is artesian, with flow approximately following the regional trend (e.g., Lawson et al. 1996), whereas the local hydraulic gradient, alluvial stratigraphy, and permafrost configuration can create flow patterns in near-surface sediments confined by

permafrost that are significantly different from subpermafrost flow patterns.

The thermal disturbance created by the landfill over the last 40 or more years has increased the depth to the top of permafrost. The deep thaw beneath the landfill is hydrologically important because it could support a near-surface supra-permafrost aquifer. We speculate that any zones of thin permafrost that existed 40 years ago may now be completely thawed, while any thicker permafrost may now have a deep layer of thawed sediments above it.

The landfill is also situated on top of at least one, and possibly three, north-south linear zones of unfrozen channel deposits (Fig. 4). Drilling revealed that unfrozen sediments extend to bedrock (about 43 m depth) in one of these north-south zones where it exits from beneath the west side of the landfill (Fig. 19).

We suspect that the suprapermafrost aquifer is connected to the subpermafrost aquifer via the unfrozen channel deposits (Fig. 17 and 20). Leachate from the landfill is likely to migrate towards such deeply thawed zones where it could be transported into the subpermafrost aquifer. Whether leachate actually migrates through the fill materials is unknown, however.

#### **Site-specific seepage data**

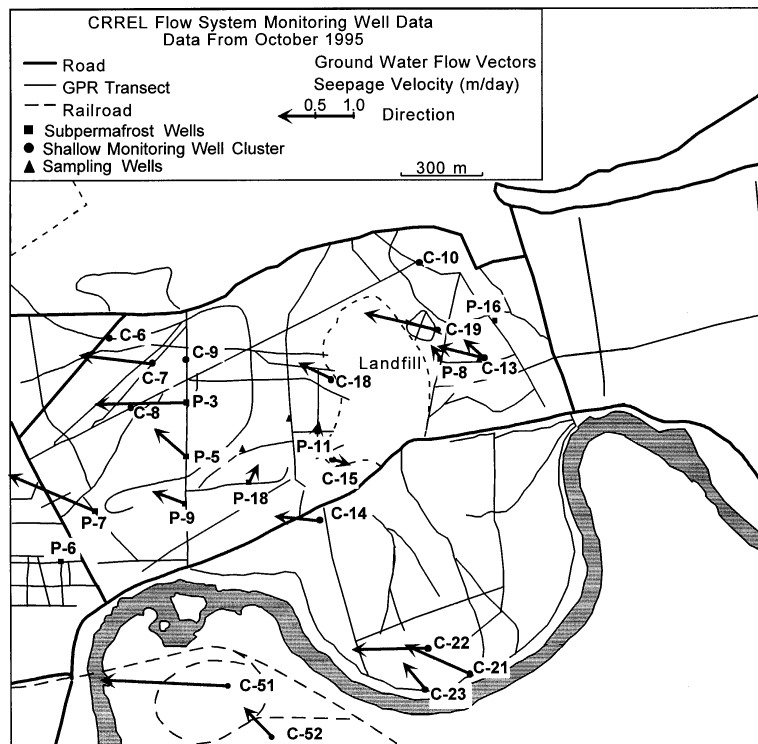
Site-specific ground water data show both seasonal and annual variability in water levels, flow

velocity, and, to a lesser extent, flow direction (App. A). The period of record is, however, too short to determine how representative these data are of long-term trends in flow.

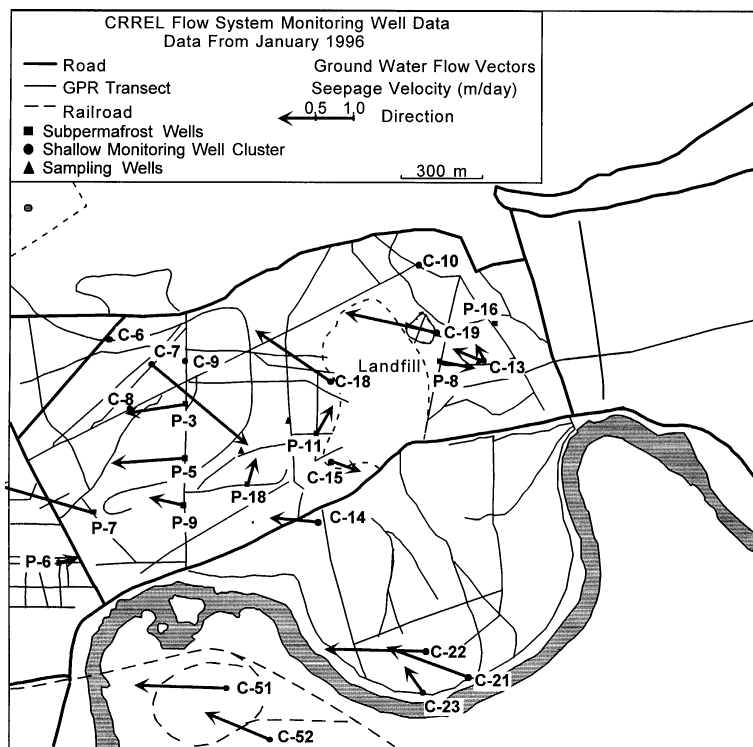
Diurnal and average weekly values are reasonably consistent in any given well; however, flow velocity may vary at depth, reflecting changes in stratigraphy that influence the hydraulic conductivity. Seepage velocities typically range from 0.3 to 1 m/day, although rates of less than 0.15 and greater than 1.5 m/day were recorded. These higher values likely reflect local differences in gradient, hydraulic conductivity, or permafrost confinement.

The velocity of near-surface flow varies inversely with seasonal water level fluctuations. Velocities generally increase as water levels decline during the fall and winter, but decrease in the spring and summer (App. A). Paino (1997) suggested that higher velocities during winter may reflect an increased confinement or changes in flow paths and water flux caused by seasonal freezing of near-surface sediments. Frost commonly extends 4 m or more in depth each winter in this region and, as a result, can completely freeze thin active layers. This can isolate parts of suprapermafrost aquifers and reduce the overall volume of a near-surface aquifer.

Flow directions in near-surface (10-m) and, to a lesser degree, deeper (20-m) wells show the effects of permafrost. Wells located in unfrozen materials that are bounded on the sides by frozen sediments tell us that flow diverges from the overall northwesterly flow pattern north of the Chena River (App. A). Flow patterns also reflect seasonal changes in water levels. With thawing of seasonally frozen ground, formerly isolated aquifers may open, permitting communication, and significantly changing flow direction (Paino 1997).

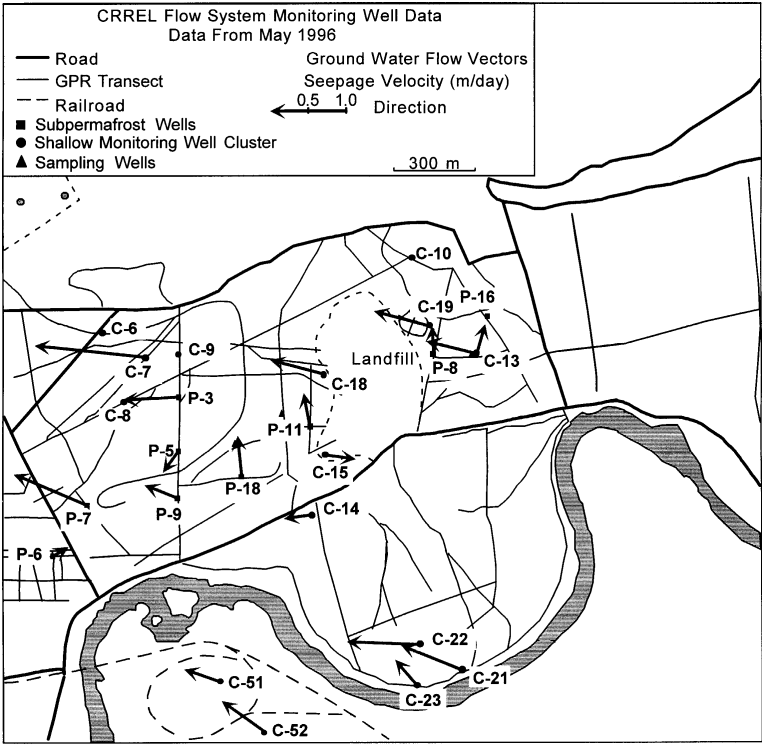


a. October 1995.

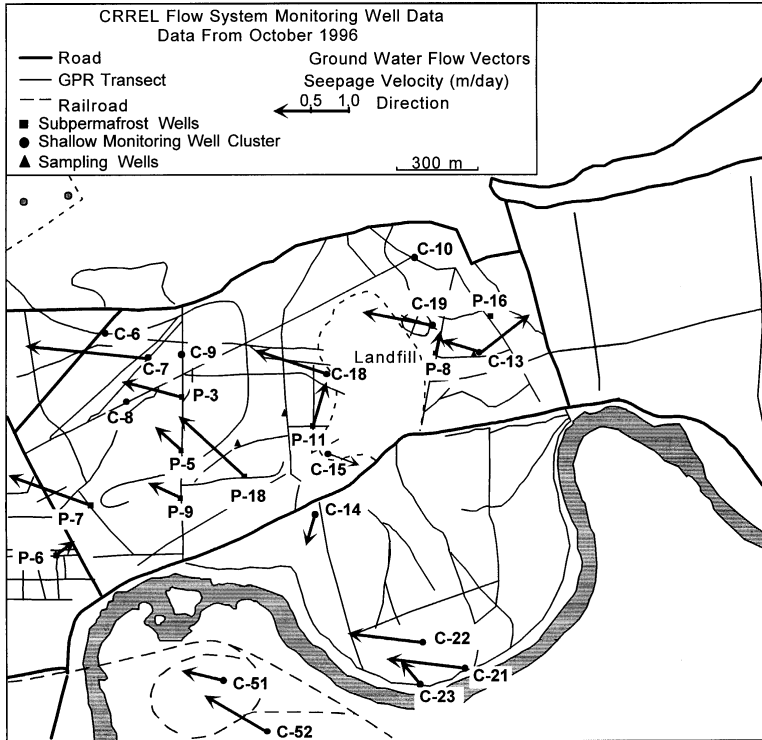


b. January 1996.

Figure 21. Averaged flow vectors for subpermafrost and deep (30-m) wells, shown with respect to permafrost distribution.



c. May 1996.



d. October 1996.

Figure 21 (cont'd).

Flow directions at 30 m below the surface are generally consistent from well to well, except where permafrost is in contact with bedrock over a large area (Fig. 21). In that situation, flow is diverted around deep permafrost and may vary by over 90° from the usual west to northwest trend. This is exemplified by a northeasterly flow of water west of a deep (more than 85 m) permafrost “plug” that is southeast of the landfill along the Chena River (Fig. 17 and 21).

A strong seasonal change in direction from the prevailing west-northwest flow pattern is evident north of River Road (Fig. 21). Lower velocities and higher water levels during the late spring and summer are associated with a more northerly flow, but shifts in flow direction to the west during fall to winter correlate with a lower water table. The direction probably changes in response to the large flux of water from the Tanana River during summer (e.g., Cedersstrom 1963, Williams 1970). Late in the year, the flux of water from the Tanana River into the alluvial aquifer declines and local factors may be controlling flow.

**HYDROGEOLOGICAL CONCEPTS**

Ground water in the north-central cantonment flows in patterns that reflect the impermeable confining conditions imposed by permafrost, the topography, and the relief of the buried bedrock surface. For example, flow directions vary from the prevailing west to northwest regional trend where permafrost extends into bedrock along the base of Birch Hill and in the area southeast of the landfill. Former channels and sloughs are unfrozen, and narrow trails, roads, and other disturbed locations are deeply thawed above permafrost, as are places with a thin (less than

2 m) active layer, particularly south of Birch Hill and east of Ski Hill Road. Unfrozen materials below the permafrost increase in thickness to the south as the depth to bedrock increases and permafrost thins. The subpermafrost aquifer increases in volume to the south as well and is more connected with the regional Tanana Valley aquifer.

Although we have limited data on ground water conditions north of the Chena River, the numerous physical constraints on aquifers and ground water movement limit the potential avenues of flow. Two “external” sources of ground water may determine the direction and velocity of flow in this area. An aquifer in Birch Hill, which

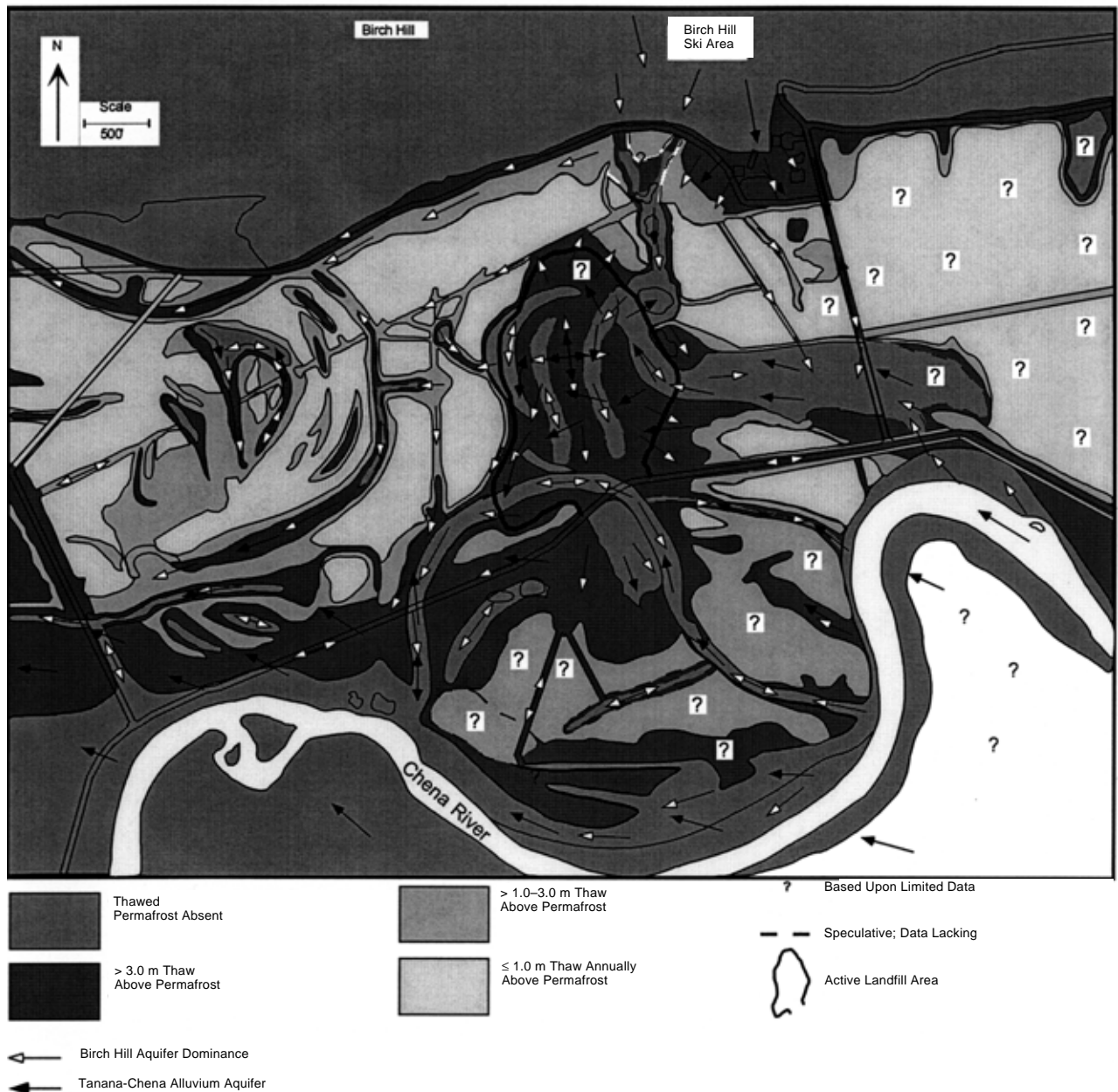


**Figure 22. Near-surface and suprapermafrost flow paths.** Depicted are ground water flow patterns possible if they are controlled by an aquifer in Birch Hill or if they result from the dominance of the subregional aquifer in the Tanana-Chena alluvium. Ground water flow is restricted to deeply thawed or unfrozen materials above bedrock; permafrost distribution and dimension are critical controls in this regard. Near-surface flow could result in off-site migration of contaminants in extremely divergent directions.

is affected by precipitation and spring runoff, may produce local differences in hydraulic gradient and therefore direction of flow north of the Chena River (Fig. 22). The subregional aquifer of the Tanana River Valley, however, is probably responsible for the prevailing hydraulic gradient and overall flow pattern, particularly in the subpermafrost aquifer. Because the flux from both aquifers varies with the season, flow direction and velocity in the subpermafrost and suprapermfrost aquifers also vary with the seasons. In the following sections, we define hypothetical ground water flow patterns, assuming that either an aquifer in Birch Hill or the Tanana Valley determines hydraulic gradients in the north-central cantonment area.

### **Suprapermfrost aquifers and near-surface flow patterns**

Figure 22 shows the potential pathways for near-surface ground water movement and the possible interactions with permafrost. The near-surface ground water system is located above the permafrost, where the seasonal thaw is sufficient to develop a mostly continuous suprapermfrost aquifer. Where the depth to permafrost is less than 1.0 m, an aquifer probably does not develop. In contrast, there is likely a significant suprapermfrost aquifer beneath the landfill and in other deeply thawed areas beneath surface disturbances. These aquifers communicate with deeper aquifers through unfrozen and deeply thawed areas of former swales and channels. Near-surface ground water may flow beneath River and Ski Hill Roads, for example, and some of the older trails that have been in existence for over 40 years (Fig. 5). Many of these suprapermfrost aquifers intercept the unfrozen zone adjacent to the Chena River.

The direction of near-surface and suprapermfrost flow depends upon whether 1) surface water migrates through the landfill and recharges the supra- and subpermafrost aquifers near it, 2) Birch Hill runoff from snowmelt or precipitation is high enough to create a southward-directed gradient, or 3) the flux of water (and hydraulic gradient) in the Tanana Valley alluvial aquifer is higher than more local sources. In addition, water tables fluctuate as the stage of the Chena River fluctuates; this will locally affect flow patterns and movement of water through the suprapermfrost aquifers. The interplay and feedback of these factors result in a strong seasonal variability to ground water movement.

### **Subpermafrost and deep flow patterns**

The hydraulic gradient of the subpermafrost aquifer may be determined by either the subregional aquifer of the Tanana Valley or by more local aquifers, such as in Birch Hill (Fig. 23). A west to northwest flow will prevail if gradients are controlled by the Tanana system, whereas control by the Birch Hill aquifer will create a southerly component. In both instances, the thickness, configuration, and extent of permafrost above the aquifer will constrain flow, while it may recharge or discharge into unfrozen zones. If an aquifer of sufficient potential exists in the bedrock, it too could modify or locally control flow in the subpermafrost aquifer. The extent of a bedrock aquifer is limited, however, as it is restricted to fracture zones (Cederstrom 1963).

### **Discussion**

Data from in-situ sensors in the north-central cantonment area support the concept of an aquifer in Birch Hill that influences flow direction and velocity seasonally, but they also suggest that the overall pattern of flow is subregionally controlled. The subregional aquifer's gradient and flux vary seasonally as well and, therefore, it interacts with the more local influx of ground water, particularly from Birch Hill. For example, the lower water table and hydraulic gradient of the Tanana Valley aquifer in fall and winter result in a more westerly flow than during early and late summer peaks in water level and flux, when a northerly flow dominates (Fig. 22). The shift in flow vectors from west to north through late spring is evident in the measurements across the area (Fig. 23, Lawson et al. 1996).

Whenever the flux of water through fracture and thaw zones originating in Birch Hill is sufficiently large (this is quantitatively unknown), the distribution of permafrost dictates that the supra- and subpermafrost aquifers will have a southerly flow. The resultant vector of flow of the subpermafrost aquifer in the area will depend largely on the subregional flux and gradient. This scenario of interacting aquifers is consistent with the vectors for the deeper (more than 30 m) flow measurements (Lawson et al. 1997, in prep., App. A).

Seasonally, there are periods of little or no flow in isolated, unfrozen deposits surrounded by permafrost and in some deeply thawed zones above the permafrost. Just south of Birch Hill, for example, potential water sources for unfrozen zones are limited to surface infiltration and adja-

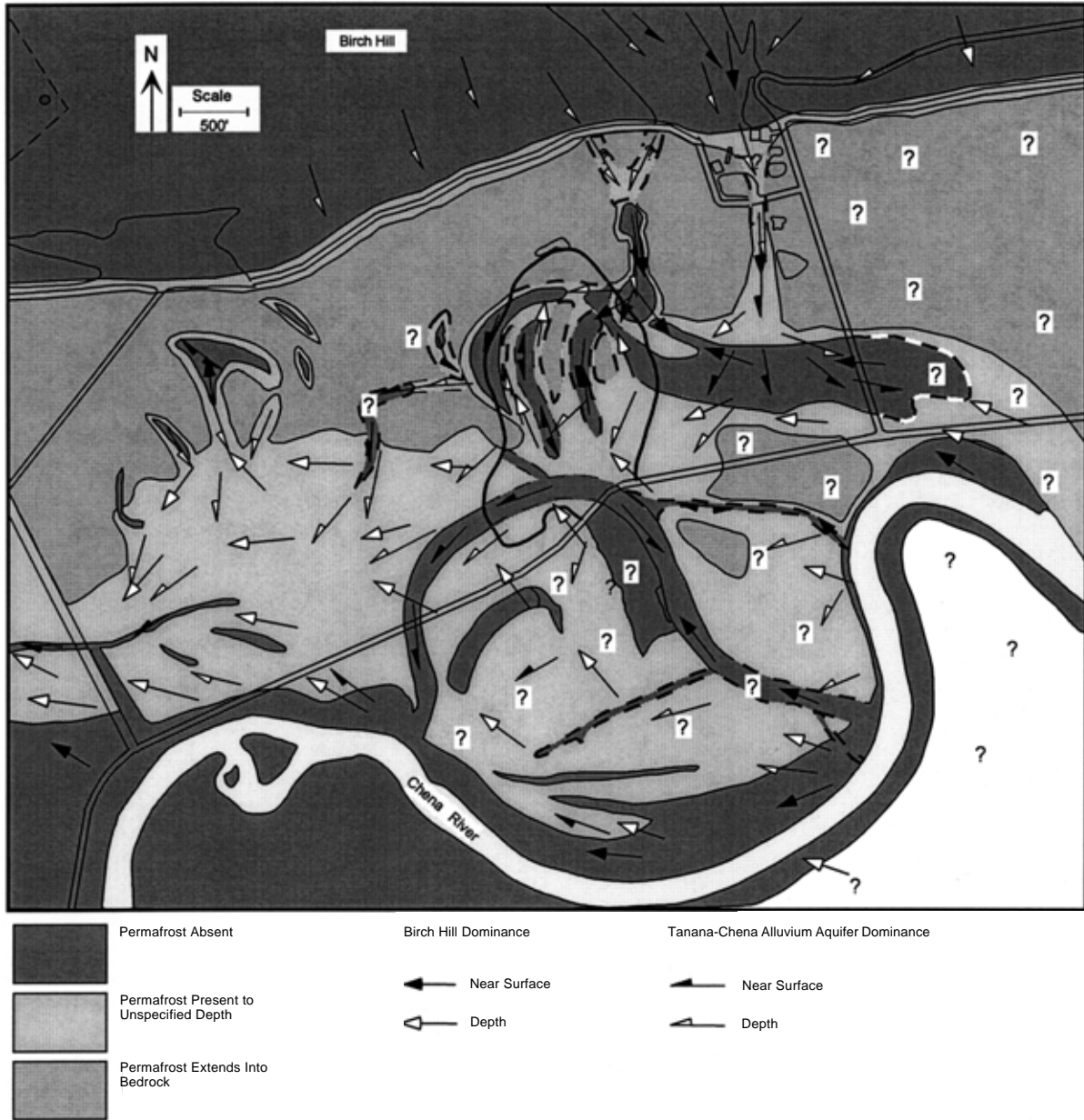


Figure 23. Hydrogeological concepts of deep aquifer flow paths depicted for two scenarios: where Birch Hill dominates and where a subregional aquifer dominates. We assumed ground water flow within the bedrock not to be significant. The direction and velocity of flow for both scenarios may differ significantly in the subpermafrost aquifer because of thaw zones that intercept it. The effect of the large area of sediments frozen to bedrock is evident for both scenarios. The prevailing flow below permafrost, regardless of source, may result in off-site migration of soluble contaminants.

cent suprapermafrost aquifers. An aquifer surrounded on four sides by permafrost would have a water table rising or falling in concert with recharge or discharge from the subpermafrost aquifer. Seepage velocity and direction would, therefore, be a response to the subpermafrost gradient. A strong gradient in the subpermafrost

aquifer south of the Chena River as opposed to one in Birch Hill will generate a more northerly component than when there is less difference in magnitude. Seepage measurements from 1995 to early 1997 demonstrate this to be the case in the area northwest of the landfill (Lawson et al. 1997, in prep.).

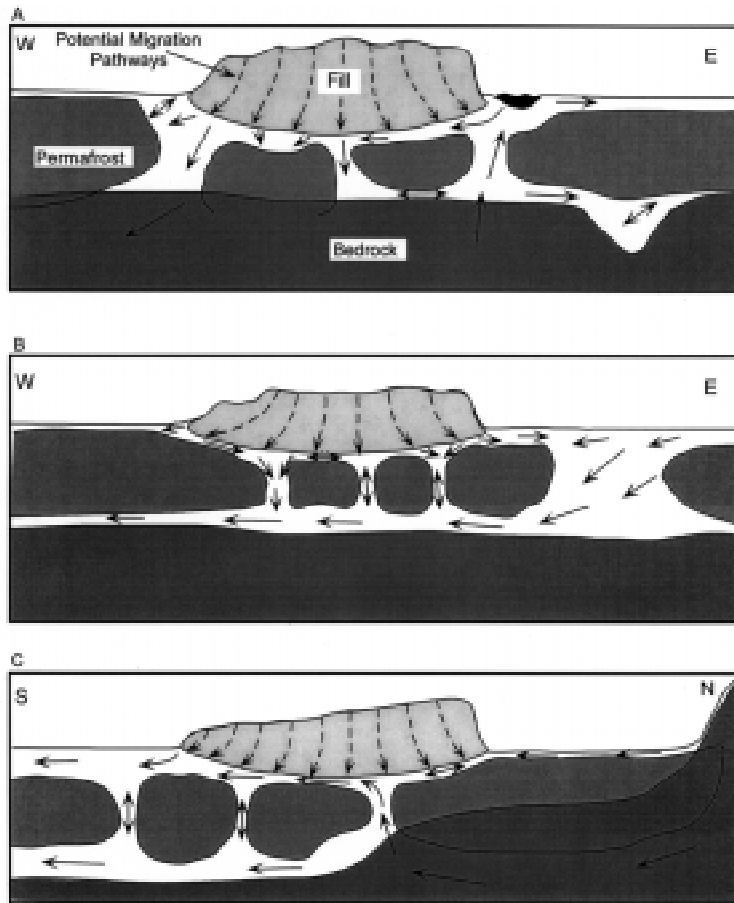


Figure 24. Idealized ground water flow patterns within and beneath the landfill. Dashed arrows show potential migration pathways if contaminants leach from the fill material. Diagram A shows the general conditions along an east to west cross section in the northern half of the fill area. Diagram B illustrates an east to west cross section in the southern half of the fill area. Diagram C gives a north to south cross section through the middle of the fill area.

The movement of ground water and the migration of contaminants beneath the landfill (Fig. 24) depend on numerous factors, some of which are as follows:

- The volume of water that seeps through the fill material, leaching contaminants in the process.
- The volume of water and leachate in surface runoff that enters laterally into the landfill through thawed materials adjacent to it.
- The hydraulic gradient and flux of the sub-regional aquifer.
- The flux of water from the Birch Hill aquifer into near-surface and subpermafrost aquifers.

In addition, the extent and depth of permafrost

and aquifers east of Ski Hill Road are unknown and their role in flow beneath the landfill is undefined.

Surface water fills low areas where the active layer is shallow (less than 1.0 m), and sometimes creates marshes. This water probably contributes little to the ground water in either the suprapermafrost or subpermafrost aquifers. In addition, those areas with a thin active layer inhibit communication between suprapermafrost aquifers and near-surface ground water movement. Directions of flow in such areas may, therefore, differ from the deeper, more continuous aquifers. Near-surface flow is mainly limited to deeply thawed areas beneath roads, trails, artificial drainage ditches, and former swales or channels. Near-surface flow is only connected to the subpermafrost aquifer where permafrost is absent, and it is seasonally controlled by depths of freezing and thawing. The combined effects of permafrost frozen to bedrock and a shallow active layer severely restrict lateral ground water movement and recharge of the subpermafrost or bedrock aquifers by suprapermafrost waters.

Water may be flowing through discrete horizontal or vertical thawed zones in the permafrost, but we have few data concerning this. Flow through taliks will probably be highly

variable in direction and rate, depending upon the size of the thaw zone, water sources, and local hydraulic gradient. Ambiguous, intense reflections on GPR records of the interface between frozen sediments and frozen bedrock suggest that water may also be present in isolated “conduits” at this interface. The number and dimensions of these interface taliks appear limited, but they could result in anomalous, but highly localized, deviations in flow.

## CONCLUSION

Hydrogeological conditions in the north-central cantonment area are controlled primarily by the distribution and geometry of discontinuous permafrost, stratigraphic variability, and inter-

actions among multiple aquifers. Site-specific conditions are extremely complex because of the diverse relationships among deeply thawed and unfrozen zones, and the subpermafrost aquifer. Deeply frozen materials interrupt the continuity of the subpermafrost aquifer, while a thin active layer interrupts the continuity of suprapermafrost aquifers. Fracture zones in bedrock are possible sources of ground water entering the subpermafrost aquifer south of Birch Hill. With sufficient flux, thaw zones that penetrate from the bedrock through the permafrost into the suprapermafrost aquifer can be created. Ground water flow rates and directions are affected seasonally by the competitive interaction of aquifers in the bedrock of Birch Hill and those in the alluvial deposits of the Chena and Tanana basins, but we do not have enough data to define fully this interaction.

Measurements with ground water flow sensors below permafrost for the period of August 1995 through July 1997 indicate that the prevailing flow direction is northwest by westerly. In unfrozen materials laterally bounded by permafrost, flow directions vary with depth, as well as from site to site. Flow in suprapermafrost aquifers is extremely variable in direction seasonally as well as from location to location.

Potential pathways through which contaminants might migrate from the landfill site include unfrozen channel sediments that existed before operations began and the thaw bulb that was created by those operations. If leachate is migrating through the landfill, it could enter the subpermafrost aquifer through these unfrozen zones. Run-off from the landfill surface may also flow into near-surface aquifers abutting the site, including those beneath trails, roads, and drainage ditches. Both flow paths could ultimately move soluble contaminants into the subregional aquifer west or southwest of the site, depending upon the local gradient.

#### LITERATURE CITED

- Abele, G., J. Brown, and M.C. Brewer** (1984) Long-term effects of off-road vehicle traffic on tundra terrain. *Journal of Terramechanics*, **21**: 283–294.
- Arcone, S.A., D.E. Lawson, A.J. Delaney, J.C. Strasser, and J.D. Strasser** (in press) Ground-penetrating radar reflection profiling of ground water and bedrock in an area of discontinuous permafrost. *Geophysics*.
- Cederstrom, D.J.** (1963) Ground water resources of the Fairbanks area, Alaska. U.S. Geological Survey Water-Supply Paper, 1590.
- Chapman, H.T., and A.E. Robinson** (1962) A thermal flowmeter for measuring velocity of flow in a well. U.S. Geological Survey Water-Supply Paper 1544-E.
- Ecology and Environment** (1994) Remedial investigations report, Operable Unit 4, Fort Wainwright, Alaska, Volumes 1 and 2; November. Prepared for U.S. Army Engineer District, Alaska, and U.S. Army Alaska, Ft. Richardson, Alaska.
- Ferriars, O.J., Jr.** (1965) Permafrost map of Alaska. U.S. Geological Survey Miscellaneous Geological Investigations Map I-445.
- Ferriars, O.J., Jr., and G.D. Hobson** (1973) Mapping and predicting permafrost in North America. A review, 1963–1973. In *Permafrost: The North American Contribution to the 2nd International Conference on Permafrost, Yakutsk, 13–28 July*. Washington, D.C.: National Academy of Sciences, p. 479–498.
- Hamilton, T.D.** (1994) Late Cenozoic glaciation of Alaska. In *The Geology of Alaska* (G. Plafker and H.C. Berg, Ed.), Geological Society of America, p. 813–844.
- Hess, A.E.** (1982) A heat-pulse flowmeter for measuring low velocities in boreholes. U.S. Geological Survey Open-File Report, 82-699.
- Hopkins, D.M., T.N.V. Karlstrom, and others** (1955) Permafrost and ground water in Alaska. U.S. Geological Survey Professional Paper 264-F.
- King, P.B.** (1969) Tectonic map of North America (1:5,000,000). U.S. Geological Survey Map.
- Lawson, D.E.** (1986) Response of permafrost terrain to disturbance: A synthesis of observations from northern Alaska. *Arctic and Alpine Research*, **18**: 1–17.
- Lawson, D.E., J.C. Strasser, and J.M. Davi** (1994) Geological and geophysical investigations of the hydrogeology of Operable Unit 3. Interim Draft Report prepared for the U.S. Army 6th ID and U.S. Army Engineer District, Alaska, by the USA Cold Regions Research and Engineering Laboratory, Hanover, New Hampshire.
- Lawson, D.E., J.C. Strasser, J.D. Strasser, S.A. Arcone, A.J. Delaney, and C.R. Williams** (1996) Geological and geophysical investigations of the hydrogeology of Fort Wainwright, Alaska. Part 1. Canol Road Area. USA Cold Regions Research and Engineering Laboratory, CRREL Report 96-4.
- Paino, C.** (1997) An investigation of the hydrogeologic environment, Fort Wainwright, Fair-

banks, Alaska. Master's Thesis, Lehigh University, Bethlehem, Pennsylvania.

**Mackay, J.R.** (1970) Disturbances to the tundra and forest tundra environment of the western Arctic. *Canadian Geotechnical Journal*, 7: 420–432.

**Péwé, T.L.** (1958) Geologic map of the Fairbanks D-2 Quadrangle, Alaska. U.S. Geological Survey Geologic Quadrangle Map GQ-110.

**Péwé, T.L., J.W. Bell, R.B. Forbes, and F.R. Weber** (1976) Geologic map of the Fairbanks D-2 SE Quadrangle, Alaska. U.S. Geological Survey Miscellaneous Investigations Series Map I-942.

**Strasser, J.D., D.E. Lawson, C.F. Paino, C.R. Williams, and T.J. Hall** (1997) Ground water flow measurements on Fort Wainwright, Alaska, for period August 1995 through December 1996. A preliminary data report, Interim Draft Report. Prepared for U.S. Army Alaska, Directorate of Public Works.

**Strasser, J.D., D.E. Lawson, C.F. Paino, C.R.**

**Williams, C.R., and T.J. Hall** (in prep.) Ground water flow measurements on Fort Wainwright, Alaska, for period January 1997 through December 1997. A preliminary data report, Interim Draft Report. Prepared for U.S. Army Alaska, Directorate of Public Works.

**Williams, J.R.** (1970) Ground water in the permafrost regions of Alaska. U.S. Geological Survey Professional Paper 696.

**Williams, J.R., and R.O. Van Everdingen** (1973) Ground water investigations in permafrost regions of North America. A review. In *Permafrost: The North American Contribution to the 2nd International Conference on Permafrost, Yakutsk, 13–28 July*. Washington, D.C.: National Academy of Sciences, p. 435–446.

**Williams, C.R., J.S. Morse, D.E. Garfield, D.E. Lawson, T. Tantillo, J.D. Strasser, and T. Hall** (In prep.) An automated ground water flow monitoring system. USA Cold Regions Research and Engineering Laboratory, CRREL Report.

## APPENDIX A: SITE-SPECIFIC GROUND WATER DATA

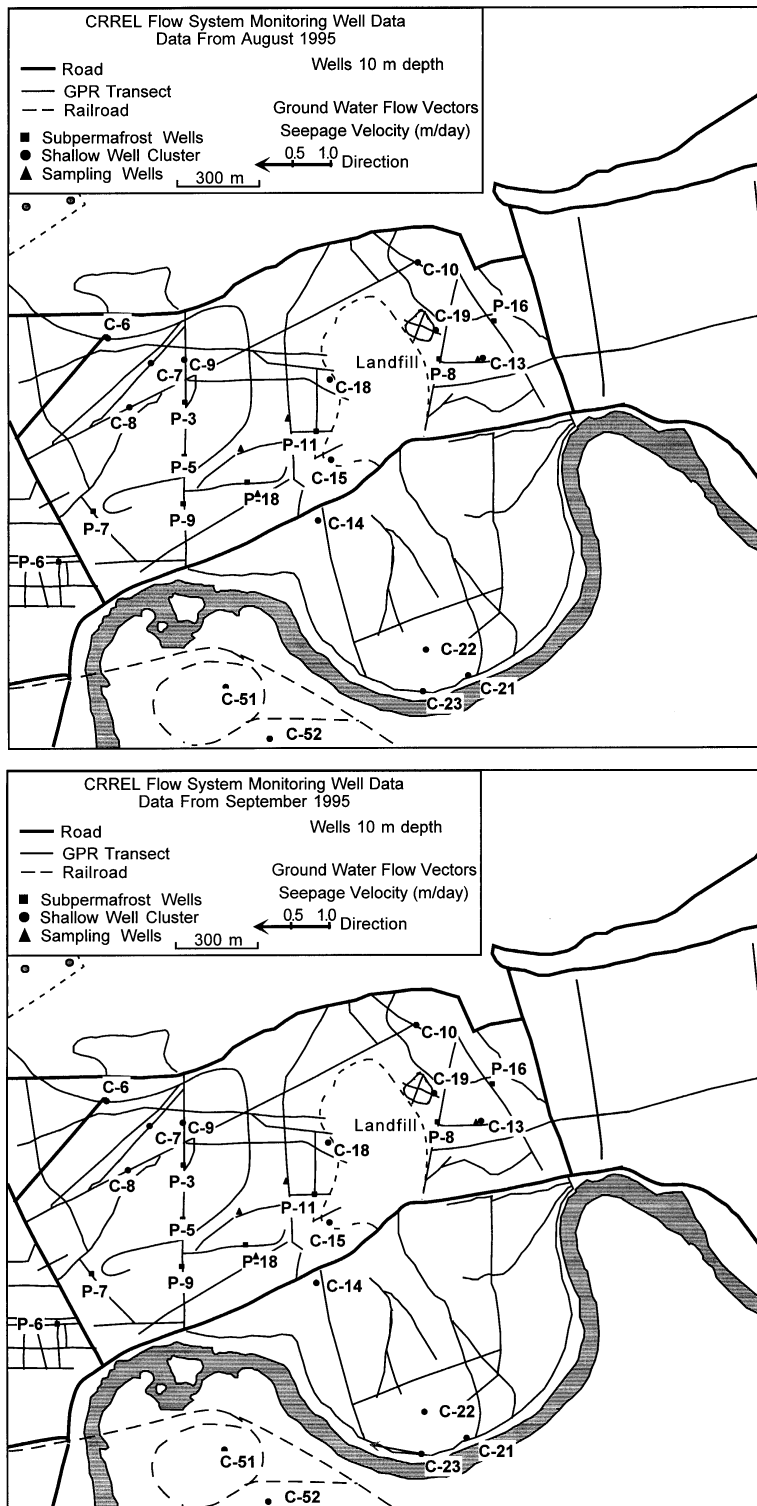


*Figure A1. Seepage velocity, flow direction, and water level in representative monitoring wells at 10 m depth. Winter flow velocities increase as water levels decline, whereas the opposite is true in summer. Frost penetration may increase confining pressures and cause the velocity to increase.*

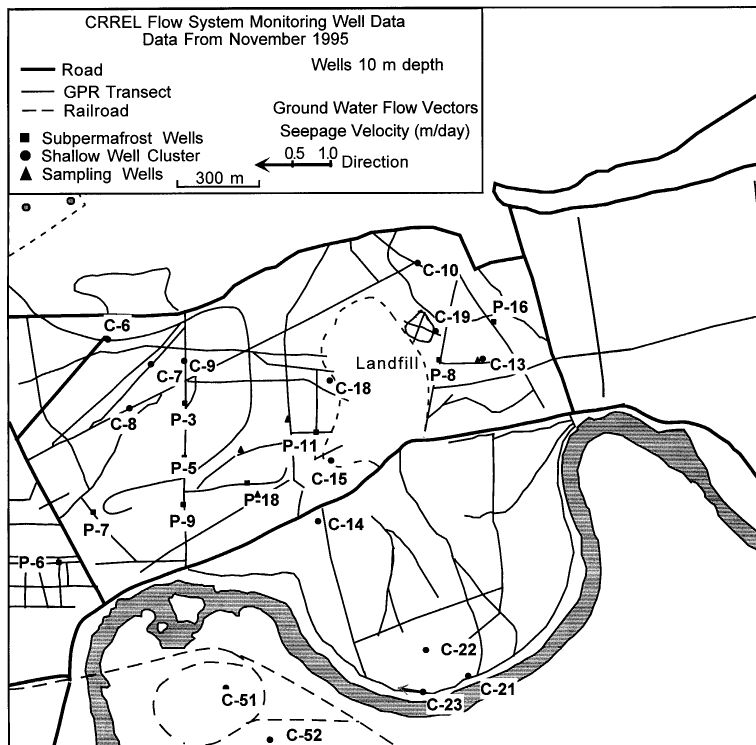
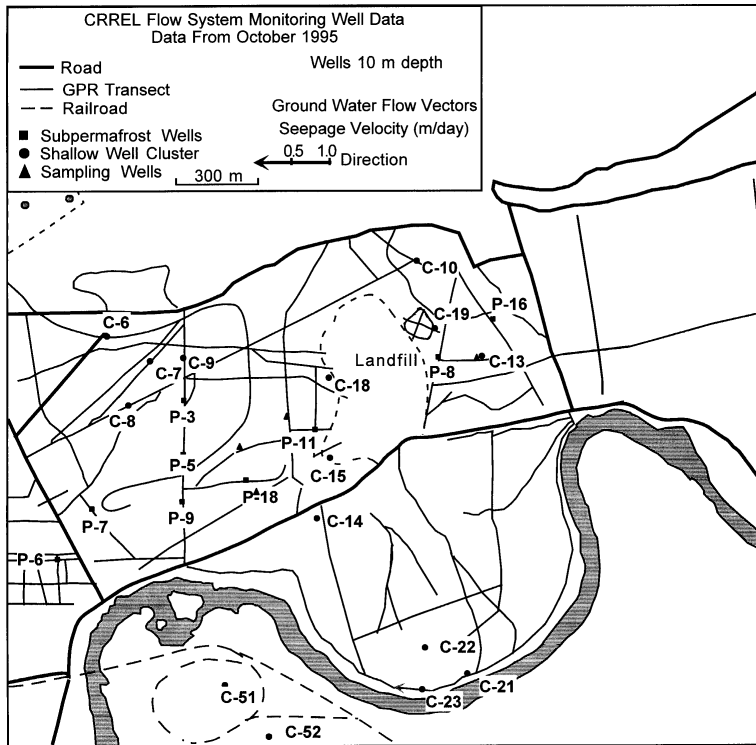


Figure A1 (cont'd). Seepage velocity, flow direction, and water level in representative monitoring wells at 10 m depth. Winter flow velocities increase as water levels decline, whereas the opposite is true in summer. Frost penetration may increase confining pressures and cause the velocity to increase.

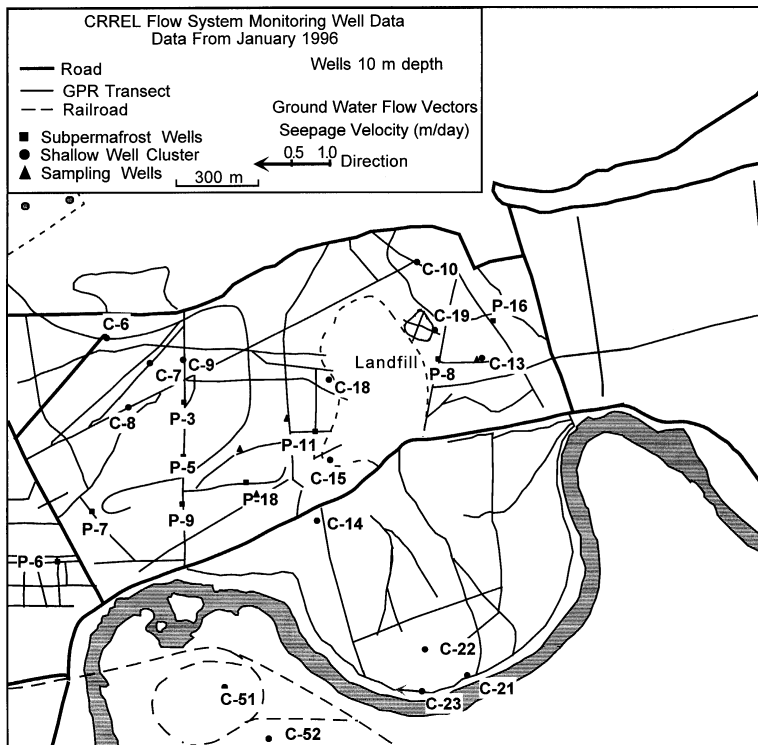
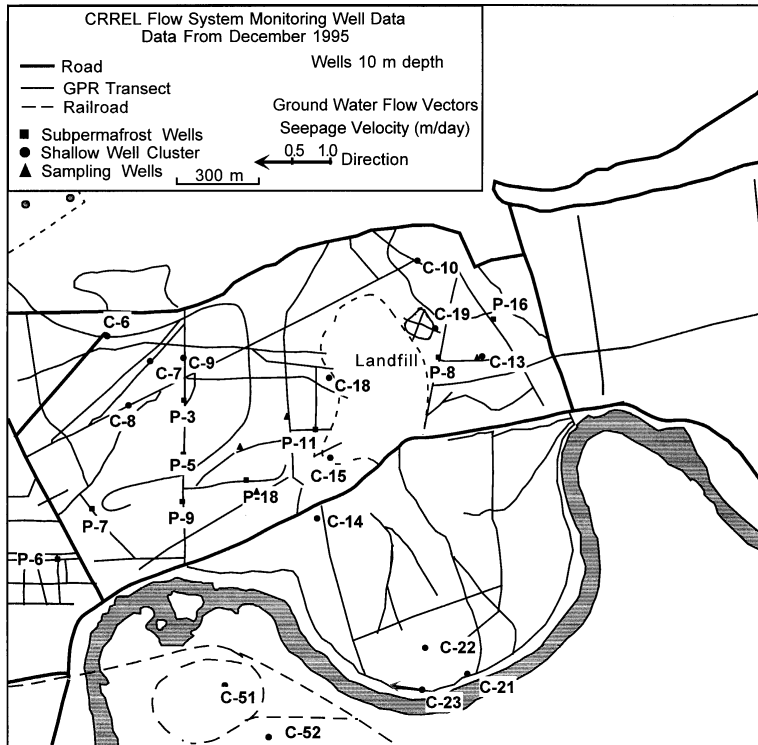


Figure A1 (cont'd).

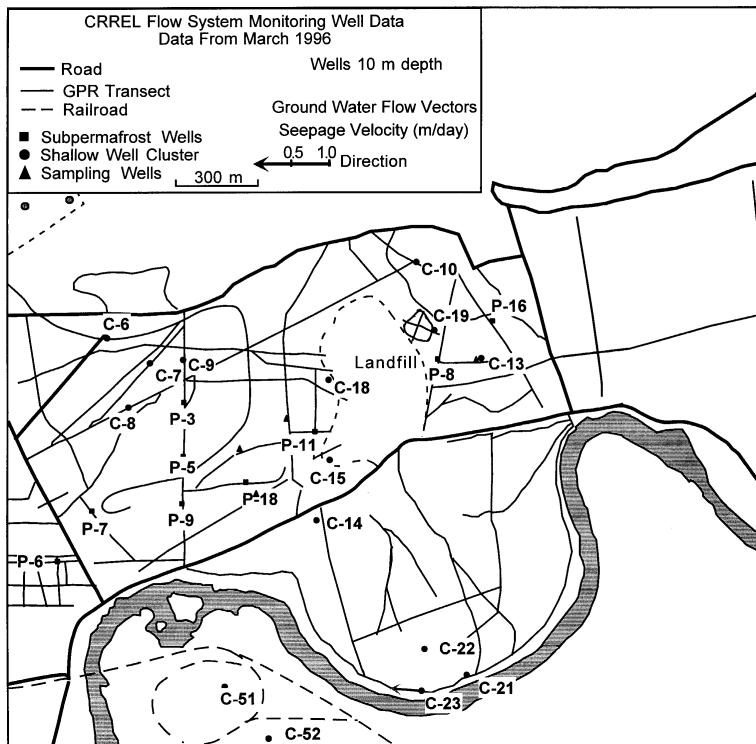
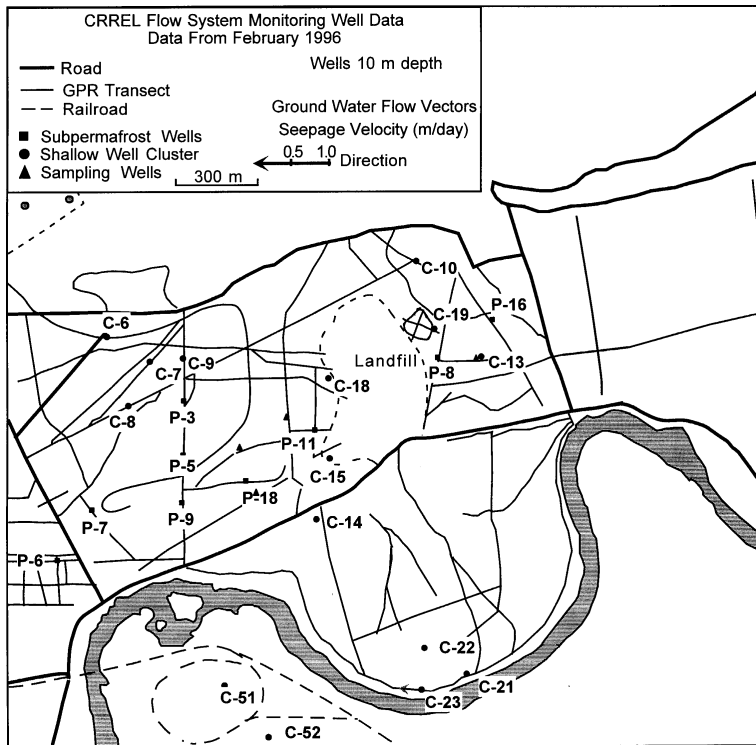


Figure A1 (cont'd). Seepage velocity, flow direction, and water level in representative monitoring wells at 10 m depth. Winter flow velocities increase as water levels decline, whereas the opposite is true in summer. Frost penetration may increase confining pressures and cause the velocity to increase.

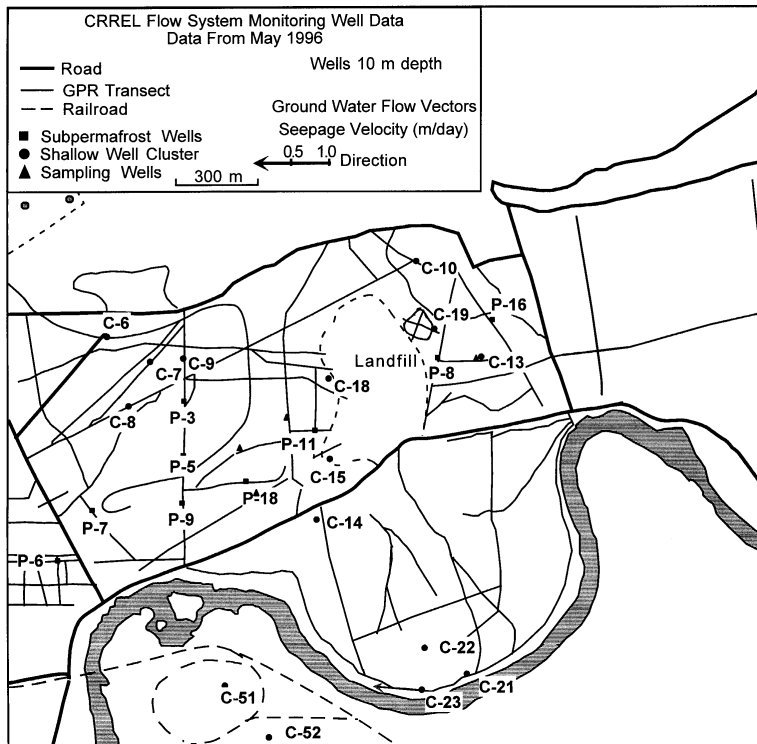
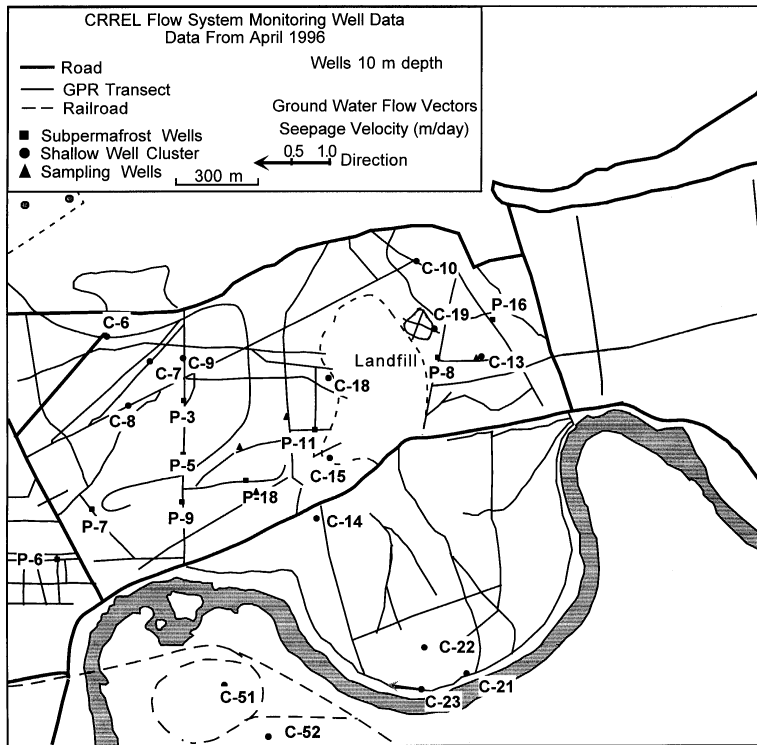


Figure A1 (cont'd).

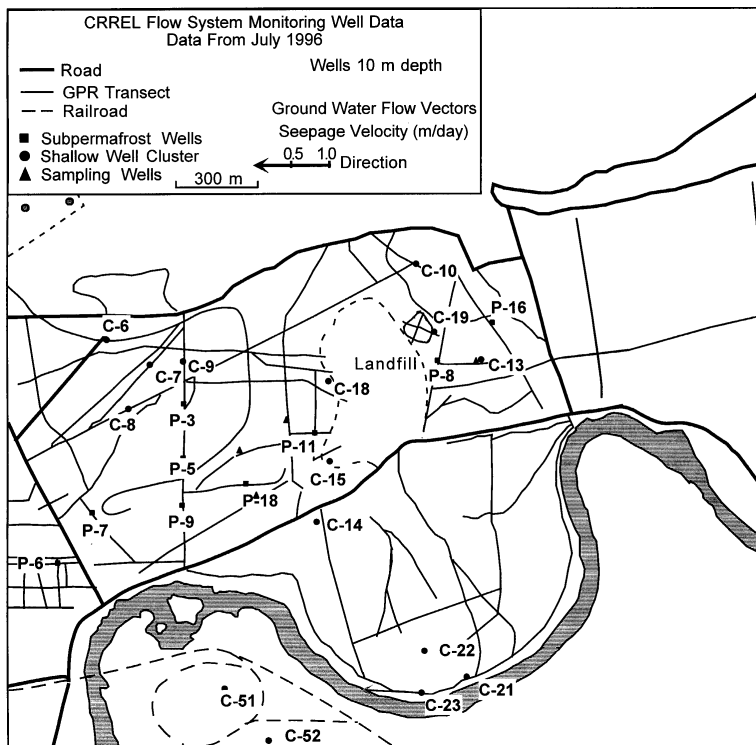
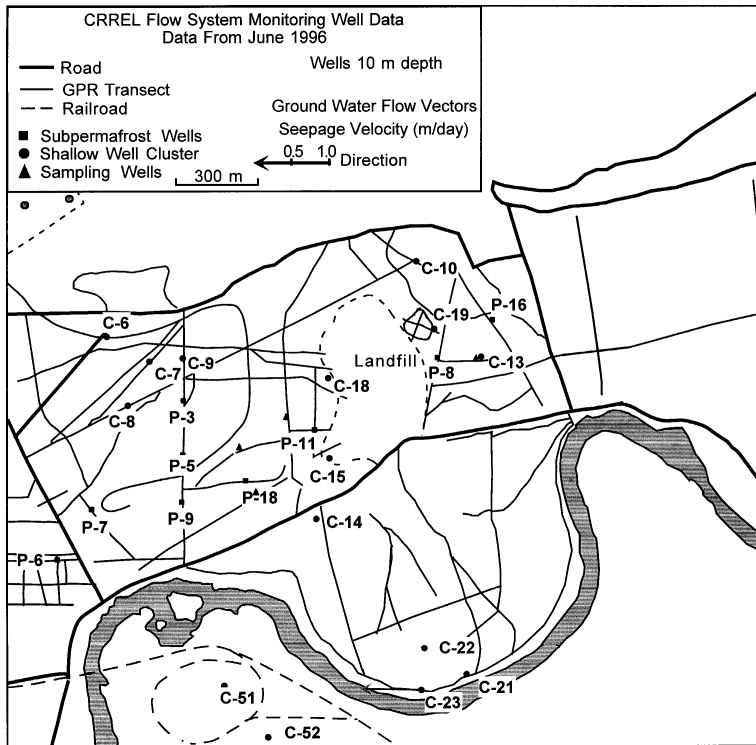


Figure A1 (cont'd). Seepage velocity, flow direction, and water level in representative monitoring wells at 10 m depth. Winter flow velocities increase as water levels decline, whereas the opposite is true in summer. Frost penetration may increase confining pressures and cause the velocity to increase.

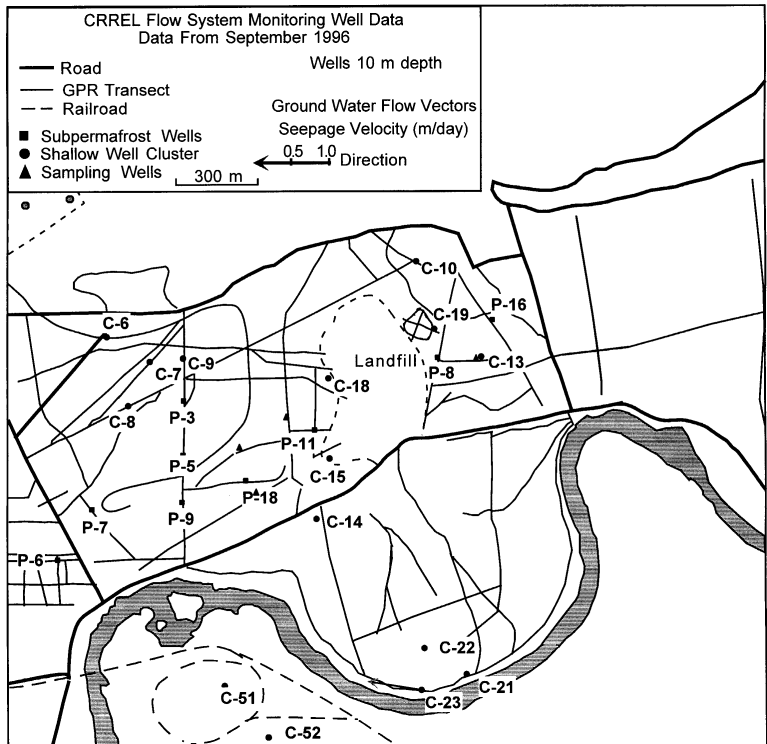
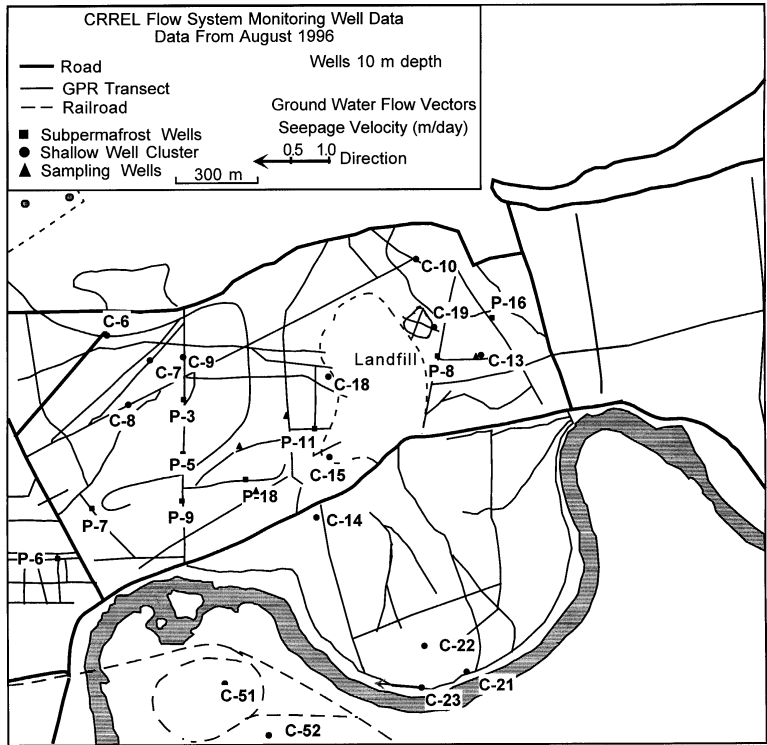


Figure A1 (cont'd).

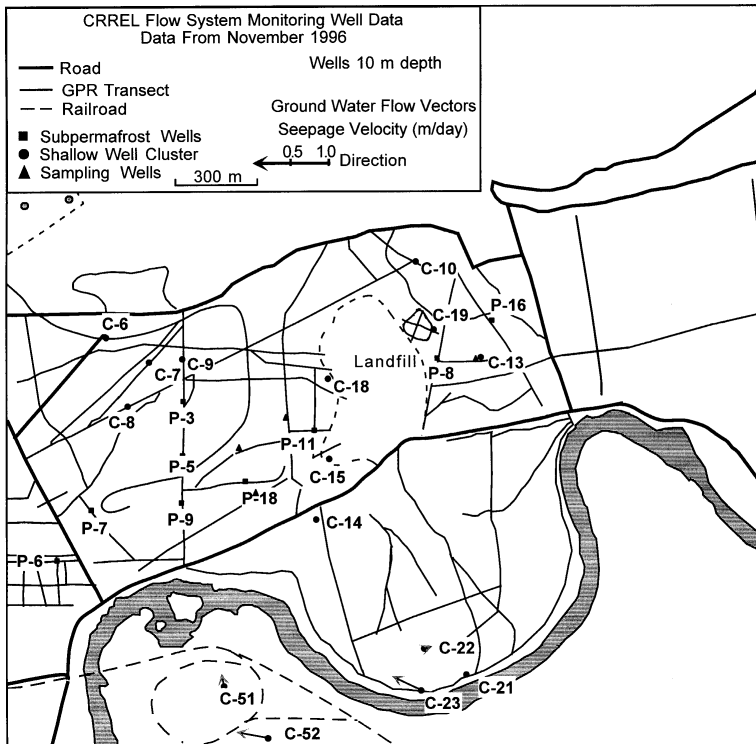
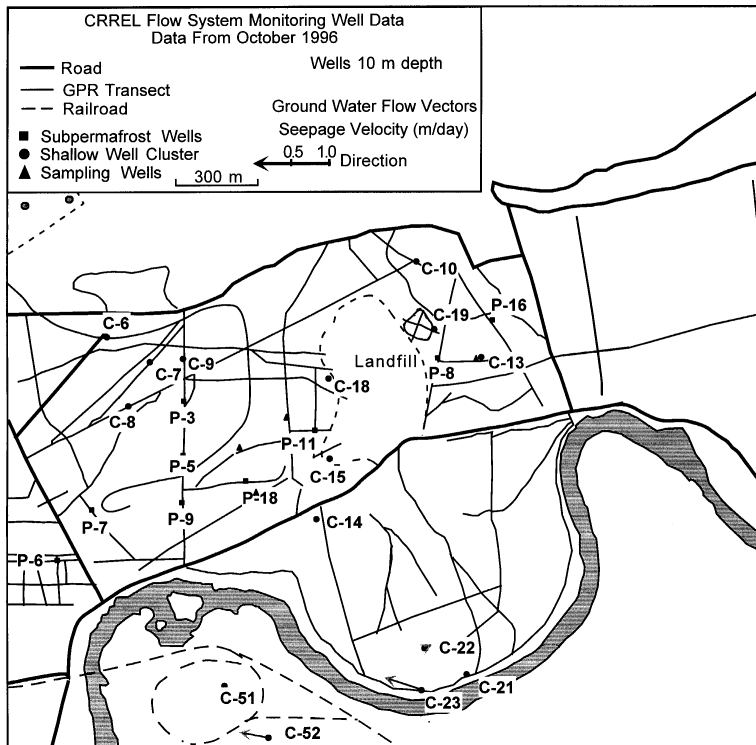


Figure A1 (cont'd). Seepage velocity, flow direction, and water level in representative monitoring wells at 10 m depth. Winter flow velocities increase as water levels decline, whereas the opposite is true in summer. Frost penetration may increase confining pressures and cause the velocity to increase.

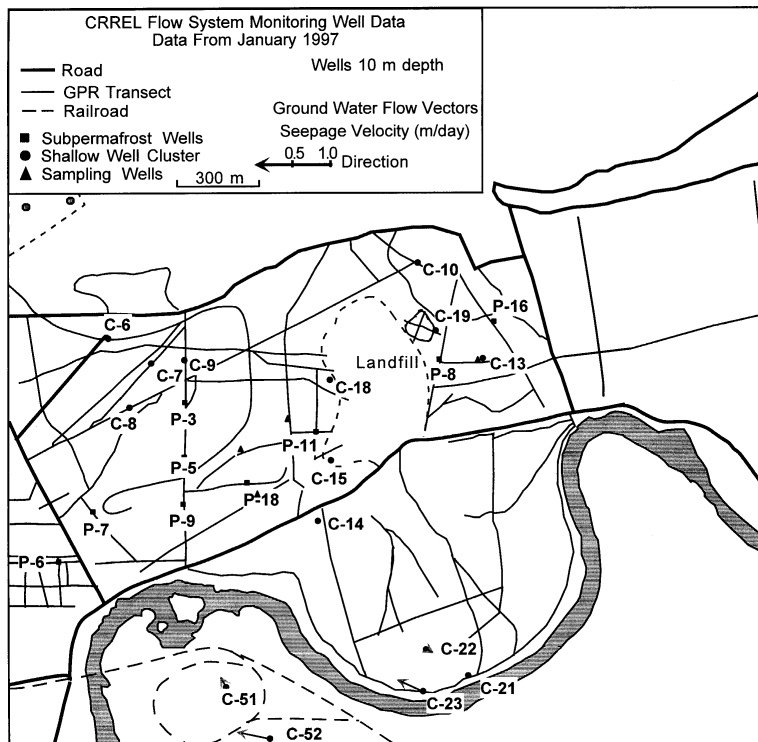
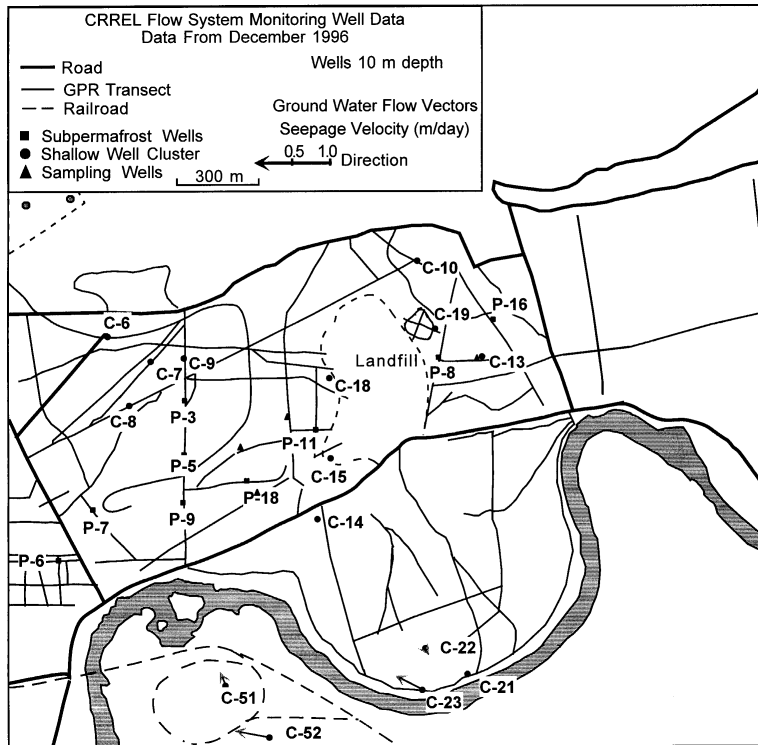


Figure A1 (cont'd).

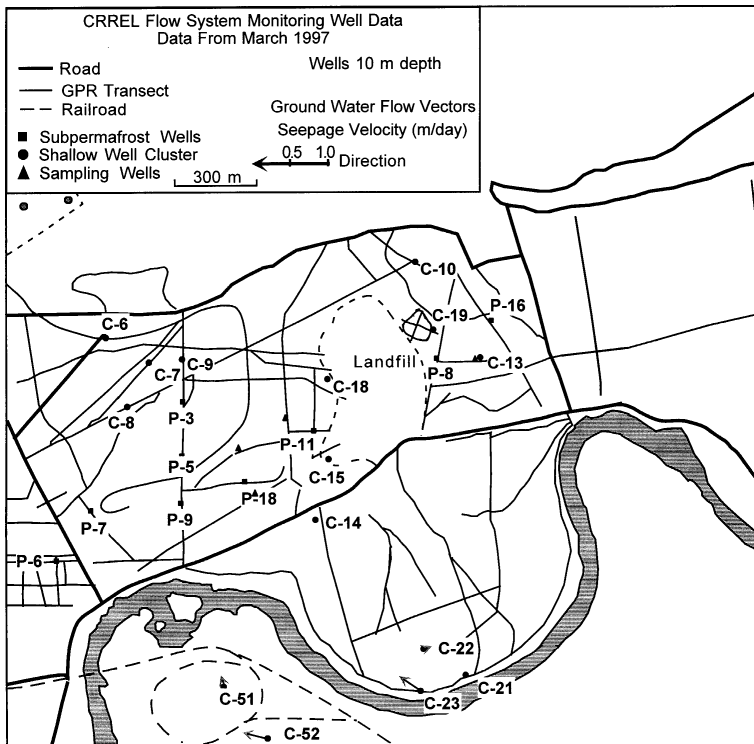
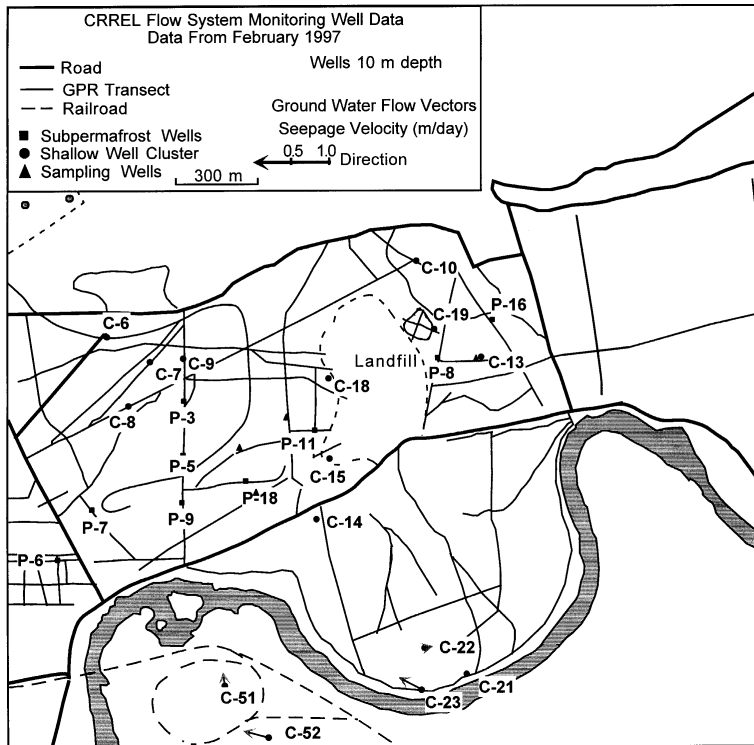


Figure A1 (cont'd). Seepage velocity, flow direction, and water level in representative monitoring wells at 10 m depth. Winter flow velocities increase as water levels decline, whereas the opposite is true in summer. Frost penetration may increase confining pressures and cause the velocity to increase.

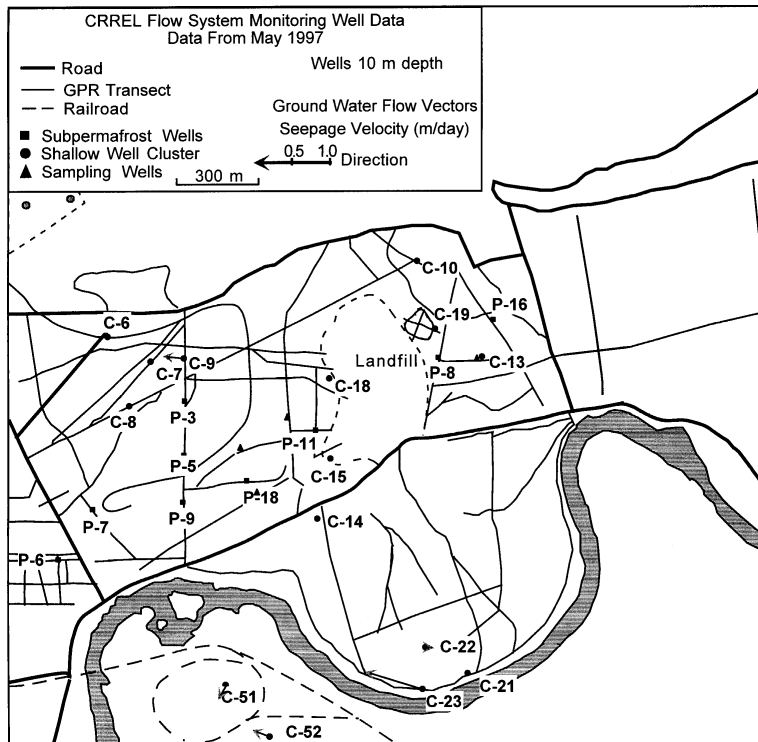
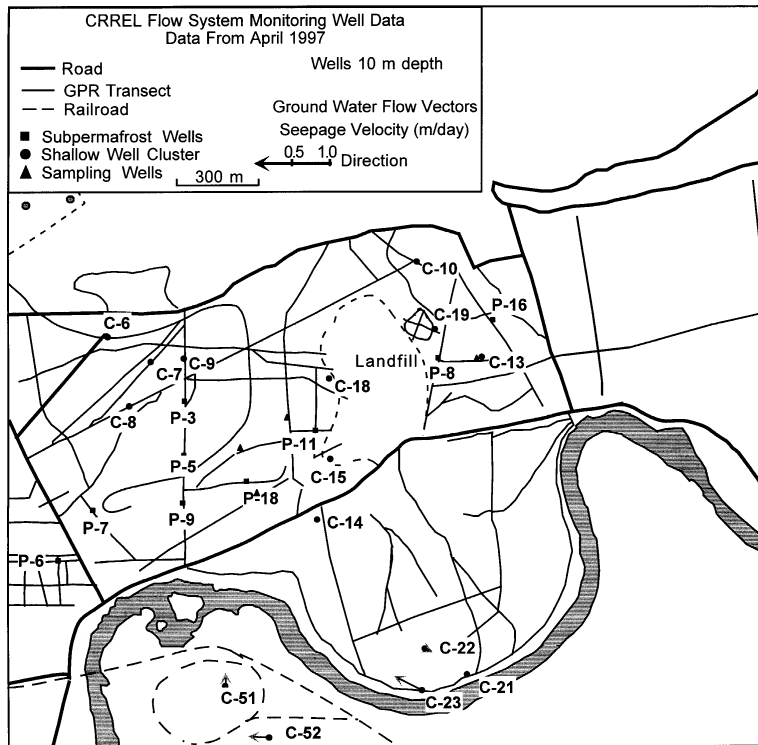
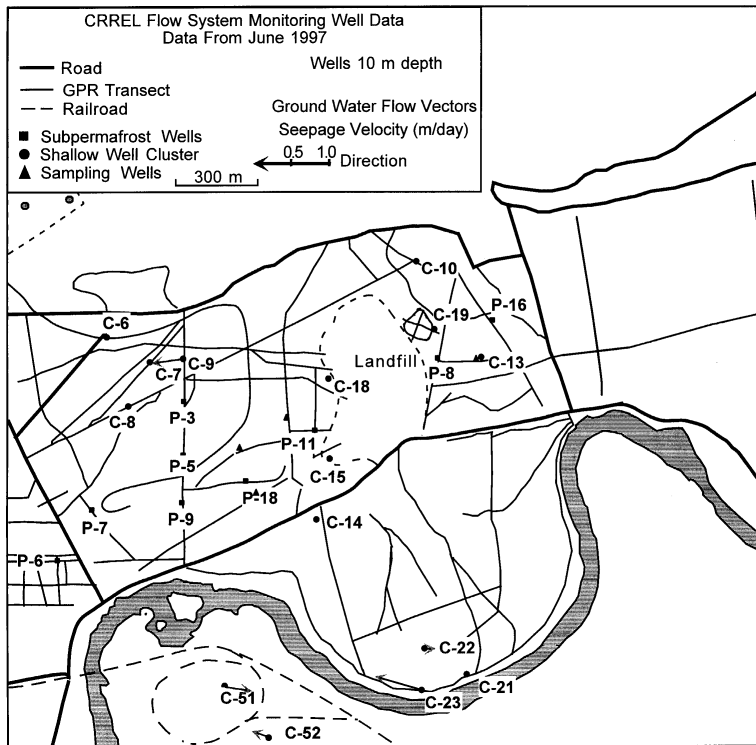


Figure A1 (cont'd).



*Figure A1 (cont'd). Seepage velocity, flow direction, and water level in representative monitoring wells at 10 m depth. Winter flow velocities increase as water levels decline, whereas the opposite is true in summer. Frost penetration may increase confining pressures and cause the velocity to increase.*

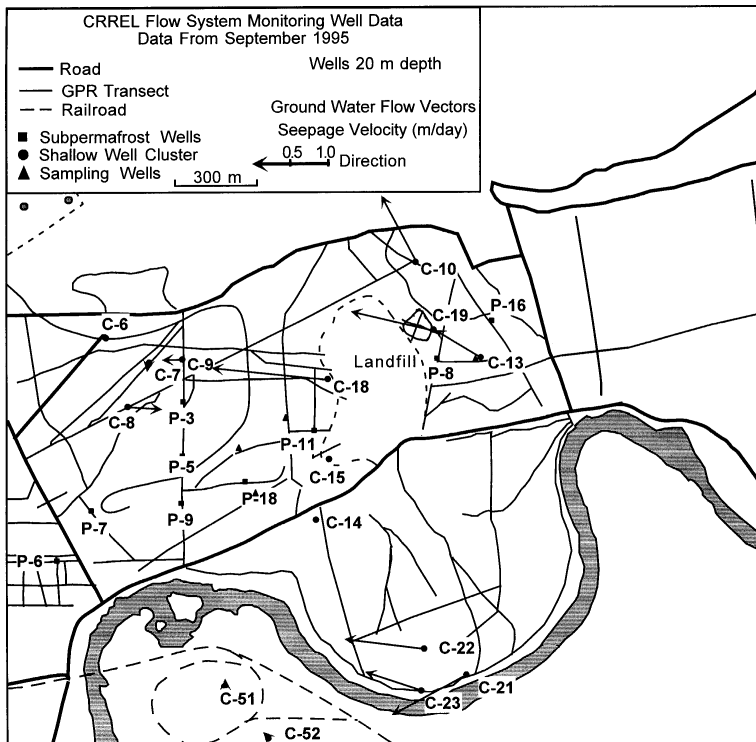
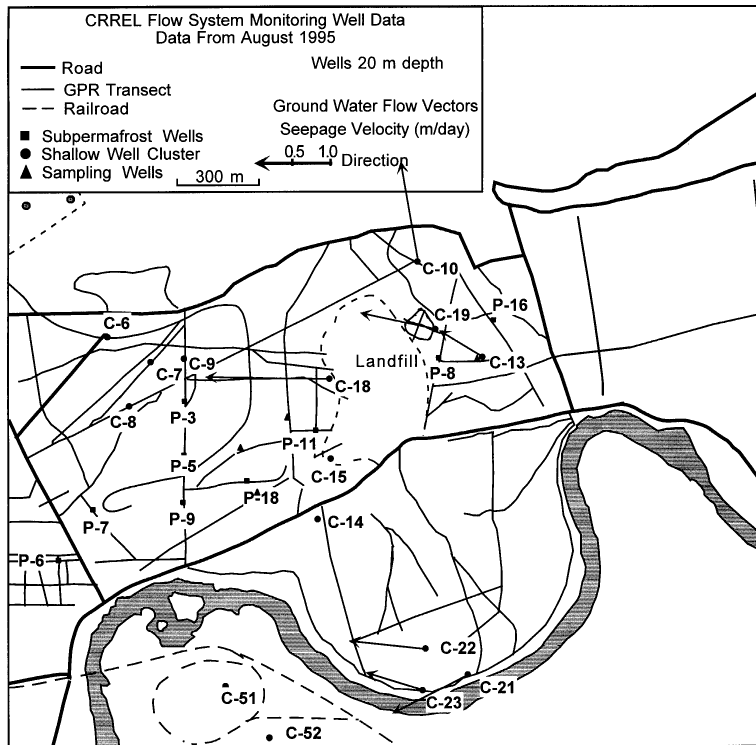


Figure A2. Mean flow directions, seepage velocities, and water levels in representative 20-m-deep monitoring wells. Vectors are calculated from ground water flow sensor data for measurements during the period of September 1995 to December 1996.

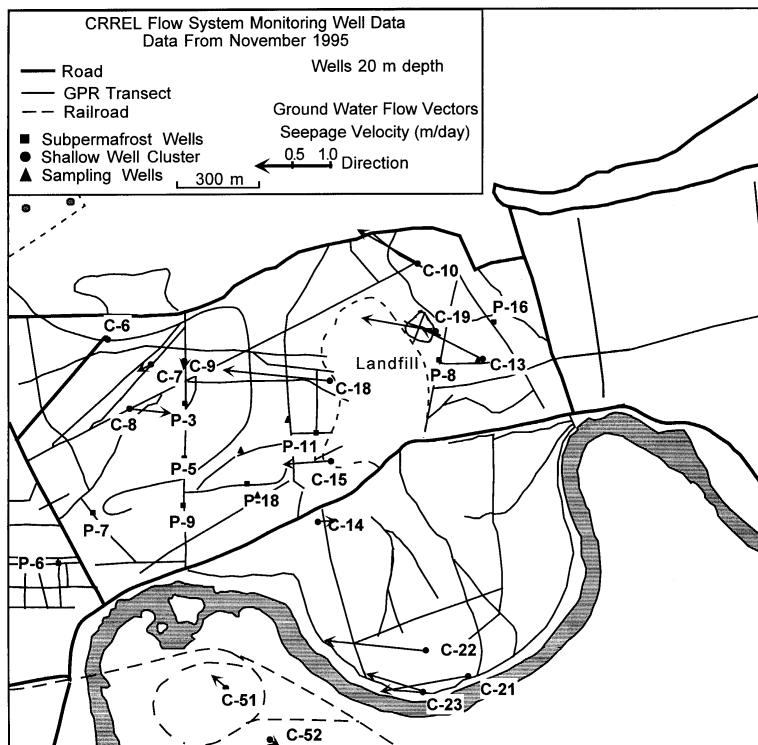
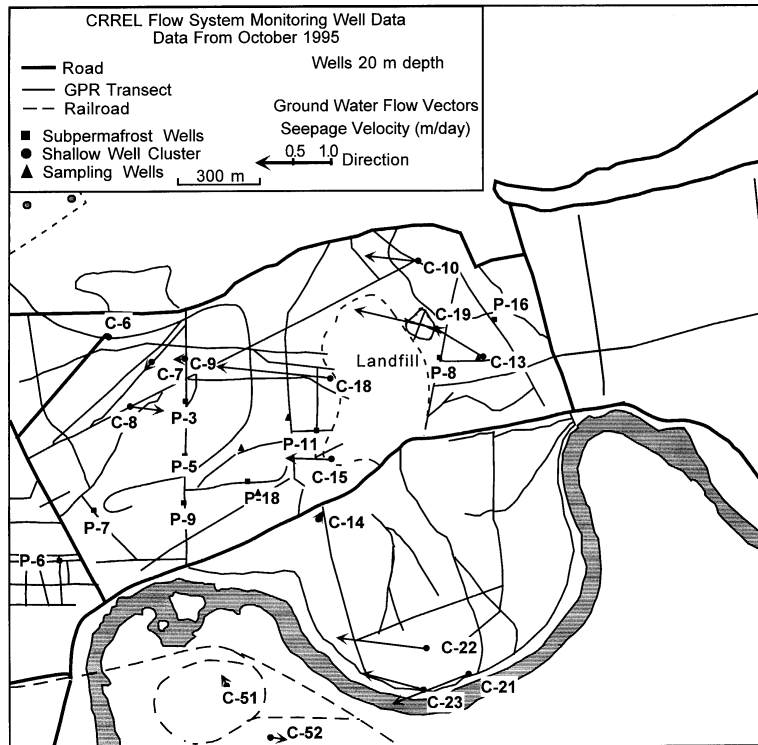


Figure A2 (cont'd). Mean flow directions, seepage velocities, and water levels in representative 20-m-deep monitoring wells. Vectors are calculated from ground water flow sensor data for measurements during the period of September 1995 to December 1996.

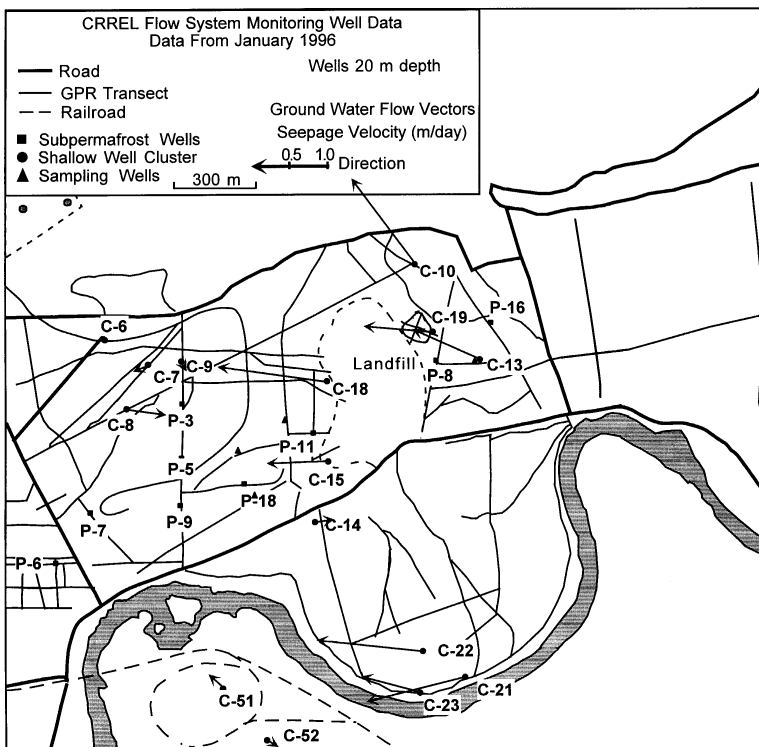
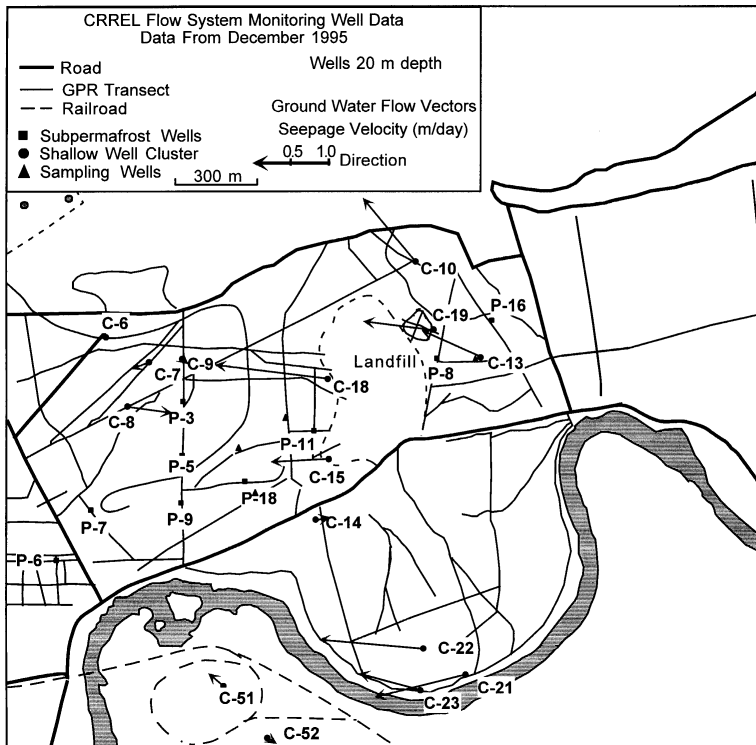


Figure A2 (cont'd).

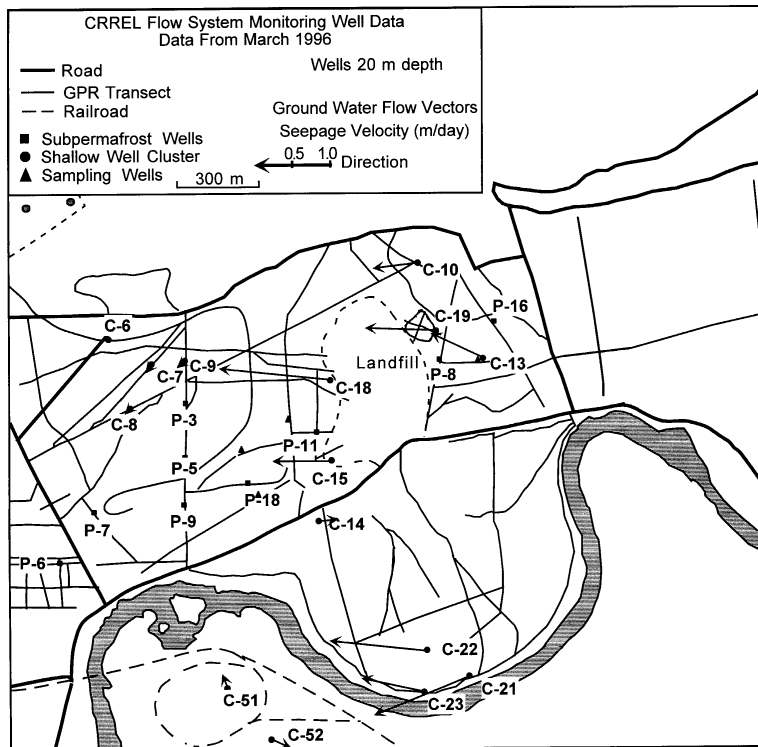
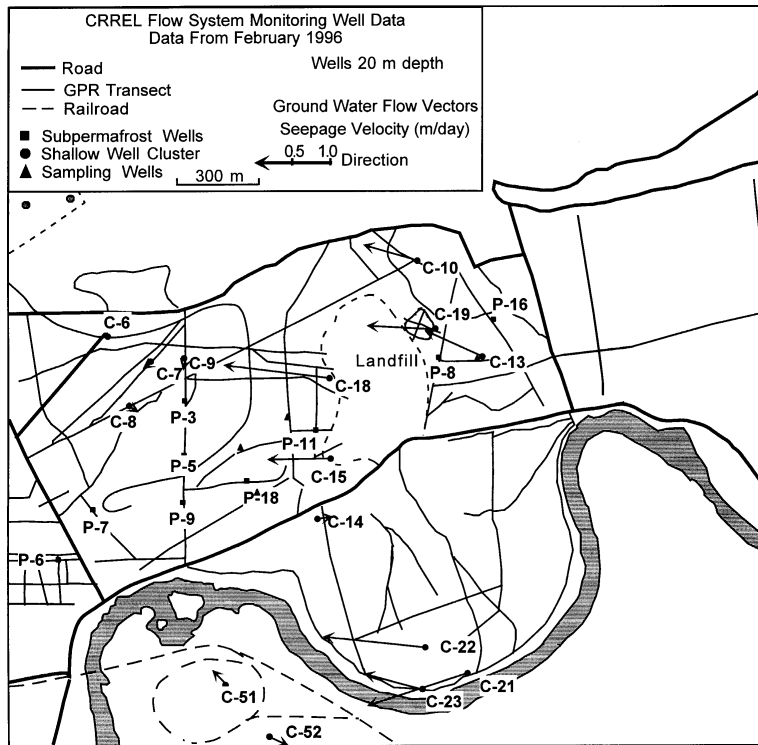


Figure A2 (cont'd). Mean flow directions, seepage velocities, and water levels in representative 20-m-deep monitoring wells. Vectors are calculated from ground water flow sensor data for measurements during the period of September 1995 to December 1996.

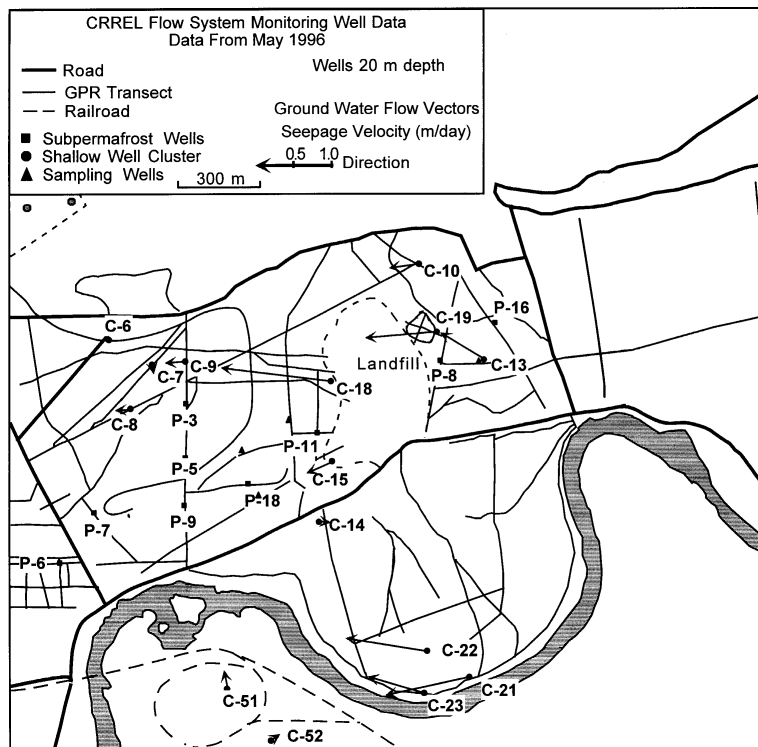
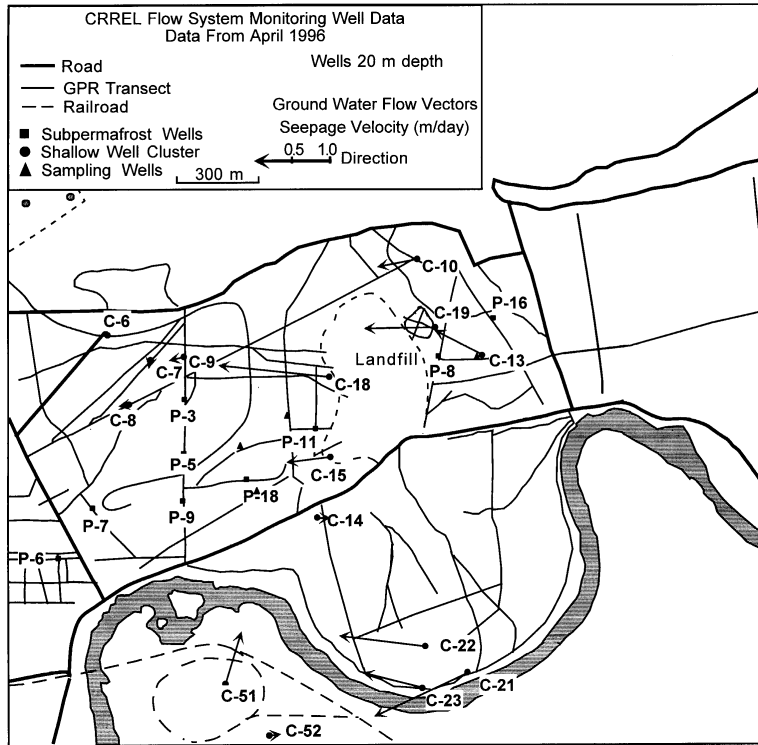


Figure A2 (cont'd).

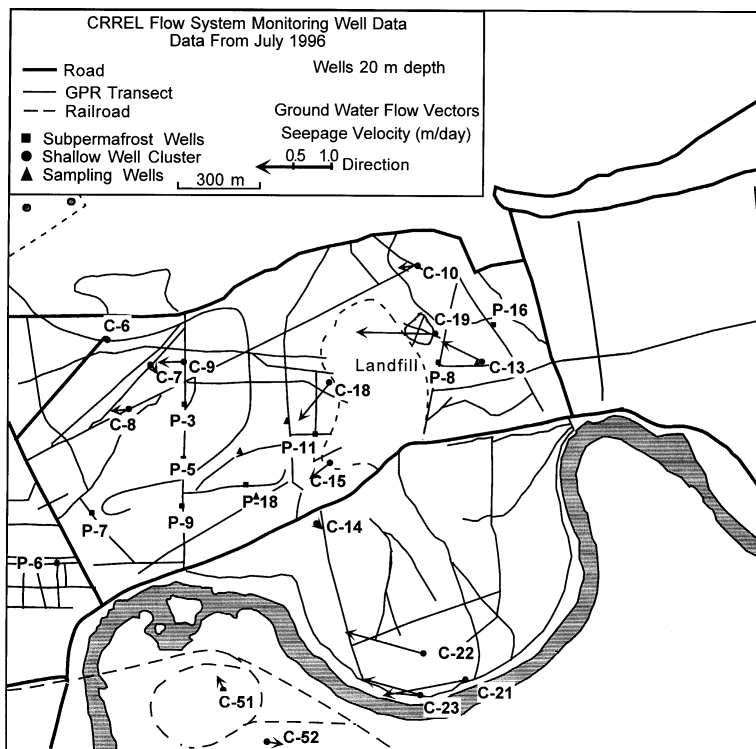
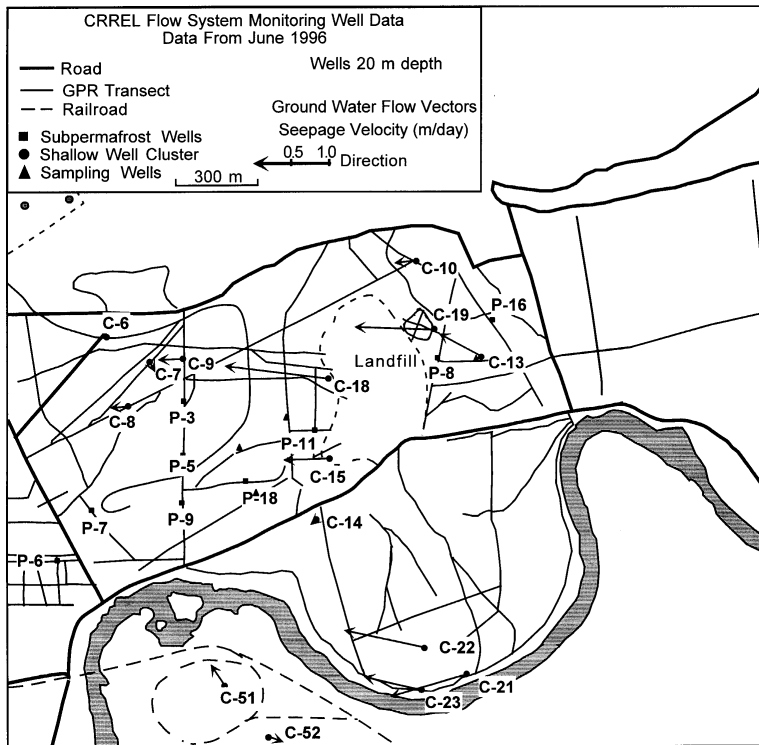


Figure A2 (cont'd). Mean flow directions, seepage velocities, and water levels in representative 20-m-deep monitoring wells. Vectors are calculated from ground water flow sensor data for measurements during the period of September 1995 to December 1996.

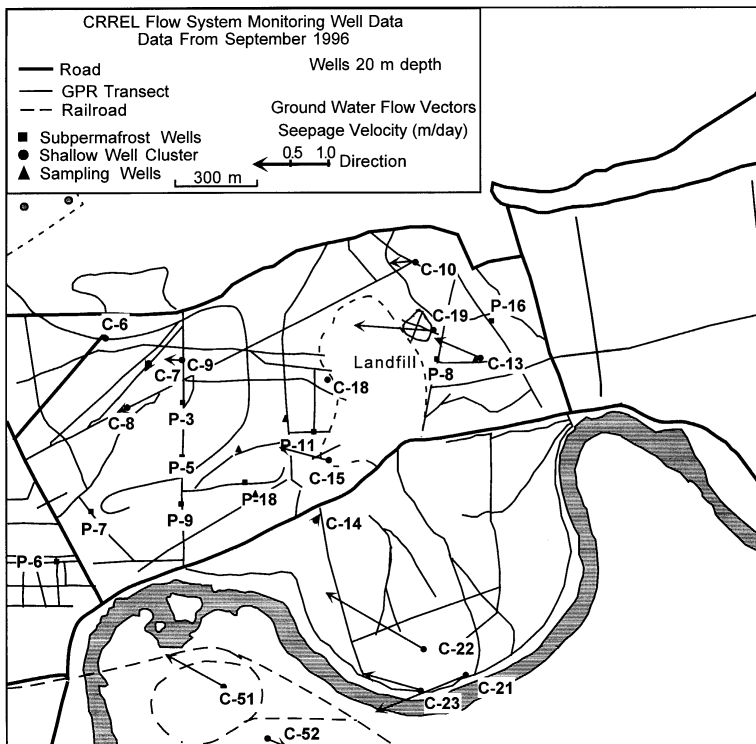
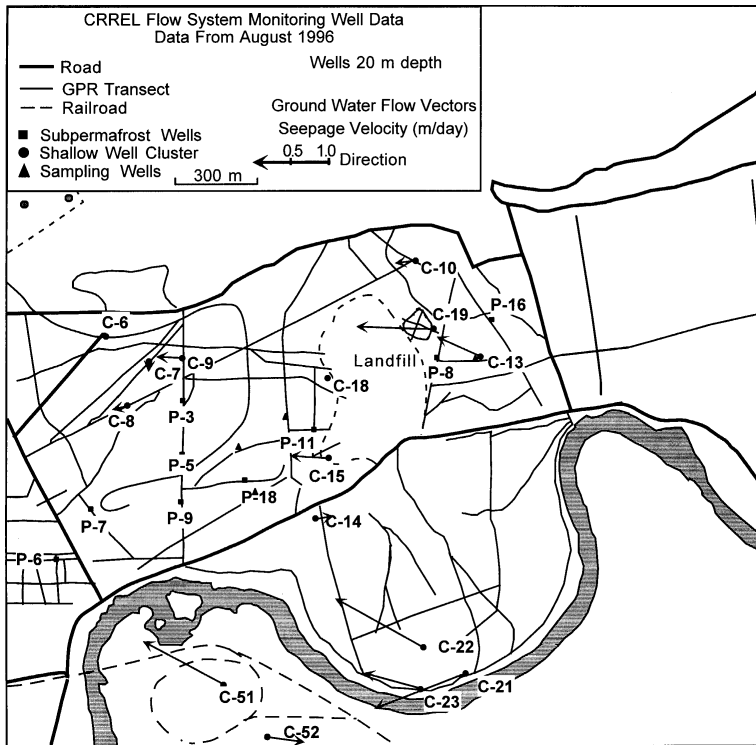


Figure A2 (cont'd).

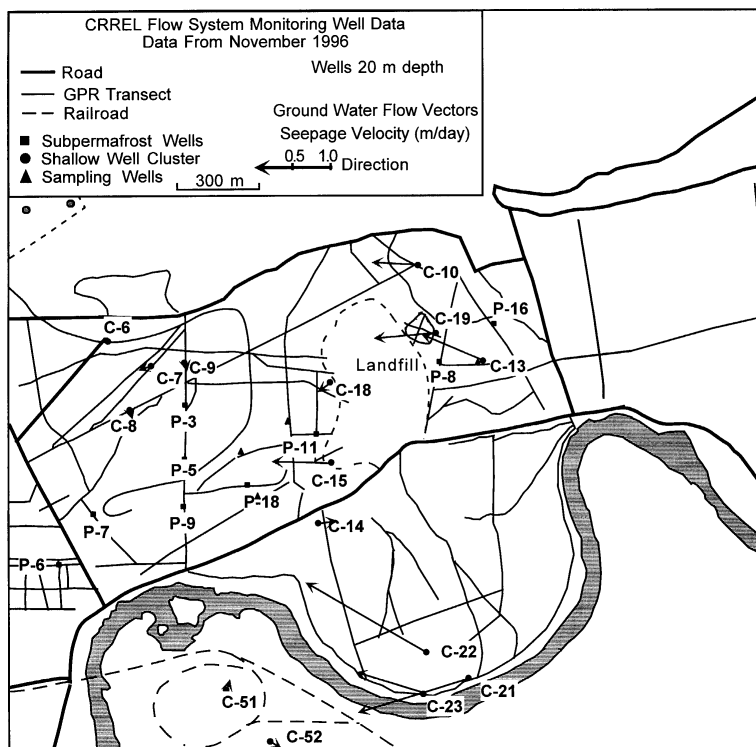
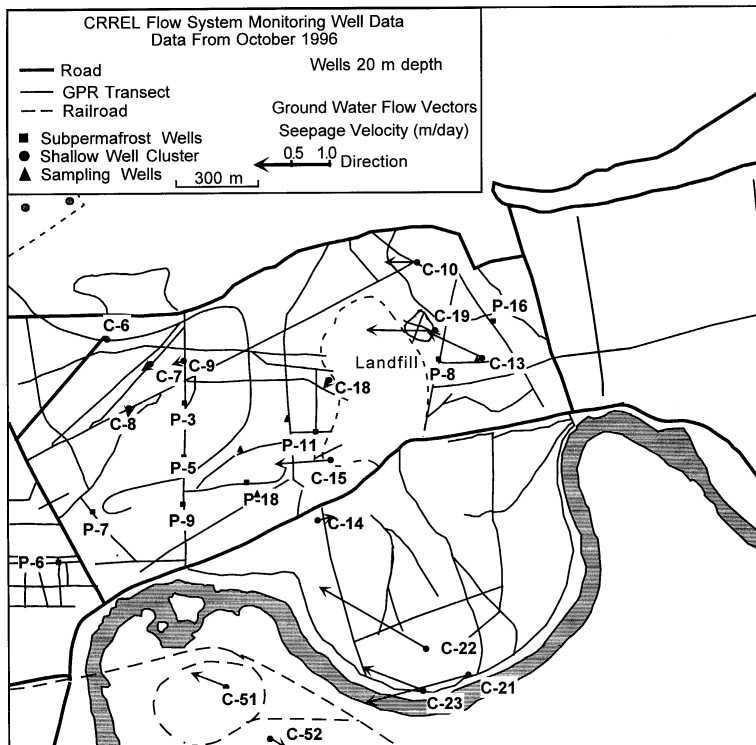


Figure A2 (cont'd). Mean flow directions, seepage velocities, and water levels in representative 20-m-deep monitoring wells. Vectors are calculated from ground water flow sensor data for measurements during the period of September 1995 to December 1996.

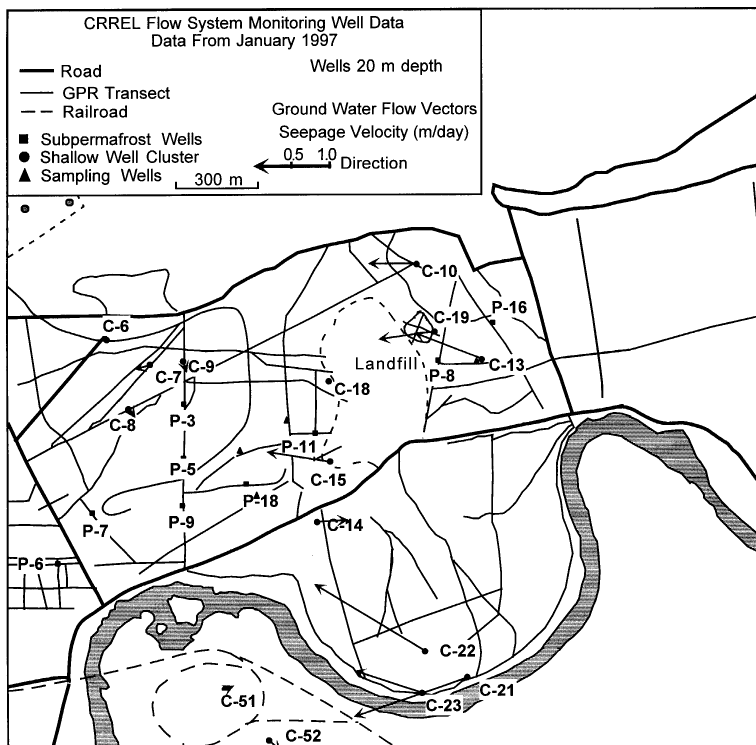
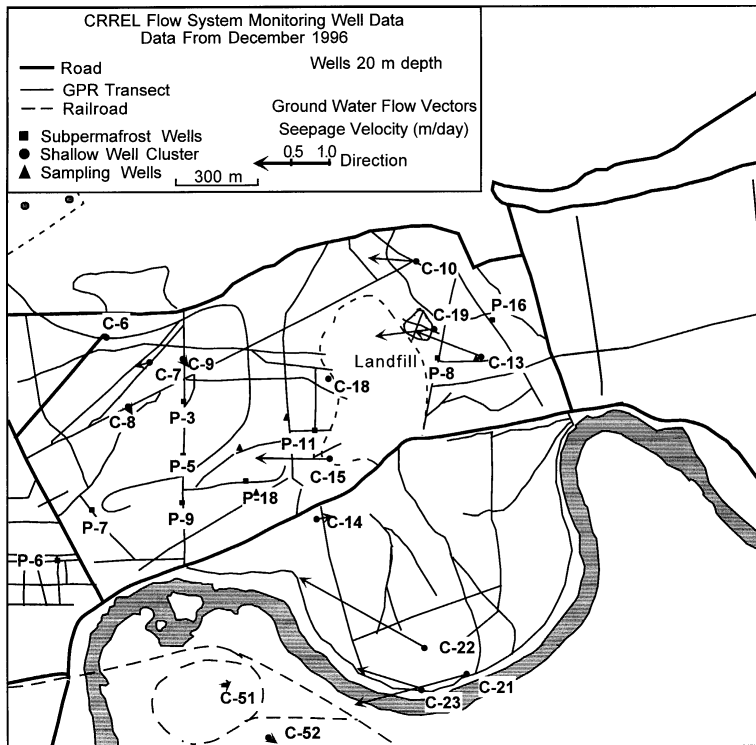


Figure A2 (cont'd).

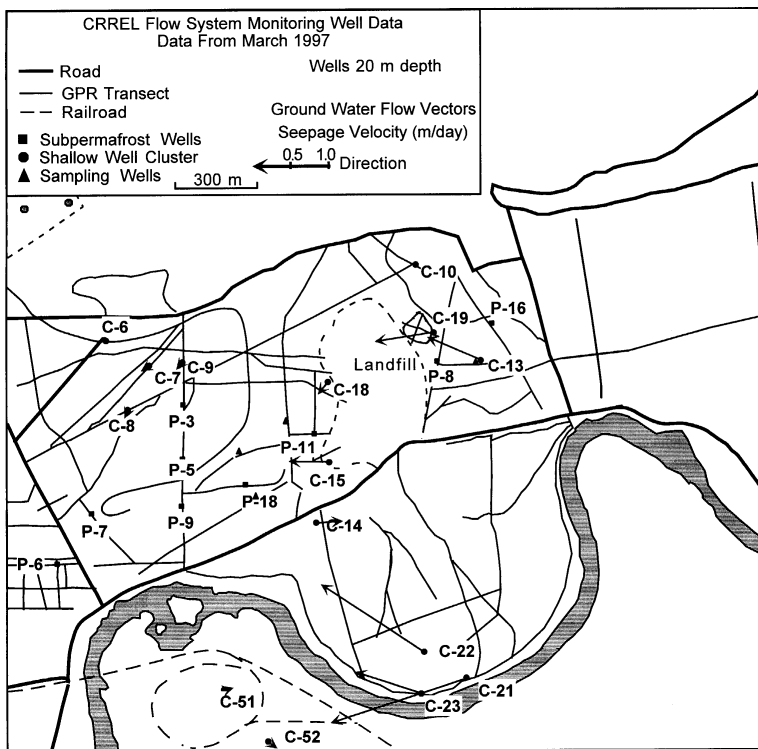
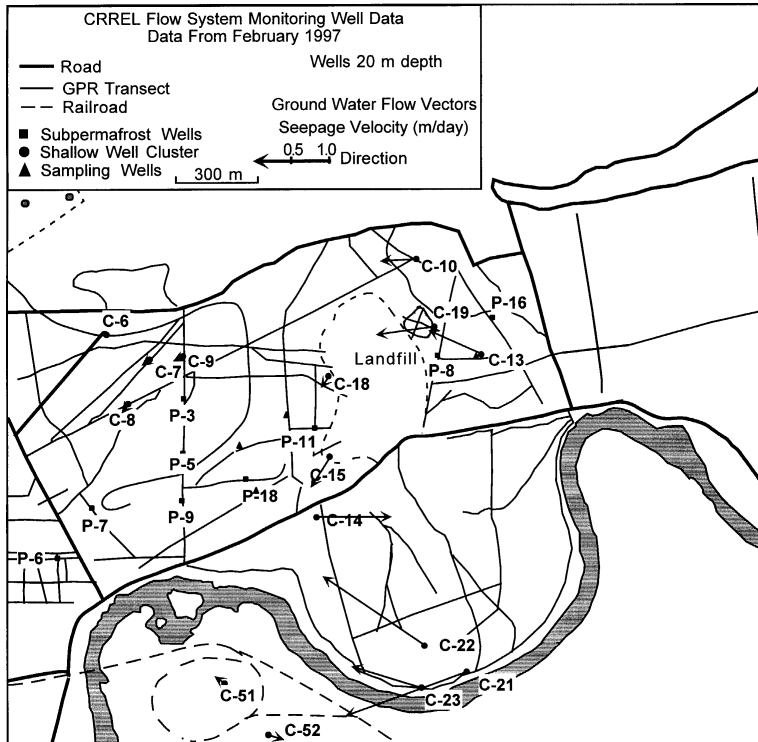


Figure A2 (cont'd). Mean flow directions, seepage velocities, and water levels in representative 20-m-deep monitoring wells. Vectors are calculated from ground water flow sensor data for measurements during the period of September 1995 to December 1996.

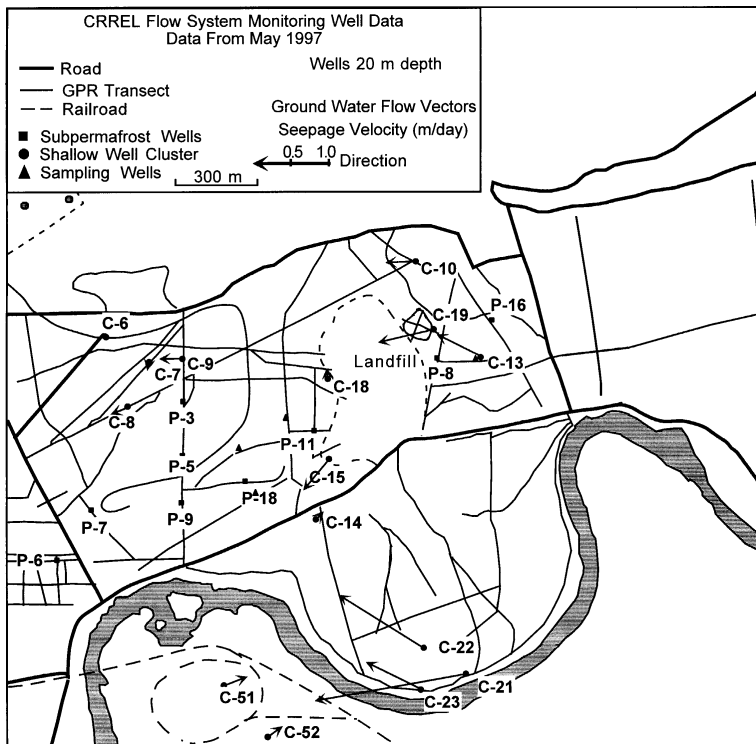
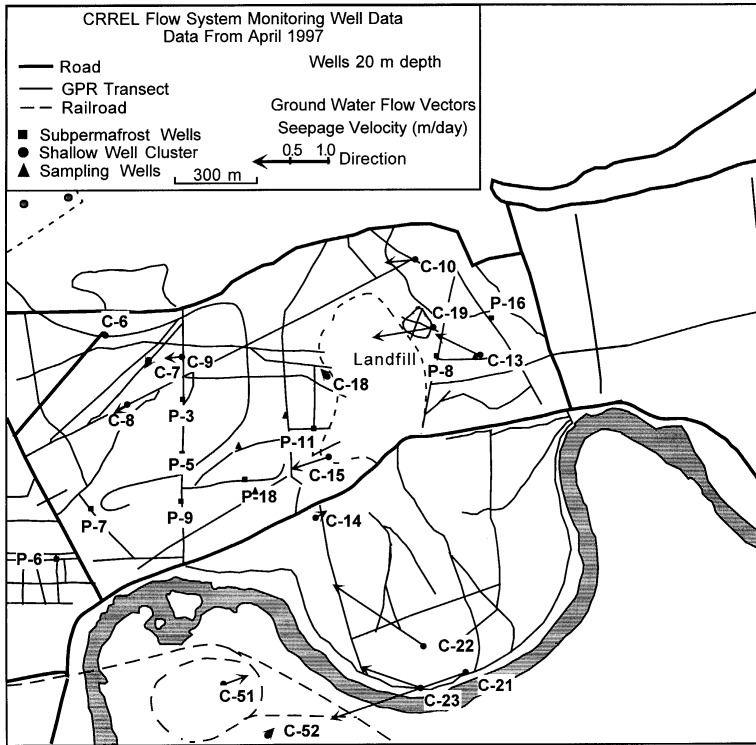


Figure A2 (cont'd).

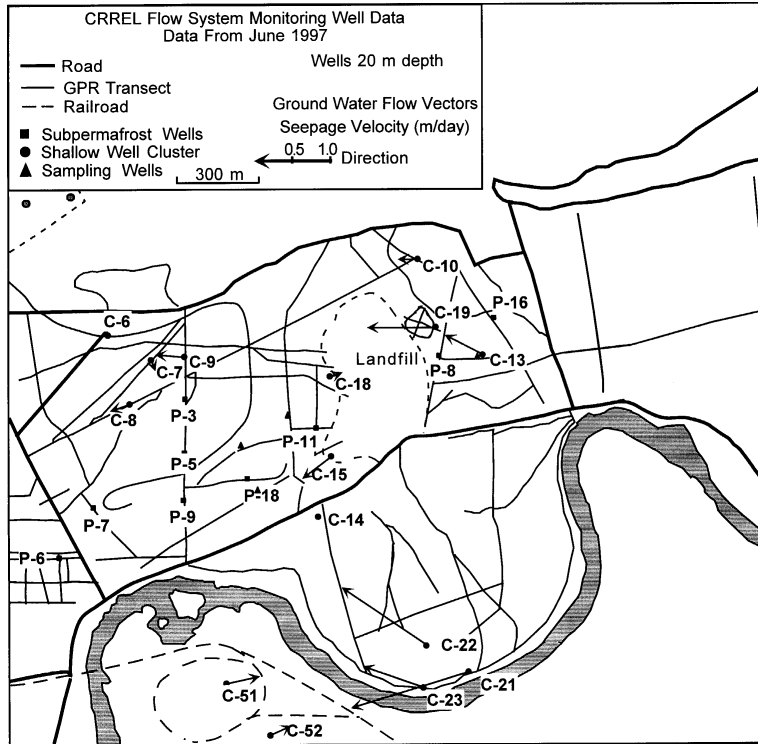


Figure A2 (cont'd). Mean flow directions, seepage velocities, and water levels in representative 20-m-deep monitoring wells. Vectors are calculated from ground water flow sensor data for measurements during the period of September 1995 to December 1996.

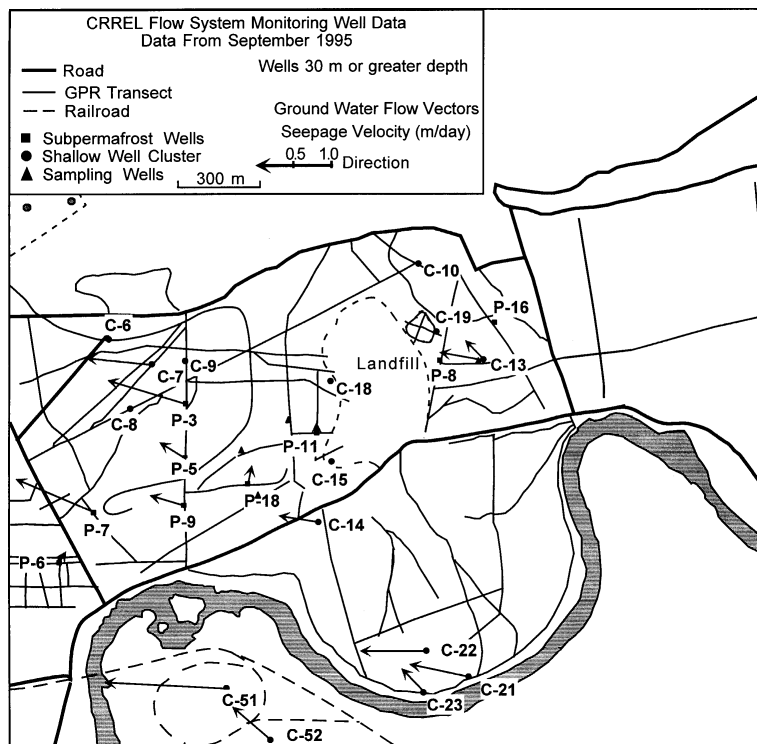
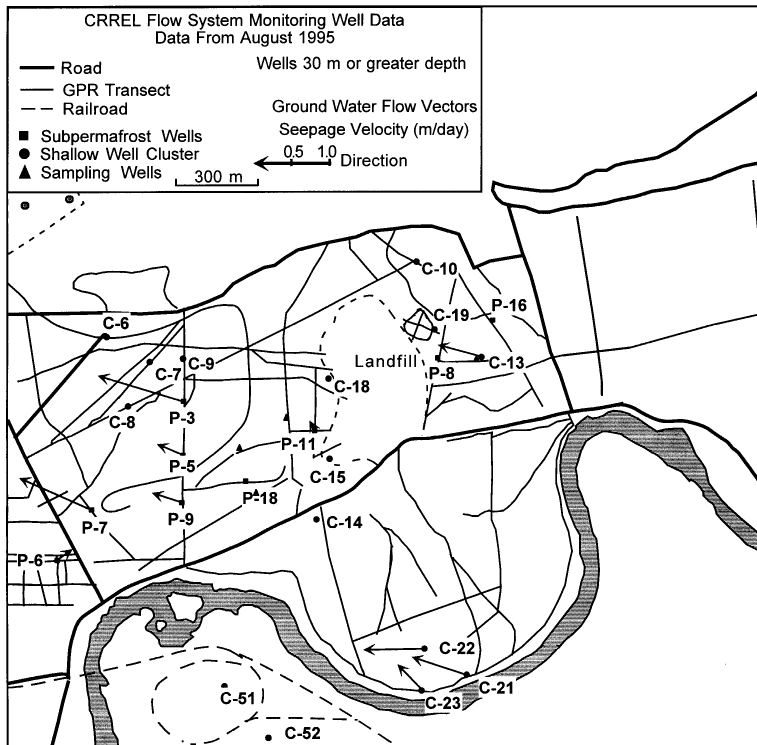


Figure A3. Mean flow directions, seepage velocities, and water levels from representative 30-m-deep monitoring wells in unfrozen thaw zones and from subpermafrost wells that exceed 30 m in depth. Vectors are calculated from ground water flow sensor data for measurements during September 1995 to January 1997.

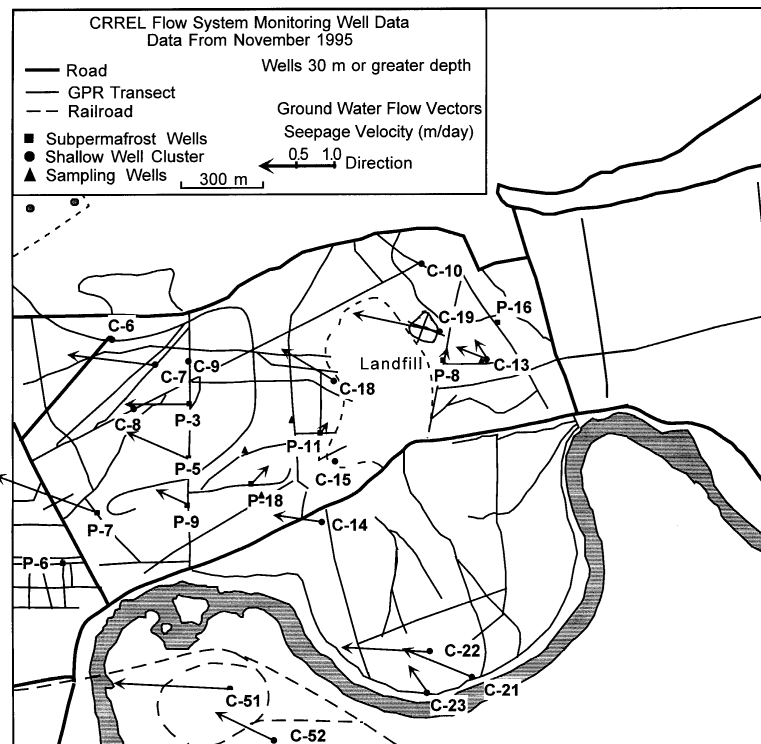
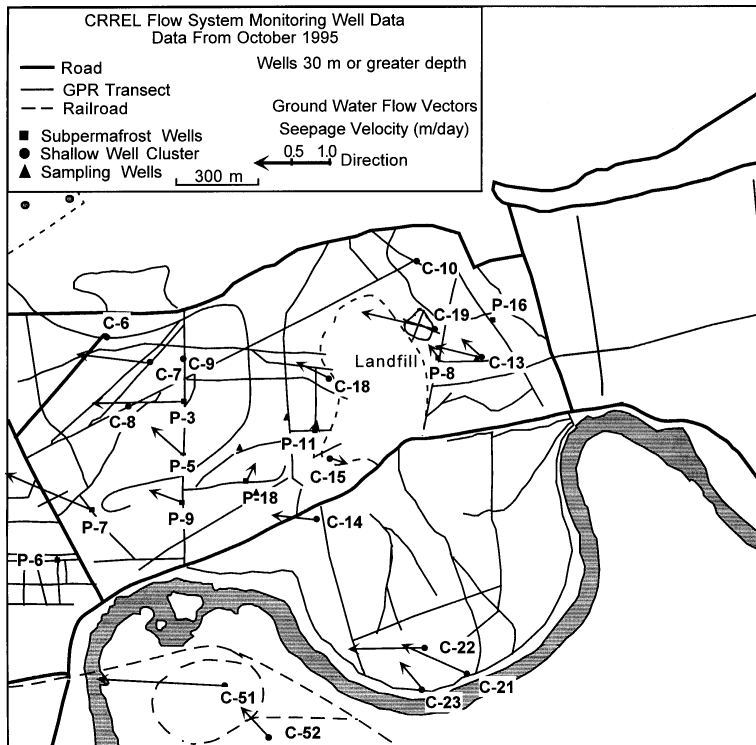
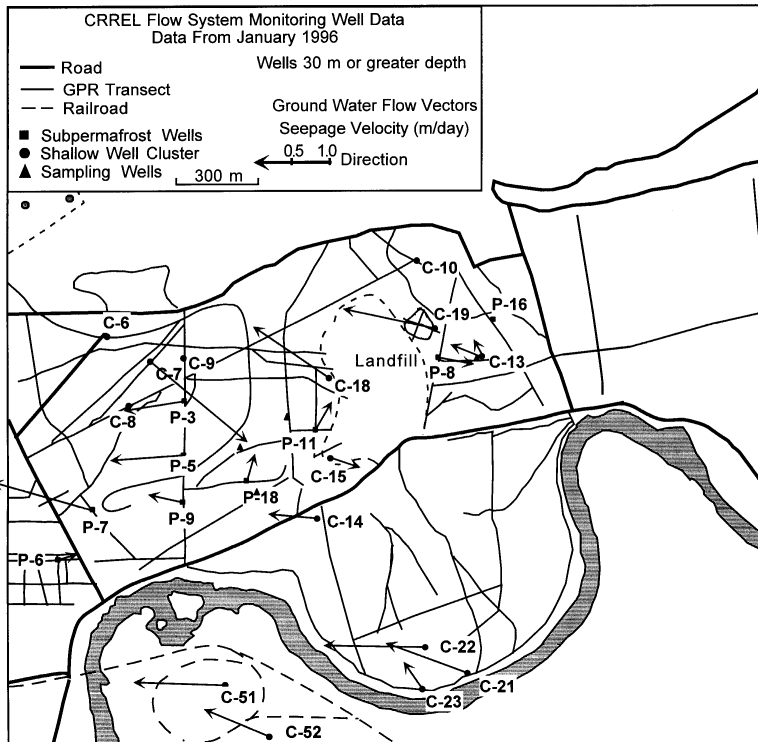
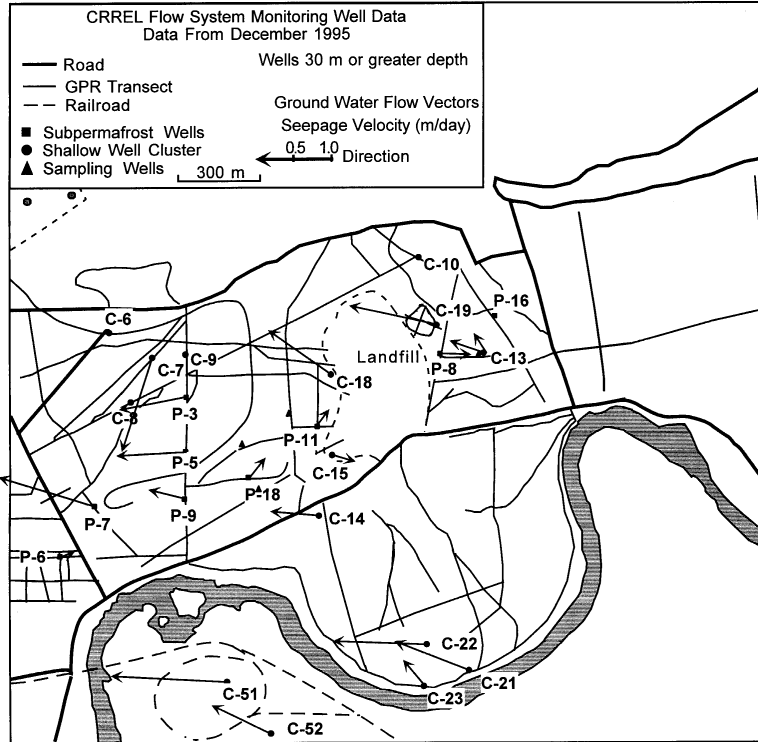


Figure A3 (cont'd). Mean flow directions, seepage velocities, and water levels from representative 30-m-deep monitoring wells in unfrozen thaw zones and from subpermafrost wells that exceed 30 m in depth. Vectors are calculated from ground water flow sensor data for measurements during September 1995 to January 1997.



*Figure A3 (cont'd).*

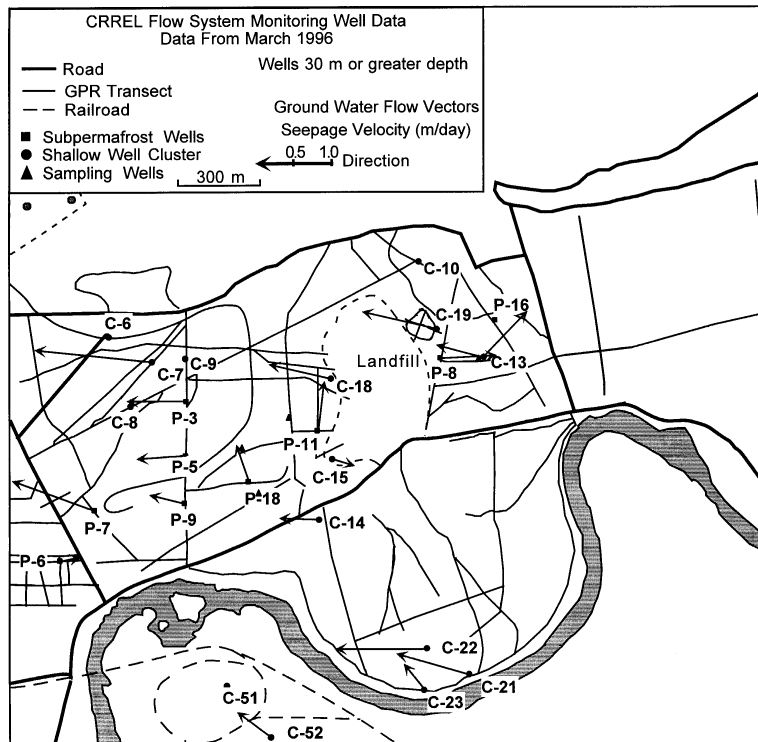
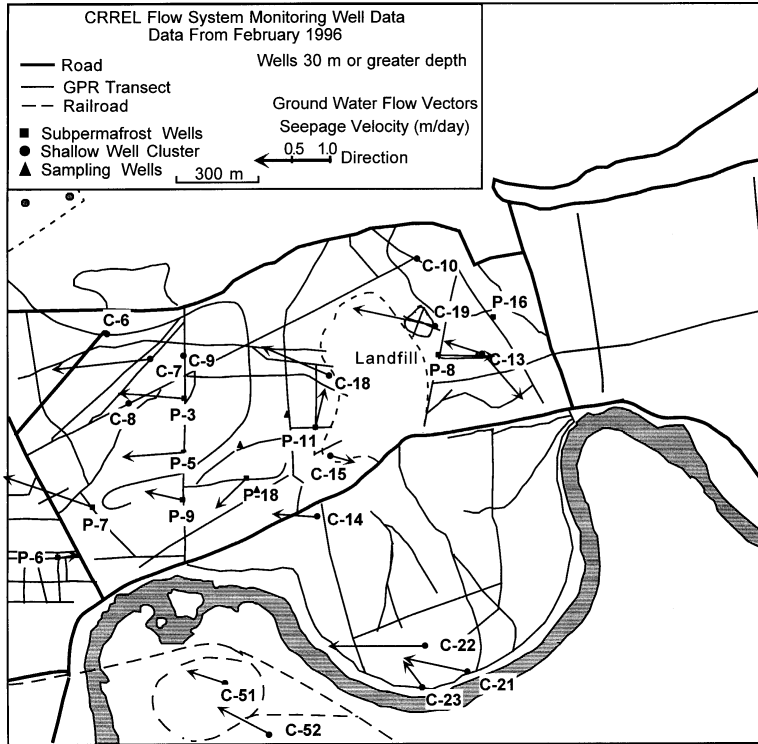


Figure A3 (cont'd). Mean flow directions, seepage velocities, and water levels from representative 30-m-deep monitoring wells in unfrozen thaw zones and from subpermafrost wells that exceed 30 m in depth. Vectors are calculated from ground water flow sensor data for measurements during September 1995 to January 1997.

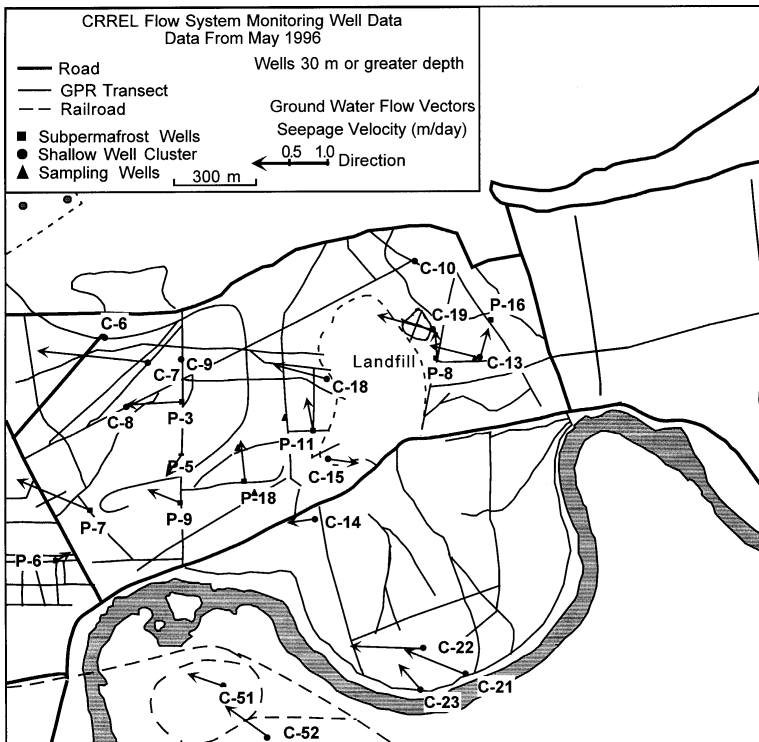
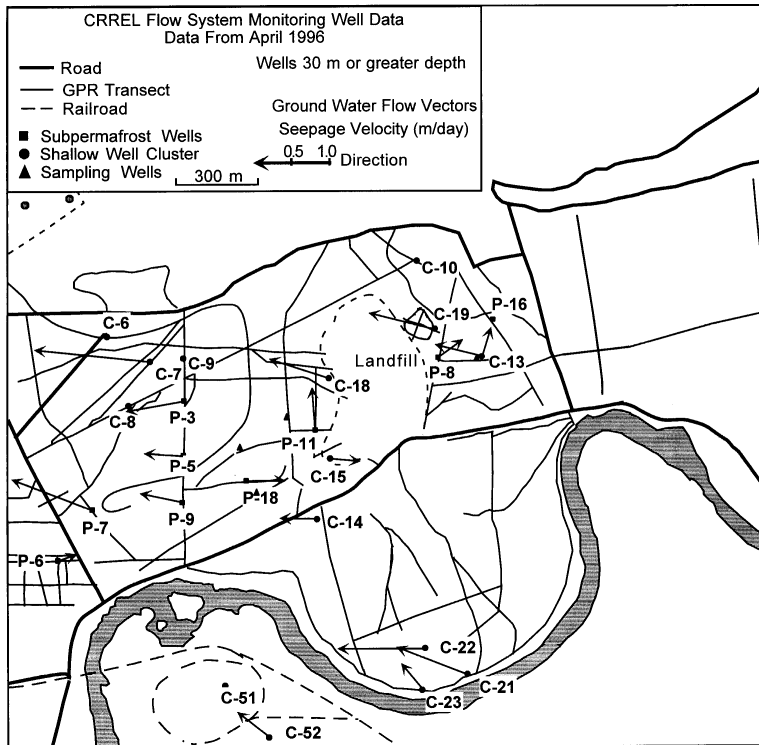


Figure A3 (cont'd).

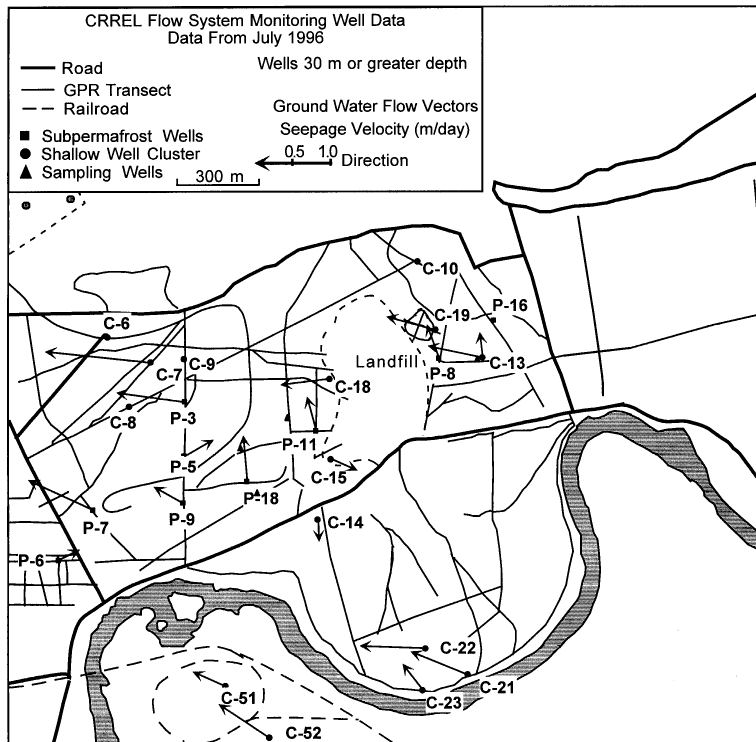
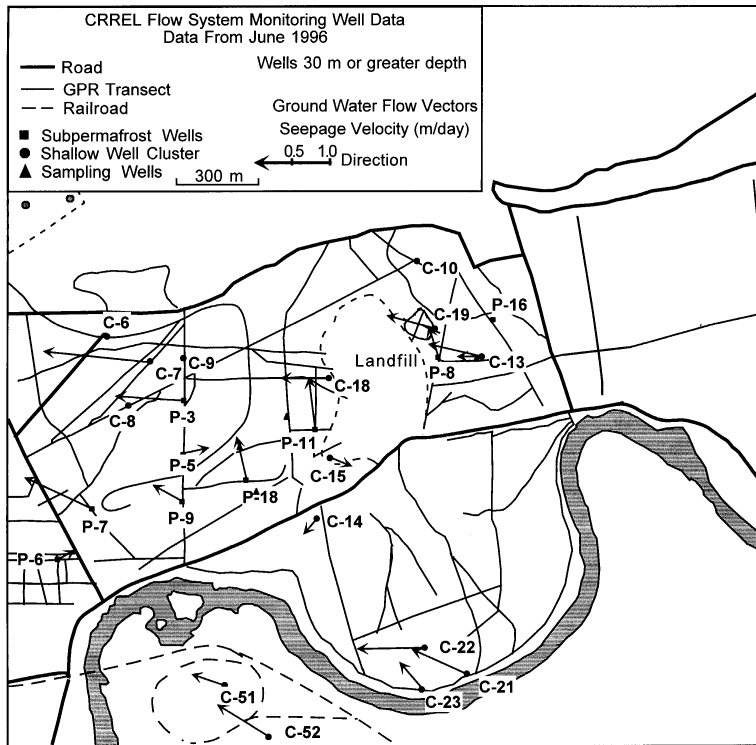


Figure A3 (cont'd). Mean flow directions, seepage velocities, and water levels from representative 30-m-deep monitoring wells in unfrozen thaw zones and from subpermafrost wells that exceed 30 m in depth. Vectors are calculated from ground water flow sensor data for measurements during September 1995 to January 1997.

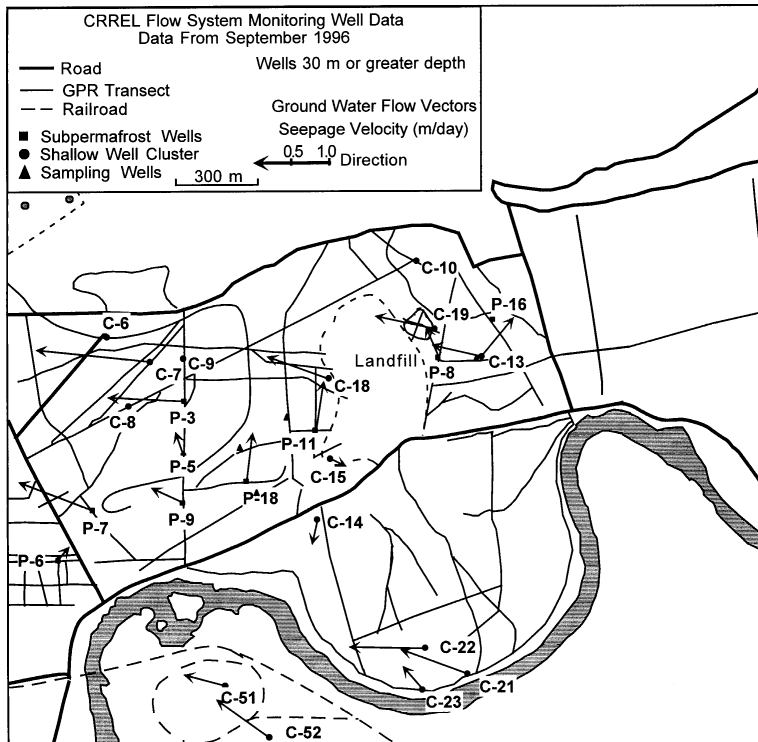
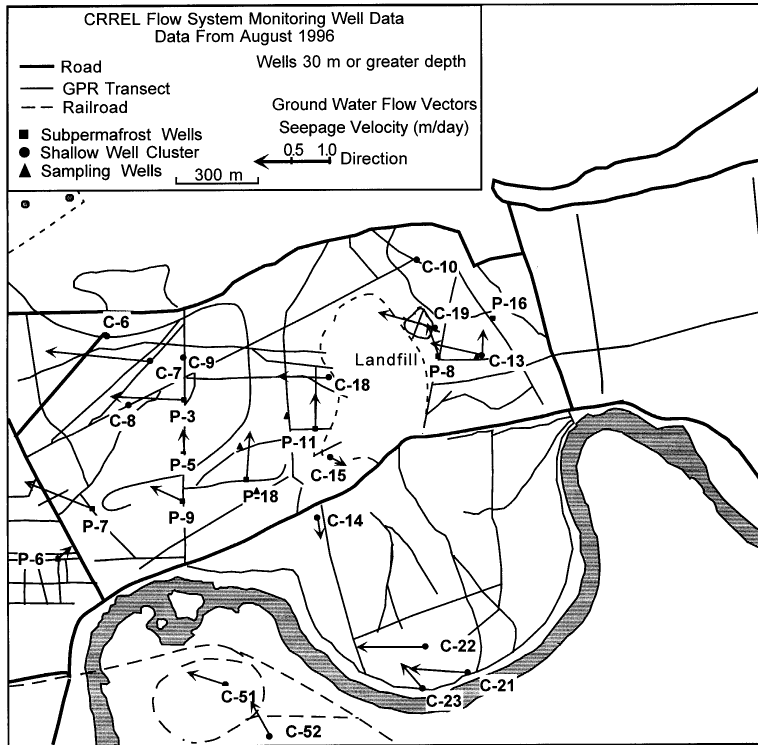


Figure A3 (cont'd).

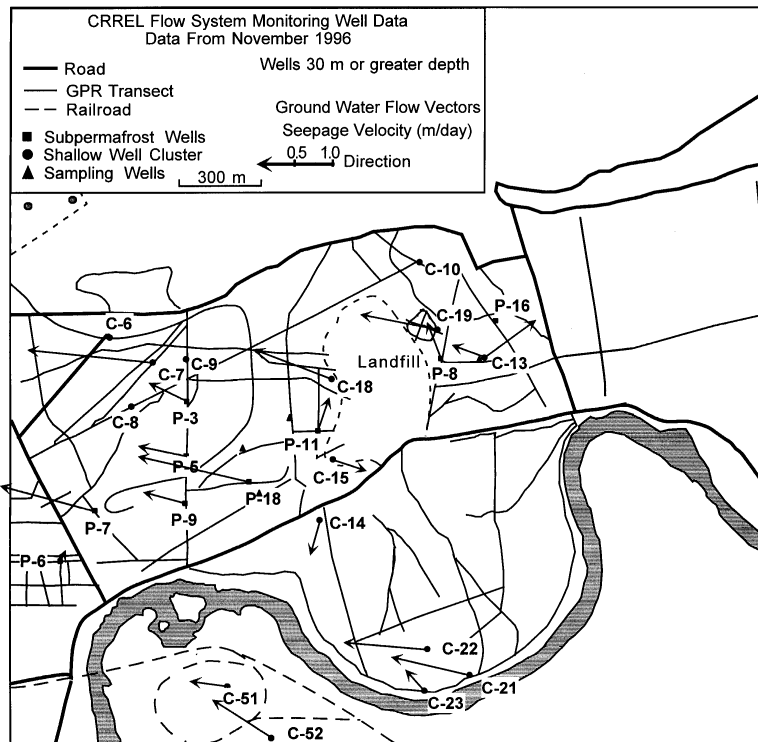
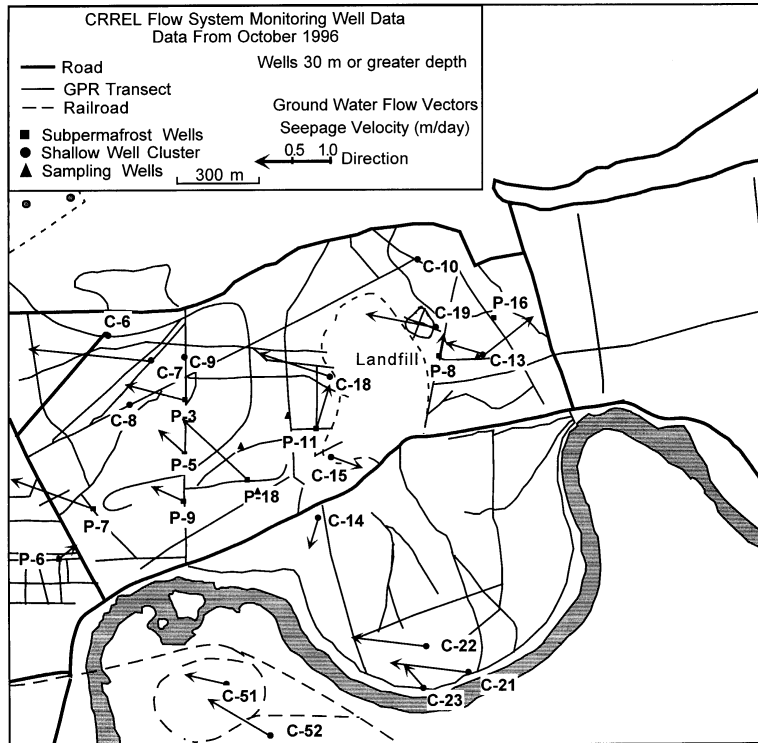
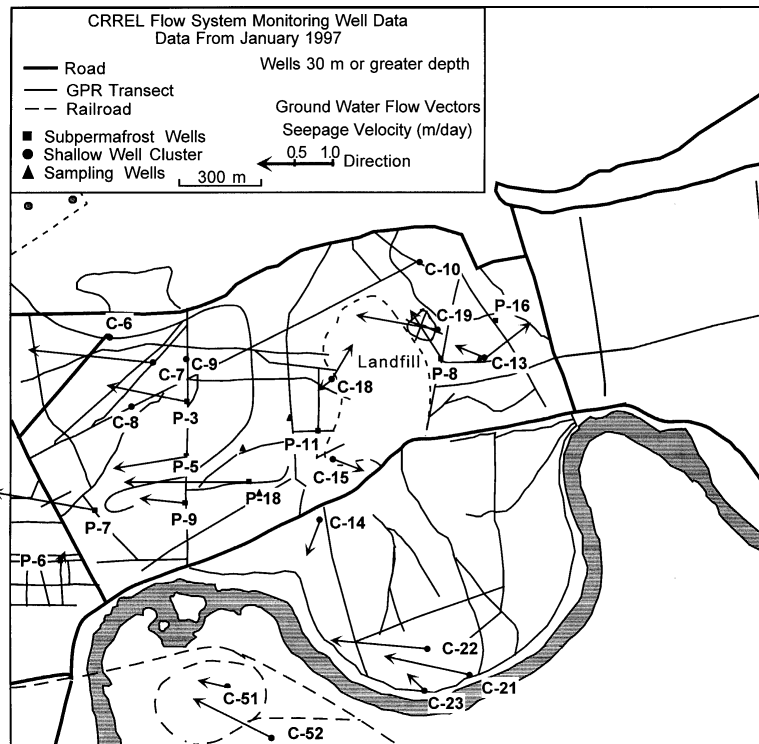
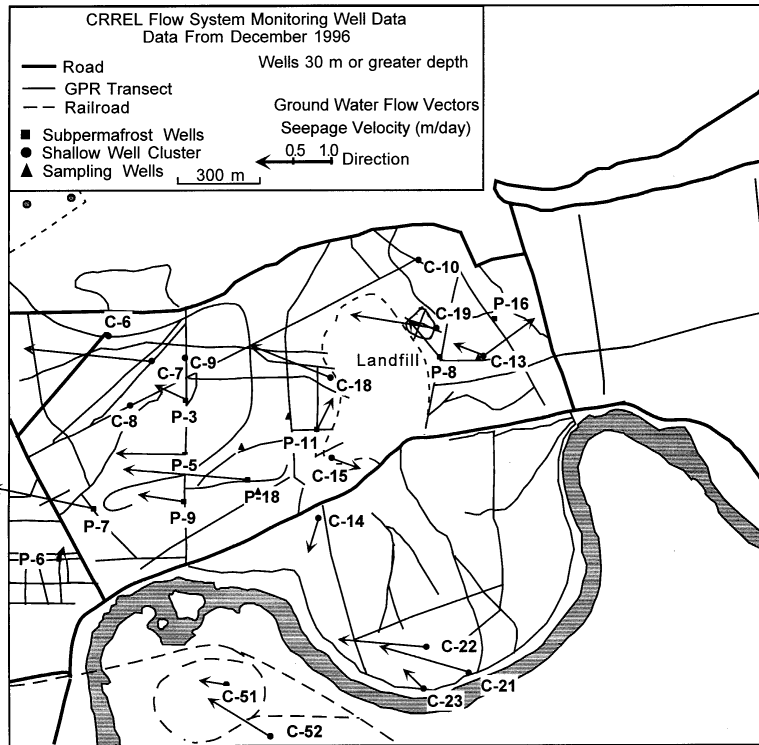


Figure A3 (cont'd). Mean flow directions, seepage velocities, and water levels from representative 30-m-deep monitoring wells in unfrozen thaw zones and from subpermafrost wells that exceed 30 m in depth. Vectors are calculated from ground water flow sensor data for measurements during September 1995 to January 1997.



*Figure A3 (cont'd).*

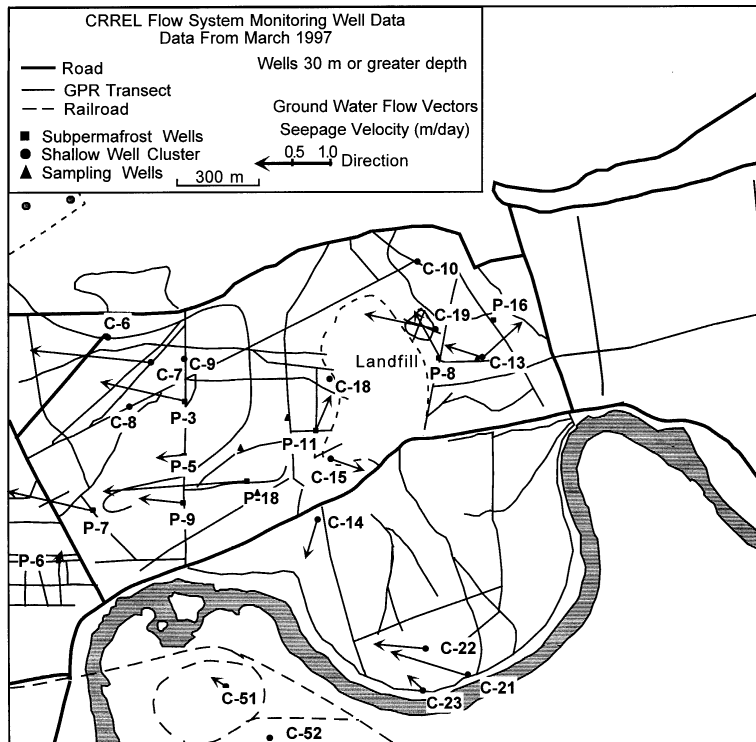
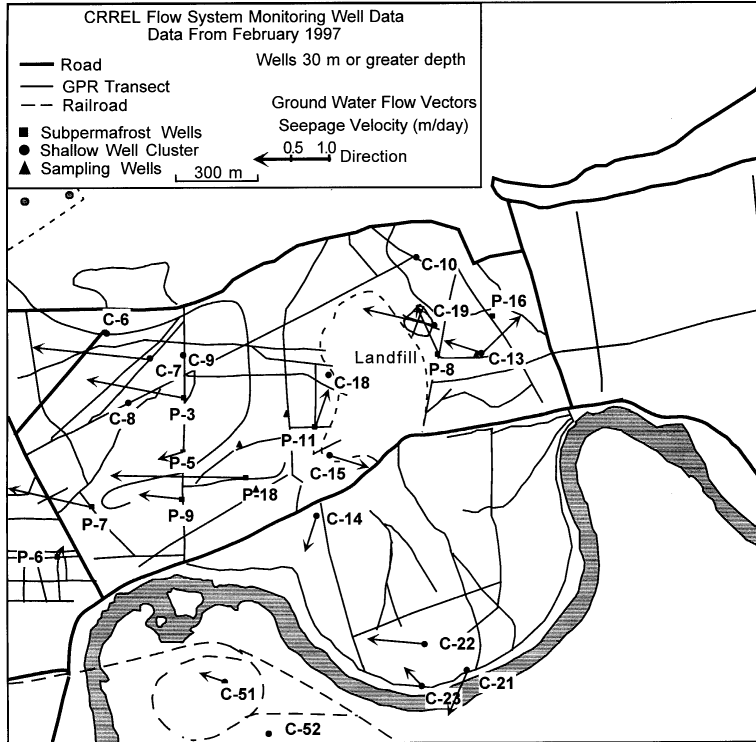


Figure A3 (cont'd). Mean flow directions, seepage velocities, and water levels from representative 30-m-deep monitoring wells in unfrozen thaw zones and from subpermafrost wells that exceed 30 m in depth. Vectors are calculated from ground water flow sensor data for measurements during September 1995 to January 1997.

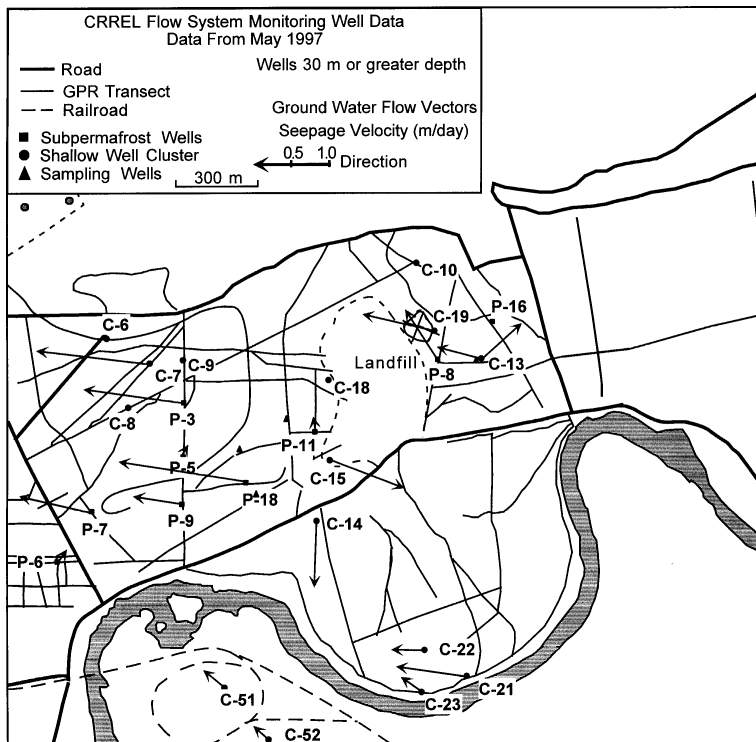
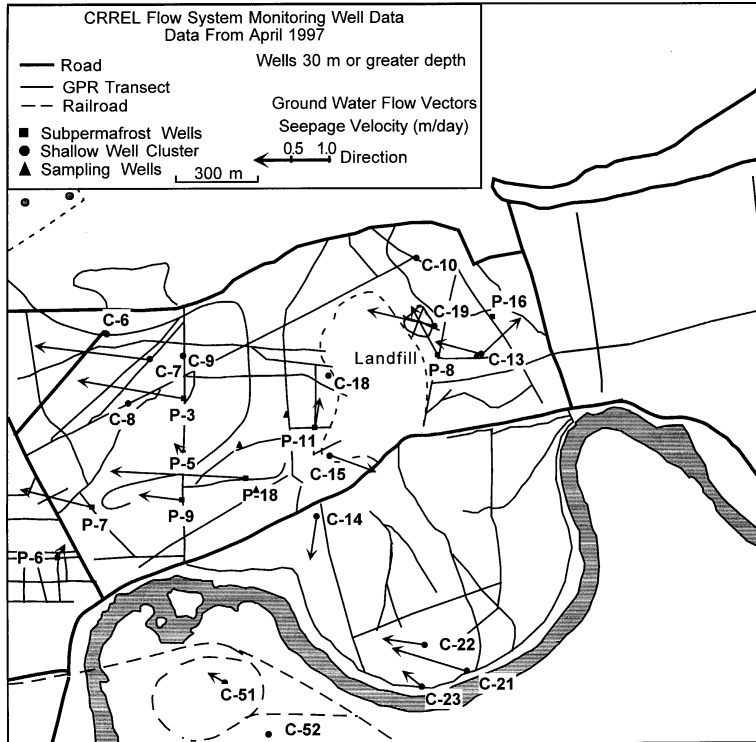
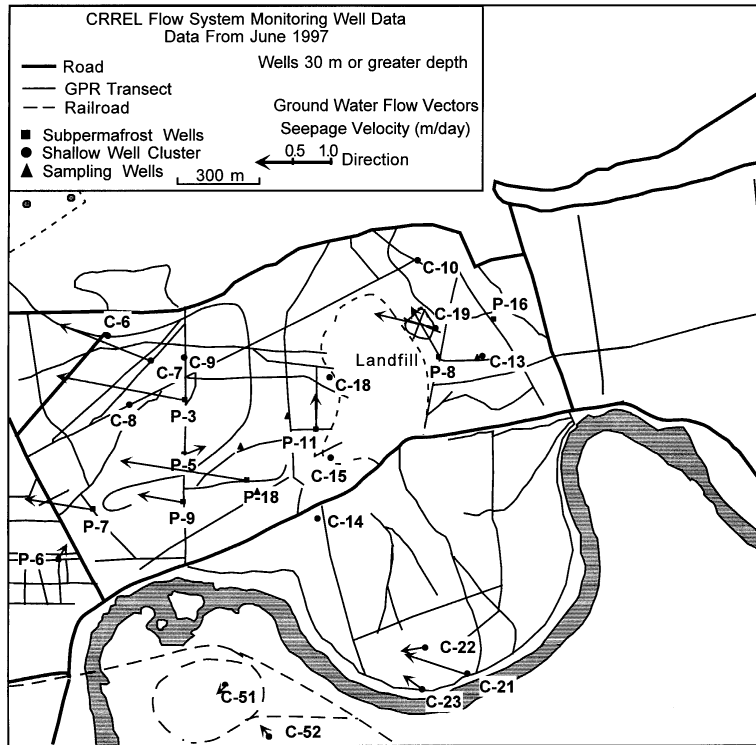


Figure A3 (cont'd).



*Figure A3 (cont'd). Mean flow directions, seepage velocities, and water levels from representative 30-m-deep monitoring wells in unfrozen thaw zones and from subpermafrost wells that exceed 30 m in depth. Vectors are calculated from ground water flow sensor data for measurements during September 1995 to January 1997.*

# REPORT DOCUMENTATION PAGE

Form Approved  
OMB No. 0704-0188

Public reporting burden for this collection of information is estimated to average 1 hour per response, including the time for reviewing instructions, searching existing data sources, gathering and maintaining the data needed, and completing and reviewing the collection of information. Send comments regarding this burden estimate or any other aspect of this collection of information, including suggestion for reducing this burden, to Washington Headquarters Services, Directorate for Information Operations and Reports, 1215 Jefferson Davis Highway, Suite 1204, Arlington, VA 22202-4302, and to the Office of Management and Budget, Paperwork Reduction Project (0704-0188), Washington, DC 20503.

1. AGENCY USE ONLY (Leave blank)		2. REPORT DATE August 1998		3. REPORT TYPE AND DATES COVERED	
4. TITLE AND SUBTITLE  Geological and Geophysical Investigations of the Hydrogeology of Fort Wainwright, Alaska. Part II: North-Central Cantonment Area				5. FUNDING NUMBERS	
6. AUTHORS Daniel E. Lawson, Steven A. Arcone, Allan J. Delaney, Jodie D. Strasser, Jeffrey C. Strasser, Christopher R. Williams, and Tommie J. Hall					
7. PERFORMING ORGANIZATION NAME(S) AND ADDRESS(ES) U.S. Army Cold Regions Research and Engineering Laboratory 72 Lyme Road Hanover, New Hampshire 03755-1290				8. PERFORMING ORGANIZATION REPORT NUMBER  CRREL Report 98-6	
9. SPONSORING/MONITORING AGENCY NAME(S) AND ADDRESS(ES) U.S. Army Engineer District, Alaska For the Environmental Resources Department Directorate of Public Works Fort Richardson, Alaska				10. SPONSORING/MONITORING AGENCY REPORT NUMBER	
11. SUPPLEMENTARY NOTES For conversion of SI units to non-SI units of measurement, consult ASTM Standard E380-93, <i>Standard Practice for Use of the International System of Units</i> , published by the American Society for Testing and Materials, 100 Barr Harbor Drive., West Conshohocken, Pennsylvania 19428-2959.					
12a. DISTRIBUTION/AVAILABILITY STATEMENT  Approved for public release; distribution is unlimited.  Available from NTIS, Springfield, Virginia 22161				12b. DISTRIBUTION CODE	
13. ABSTRACT ( <i>Maximum 200 words</i> )  Ongoing investigations of the permafrost and ground water conditions in the north-central area of the Fort Wainwright, Alaska, cantonment, north of the Chena River, show the hydrogeology of the site to be extremely complex. Permafrost, being impermeable and discontinuous, controls the distribution and dimensions of ground water aquifers to a great degree. Aquifers are above, below, and adjacent to permafrost, and in some locations are within unfrozen zones surrounded by it. This complexity makes it difficult to predict the direction and velocity of ground water flow, as well as its seasonal and annual variability. Data have been obtained from ground-penetrating radar surveys, borehole logs, and ground water instruments. They have then been combined with interpretations of aerial photographs and ground observations to delineate the permafrost and aquifer distribution. They have also been used to develop conceptual hydrogeological models of the area. This information is necessary to remediate ground water contamination, while furthering the basic understanding of aquifer distribution and ground water flow in discontinuous permafrost terrain.					
14. SUBJECT TERMS  Ground penetrating radar Ground water  Hydrogeology Permafrost  Seepage rate/direction				15. NUMBER OF PAGES 73	
				16. PRICE CODE	
17. SECURITY CLASSIFICATION OF REPORT UNCLASSIFIED		18. SECURITY CLASSIFICATION OF THIS PAGE UNCLASSIFIED		19. SECURITY CLASSIFICATION OF ABSTRACT UNCLASSIFIED	
				20. LIMITATION OF ABSTRACT UL	